

Chapter III

Results

The Spray-drying Conditions.

Before proceeding with the preparation of co-spray dried powder, preliminary investigation of spray-drying process was carried out to determine optimum conditions. During the feasibility trial, the batch sizes of 100 g. were used.

Table 14 summarized the conditions which were interchanged to determine the optimum condition for the spray-drying of theophylline-polymer and theophylline-polymer-channeling agent. The main factors which could be changed were: air pressure, liquid feed rate and inlet air temperature.

Table 14. Summary of the spray-drying conditions used in preparation of co-spray dried powder.

Condition	Formulation			
	I-IV	V-VIII	IX-XII	XIII-XIX
Inlet Air Temperature(°C)	140	140	130	130
Feed Rate(ml/minute)	23.8	22.6	23.8	23.8
Compression Air(bar)	4	4	4	4
Dilution Medium	water	water	2% NH ₃	2% NH ₃

In Formulation I-IV, the maximum liquid feed rate was used and air pressure of 4 bar was chosen. Air inlet temperature, 140°C, was used to avoid melting of ethylcellulose.

In Formulation IV-VIII, air pressure was maintained at 4 bar but the feed rate was decreased to avoid the condition that led to agglomerated powder that stucked to the chamber wall. It was found that the concentration of HPMC in formulation must be decreased in order to reduce the viscosity of the mixture. In the experiment with the formulation containing HPMC, large amount of powder products adhered to the wall of drying chamber, and could not be recovered from the chamber.

In Formulation IX-XII and Formulation XIII-XIX, the same conditions as Formulation I-IV were used, except that the inlet air temperature was lowered because 2% ammonia solution had a lower boiling point.

The Percent Yield of Co-Spray Dried Powder.

The percent recovery were shown in Table 15. It was seen that Formulation V-VIII, using HPMC, had low percent recovery, because a lot of powder adhered to the chamber wall. The other formulations had good percent yield, above 70%.

Table 15. The percent recovery from spray drying procedure.

Formulation	Percent Recovery		
	Collector	Chamber	Total
I	27.56	51.66	79.22
II	23.01	55.84	78.85
III	30.65	48.92	79.57
IV	40.18	44.06	84.24
V	16.22	22.80	39.02
VI	4.88	10.70	15.58
VII	8.85	11.22	20.07
VIII	10.47	9.62	20.09
IX	55.42	28.56	83.98
X	58.33	25.70	84.03
XI	45.94	28.62	74.56
XII	43.28	25.69	68.97
XIII	70.75	18.15	88.90
XIV	62.40	24.60	87.00
XV	55.58	22.28	77.86
XVI	57.70	18.40	76.10
XVII	70.45	18.55	89.00
XVIII	66.50	18.60	85.30
XIX	65.80	18.20	84.00

Physical Properties of Co-spray Dried Powders.

1. Morphology of Powders.

The shape and surface topography of co-spray dried particles were found to be affected by the formulation and method of the drug mixture preparation. When the distilled water was used as a dilution solution (Formulation I-VIII), high quantity of

agglomerated crystals of theophylline were observed in the co-spray dried particles. In the contrary, most of the co-spray dried powder of the mixture prepared by using 2% ammonia solution (Formulation IX-XIX) was in the form of microspheres with smooth surface.

The microscopic appearance of theophylline powder in different magnification were presented in Figure 5. Theophylline powder composed of thick rod shapes in various length. The surface of powder was rough.

The photomicrographs of Formulation I-IV were shown in Figures 6-9. The shape of particles could be seen in two forms as microsphere and rod shape. The co-spray dried powder of Formulation I-IV exhibited microsphere and fine needle shape particles coated on the surface of the agglomerated particles. The shape of agglomerated particles were nearly spherical with fairly uniform sizes.

The photomicrographs of Formulation V-VIII in different magnification were shown in Figures 10-13. The agglomerated particles were consisted of bigger, irregular shape particles and smaller microspheres. The overall shape of agglomerated particles were fairly ball shape. The surface of microspheres were not smooth but was embedded by small rods. The agglomerated particles were relatively larger than of other polymer formulations.

The microscopic images of Formulation IX-XII in different magnification were shown in Figures 14-17. The particle shape was microball with different sizes. The surfaces of some microballs were rough but some of them were smooth.

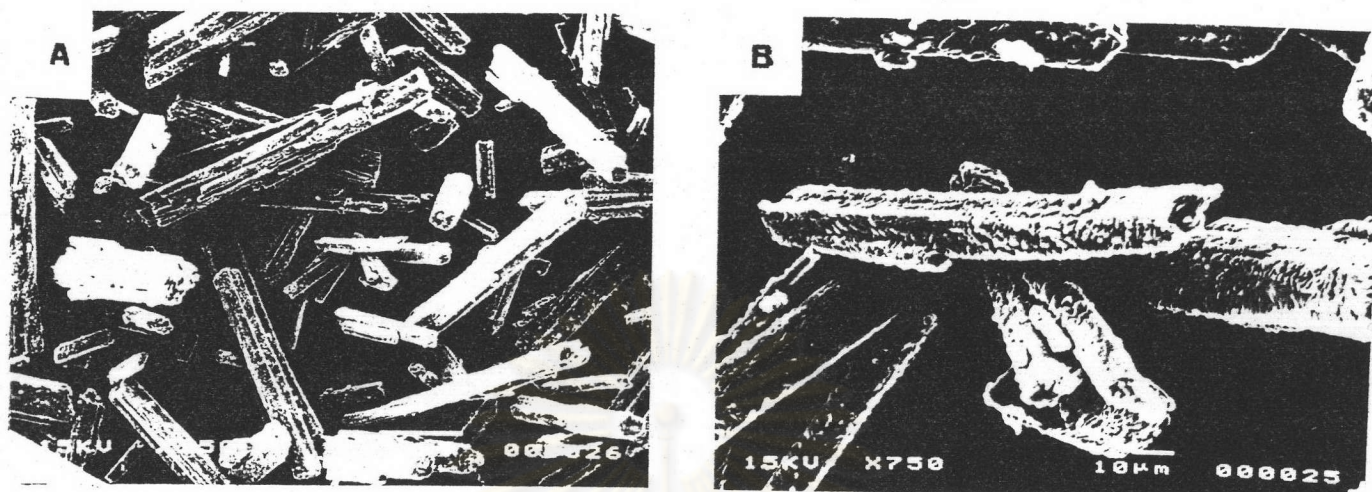


Figure 5. Photomicrographs of Original Theophylline Powders

(Key: A x 150 , B x 750)

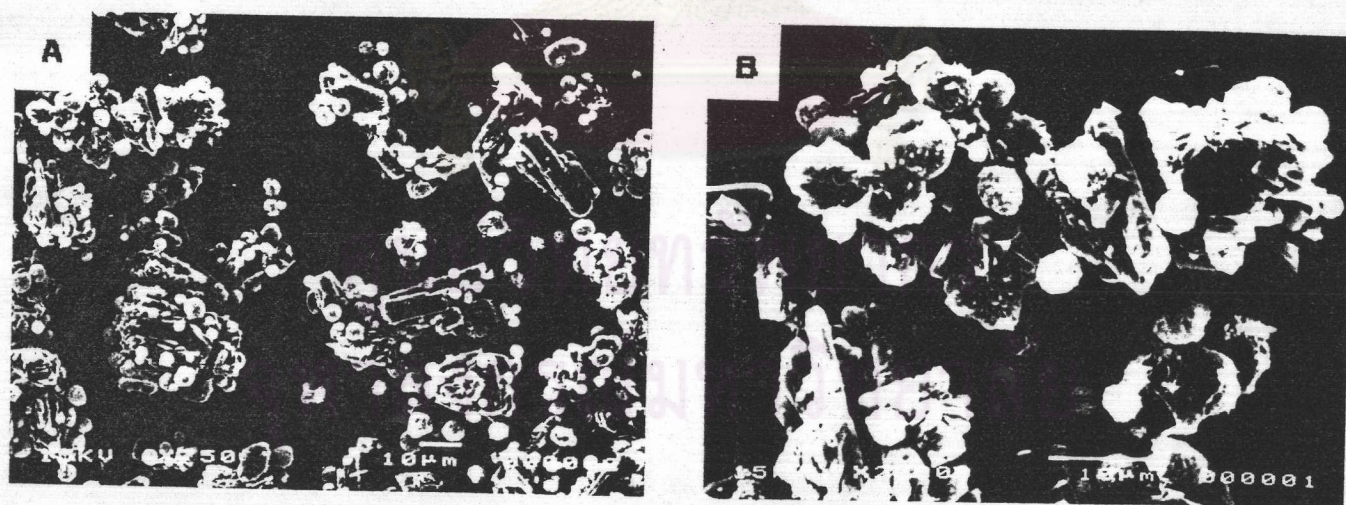


Figure 6. Photomicrographs of Co-Spray Dried Formulation I

(Key: A x 750 , B x 2,000)

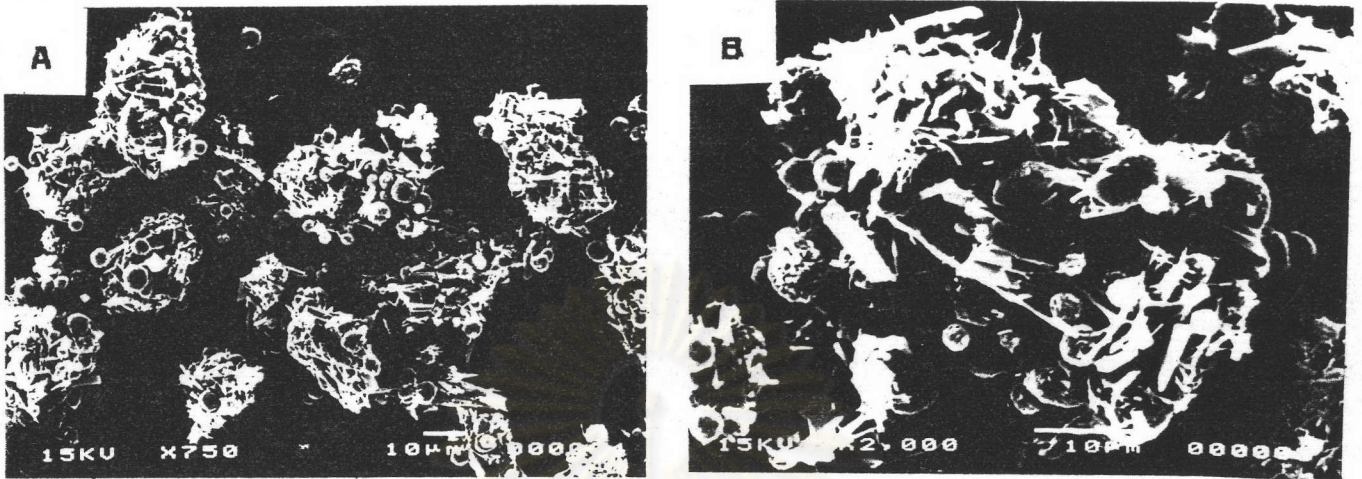


Figure 7. Photomicrographs of Co-Spray Dried Formulation II

(Key: A x 750 , B x 2,000)

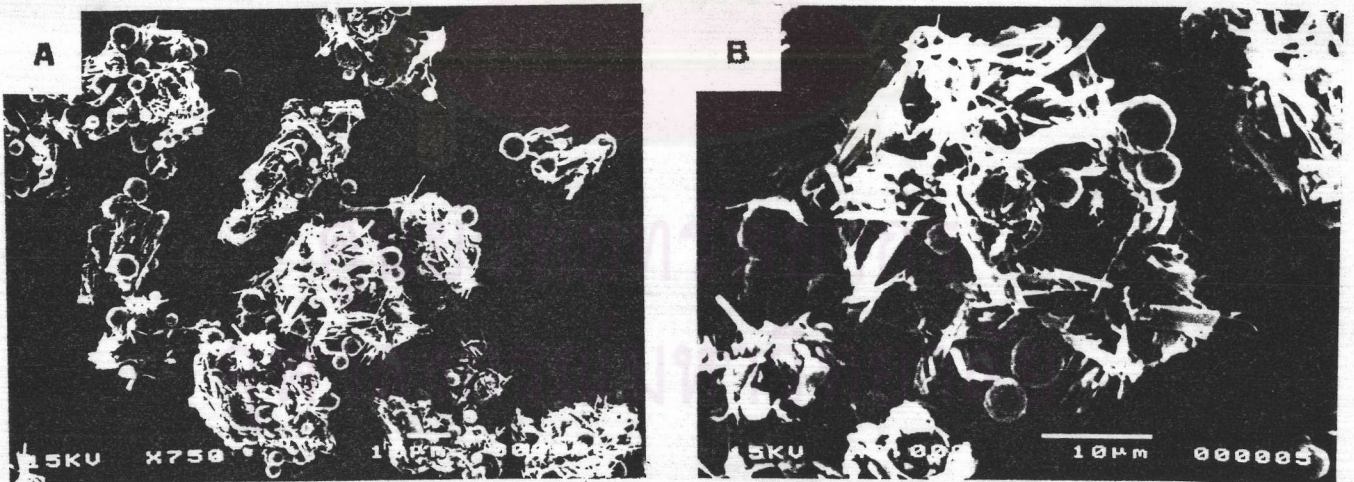


Figure 8. Photomicrographs of Co-Spray Dried Formulation III

(Key: A x 750 , B x 2,000)

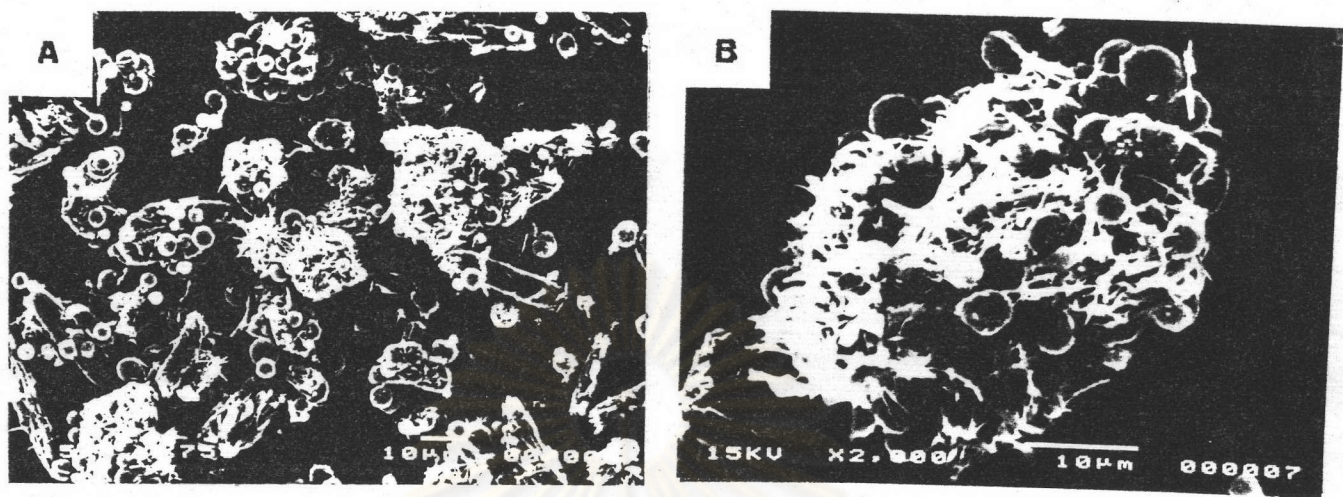


Figure 9. Photomicrographs of Co-Spray Dried Formulation IV
(Key: A x 750 , B x 2,000)

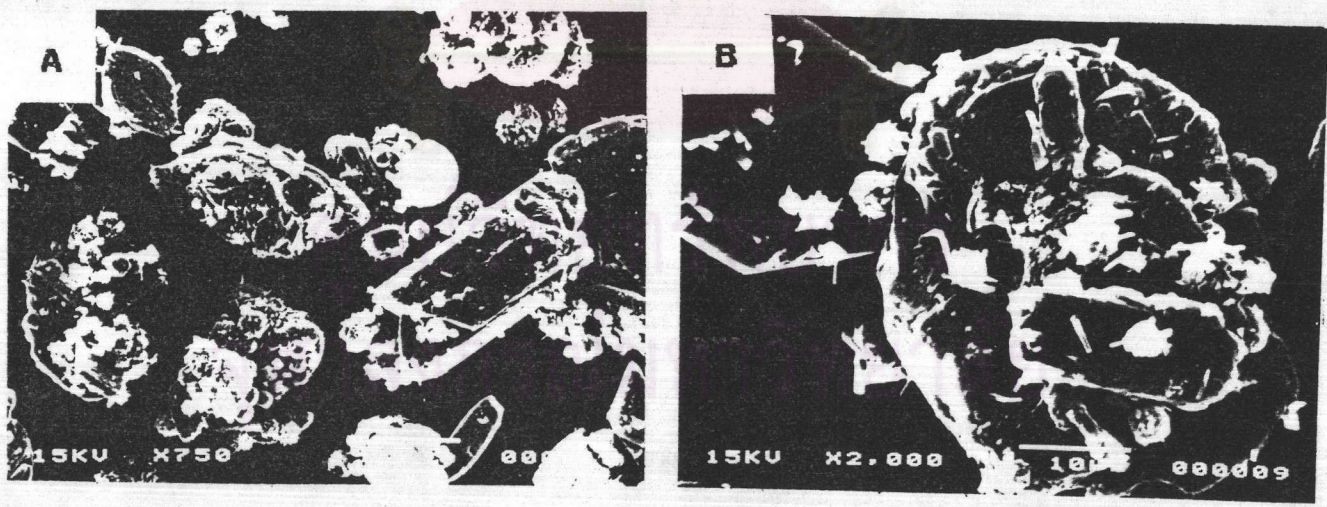


Figure 10. Photomicrographs of Co-Spray Dried Formulation V
(Key: A x 750 , B x 2,000)

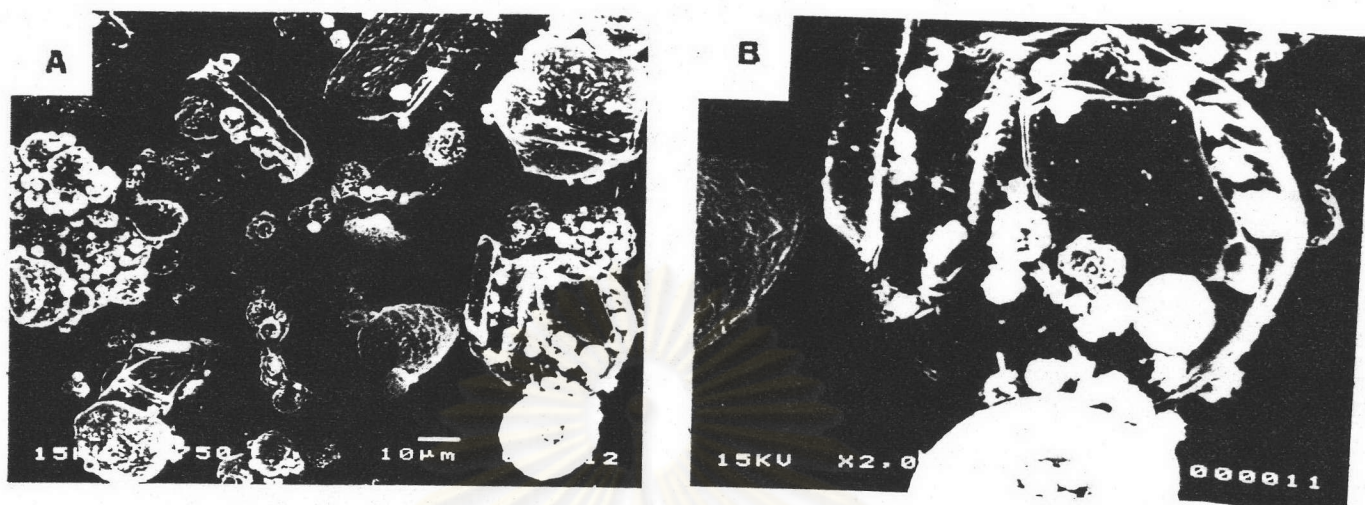


Figure 11. Photomicrographs of Co-Spray Dried Formulation VI

(Key: A x 750 , B x 2,000)

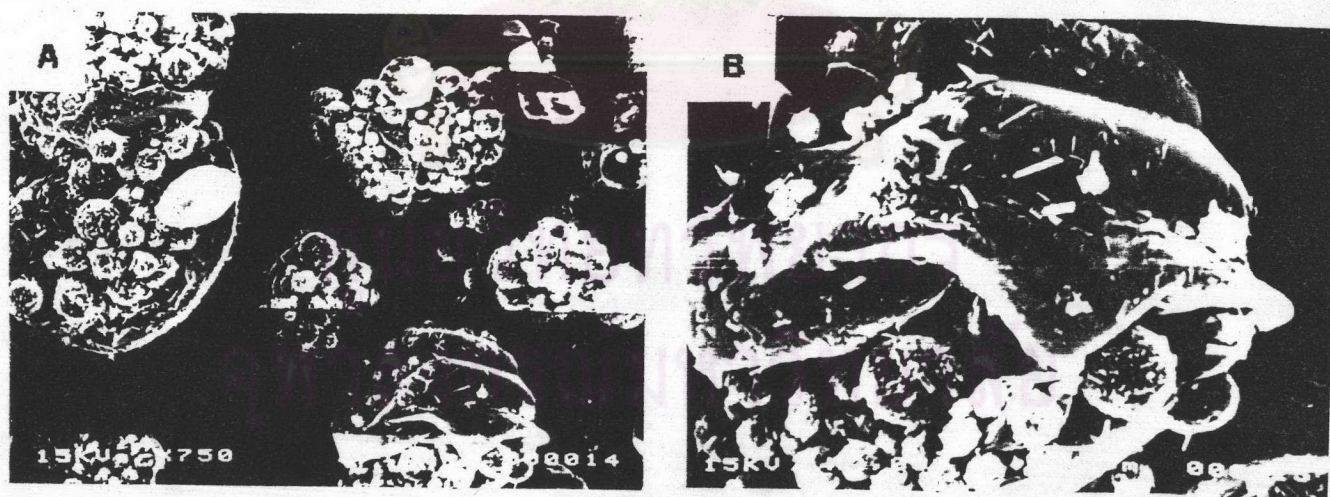


Figure 12. Photomicrographs of Co-Spray Dried Formulation VII

(Key: A x 750 , B x 2,000)

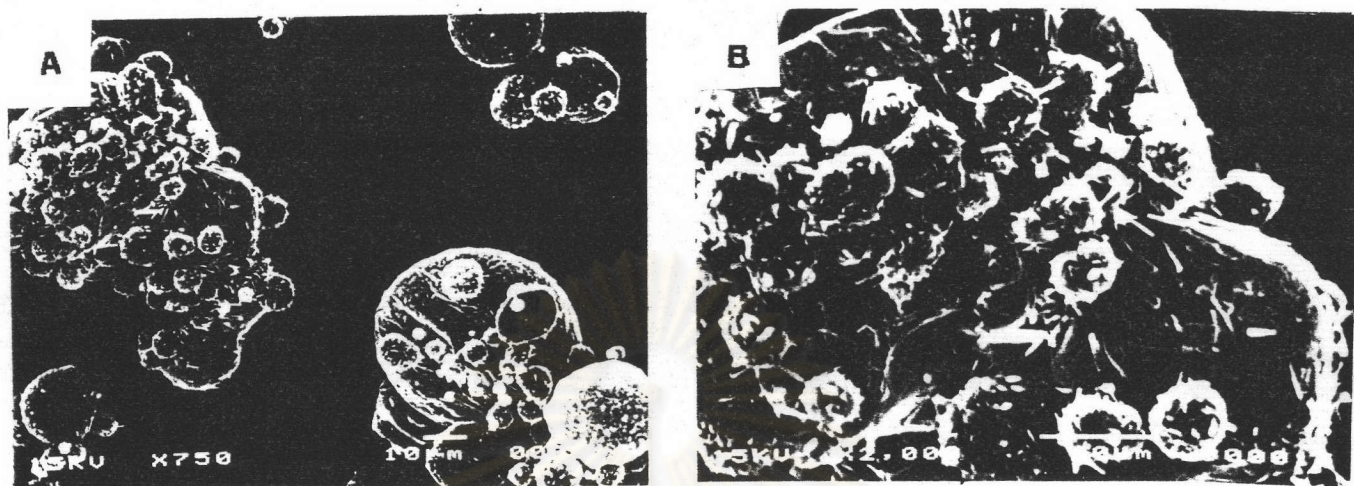


Figure 13. Photomicrographs of Co-Spray Dried Formulation VIII

(Key: A x 750 , B x 2,000)

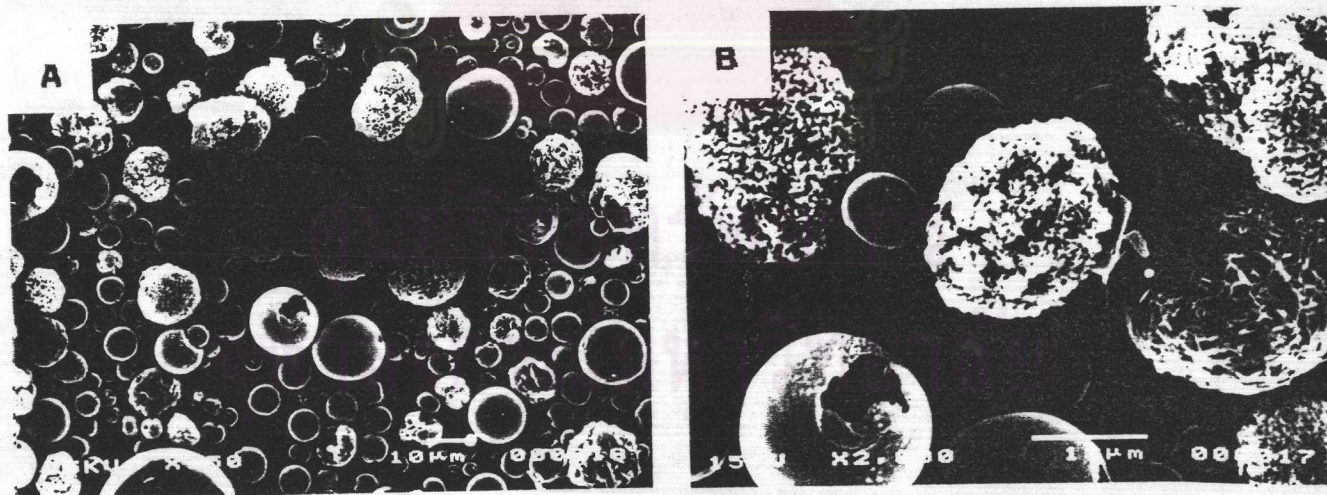


Figure 14. Photomicrographs of Co-Spray Dried Formulation IX

(Key: A x 750 , B x 2,000)

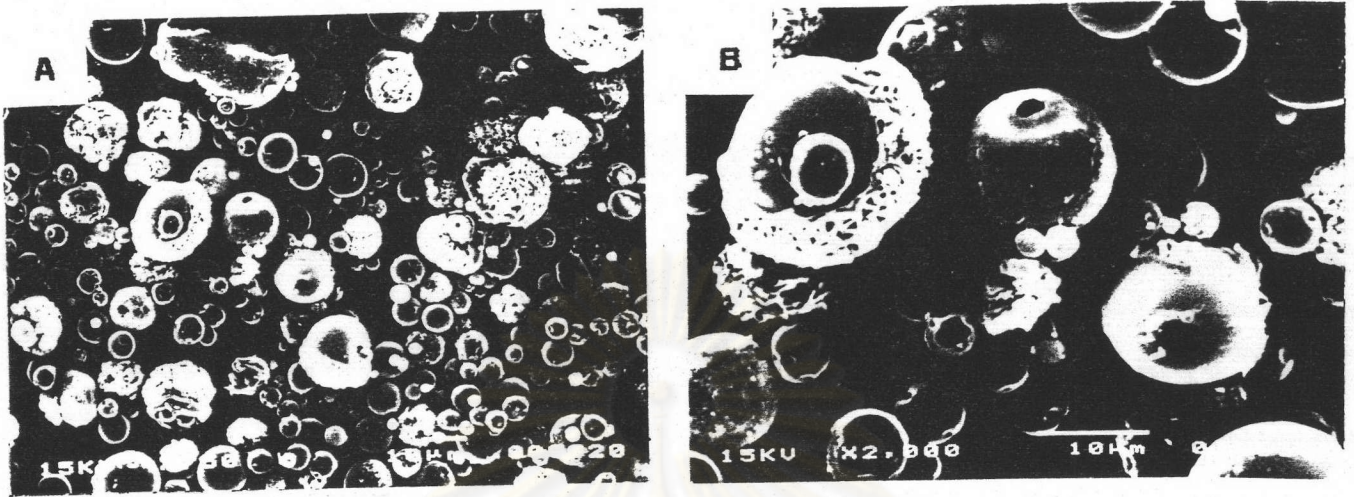


Figure 15. Photomicrographs of Co-Spray Dried Formulation X

(Key: A x 750 , B x 2,000)

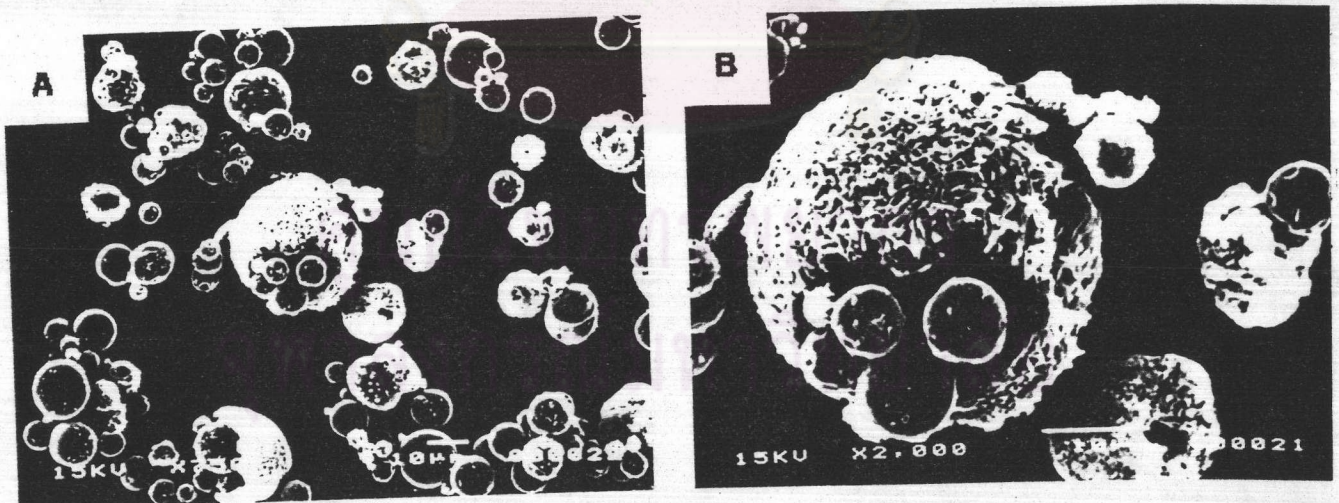


Figure 16. Photomicrographs of Co-Spray Dried Formulation XI

(Key: A x 750 , B x 2,000)

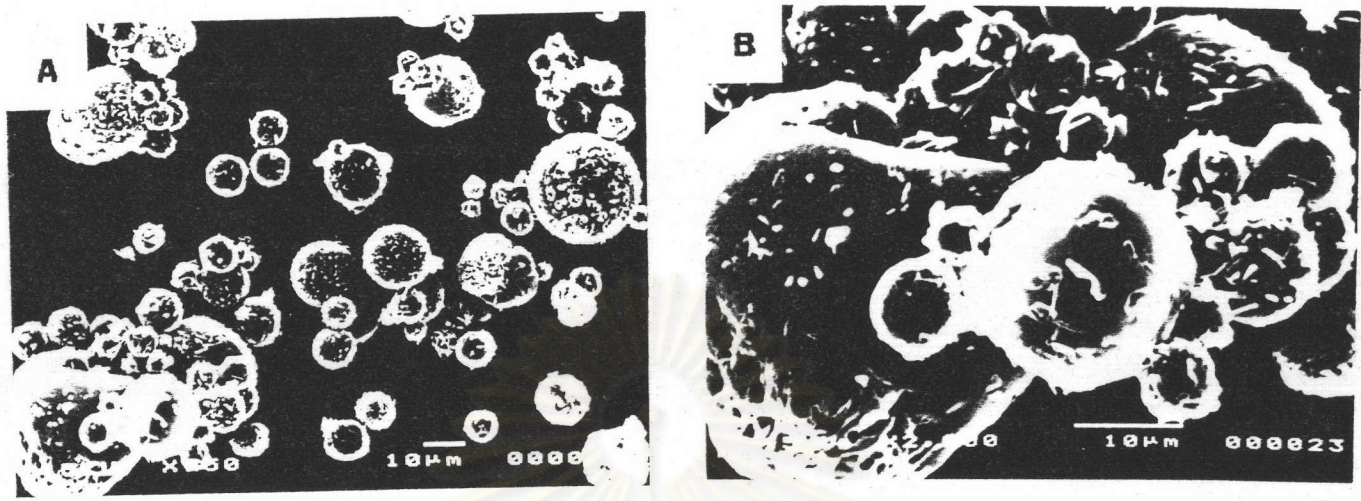


Figure 17. Photomicrographs of Co-Spray Dried Formulation XII
(Key: A x 750 , B x 2,000)

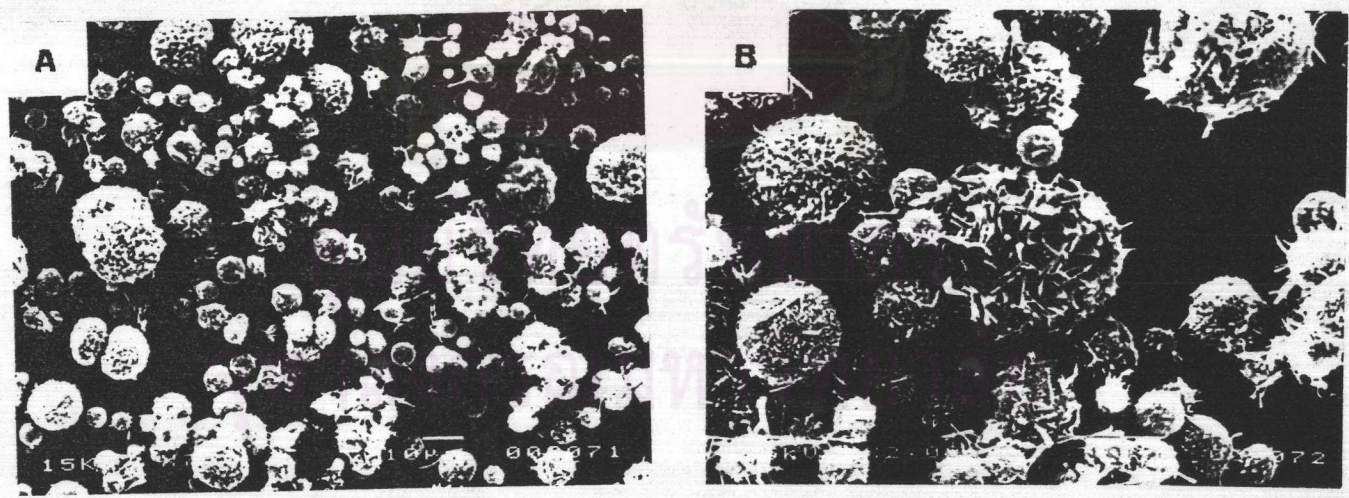


Figure 18. Photomicrographs of Co-Spray Dried Formulation XIII
(Key: A x 750 , B x 2,000)

The photomicrographs of Formulation XIII - XIX were shown in Figures 18-24. The shape of particles were microspheres in different sizes. The surface of microspheres were covered with microcrystal that made rough surface. However, some of them had rather smooth surface.

2. Drug Content.

The percent drug content of co-spray dried powder prepared from various formulation were shown in Table 16. The Formulations I-VIII in which water was used as a medium had different drug content between the products collected from the chamber and collector. However, for Formulations I-IV, the drug contents from collector were higher than those collected from chamber, but opposite results were obtained for Formulations V-VIII. The drug content of powder prepared according to Formulations IX-XII and XIII-XIX were relatively indifferent.

3. Moisture Content.

The moisture content of co-spray dried powder were also reported in Table 16. The moisture content was in the range of 0.42-4.00. The formulations that contained channeling agent had higher moisture content than of the other formulations.

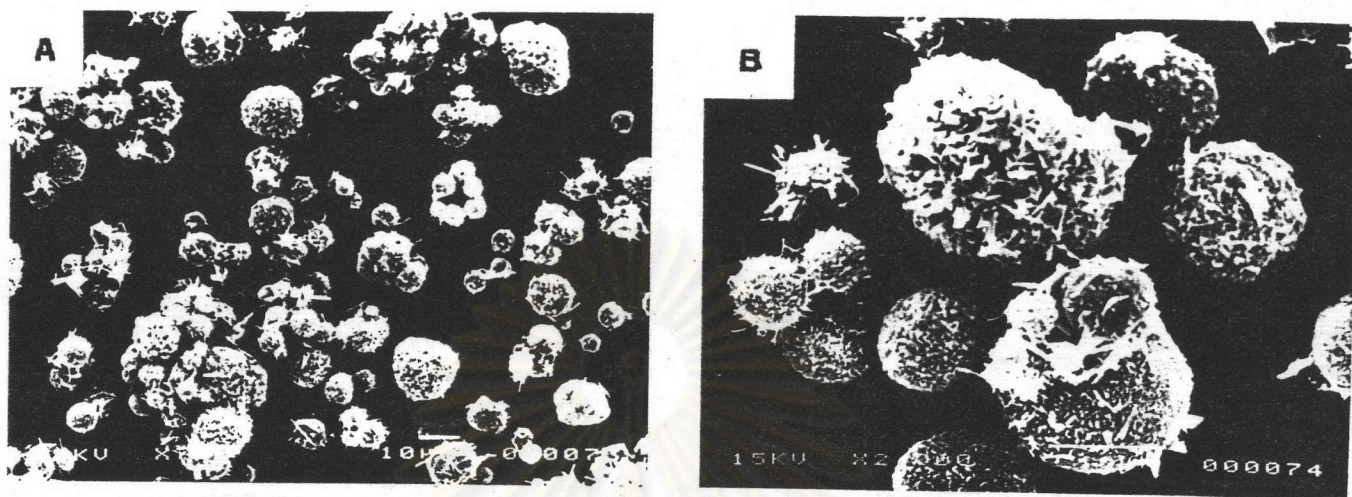


Figure 19. Photomicrographs of Co-Spray Dried Formulation XIV

(Key: A x 750 , B x 2,000)

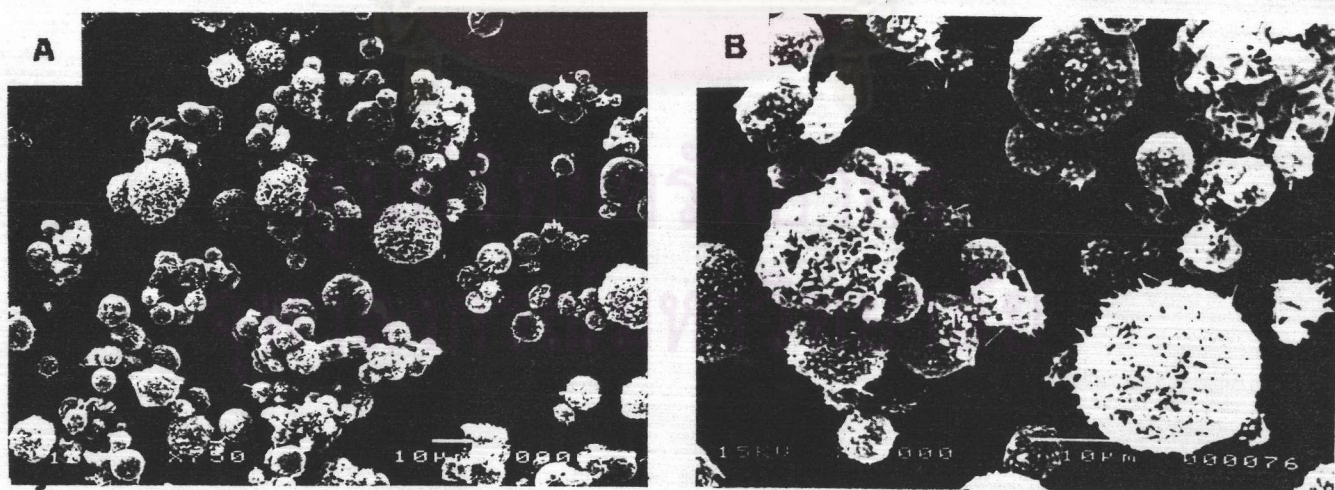


Figure 20. Photomicrographs of Co-Spray Dried Formulation XV

(Key: A x 750 , B x 2,000)

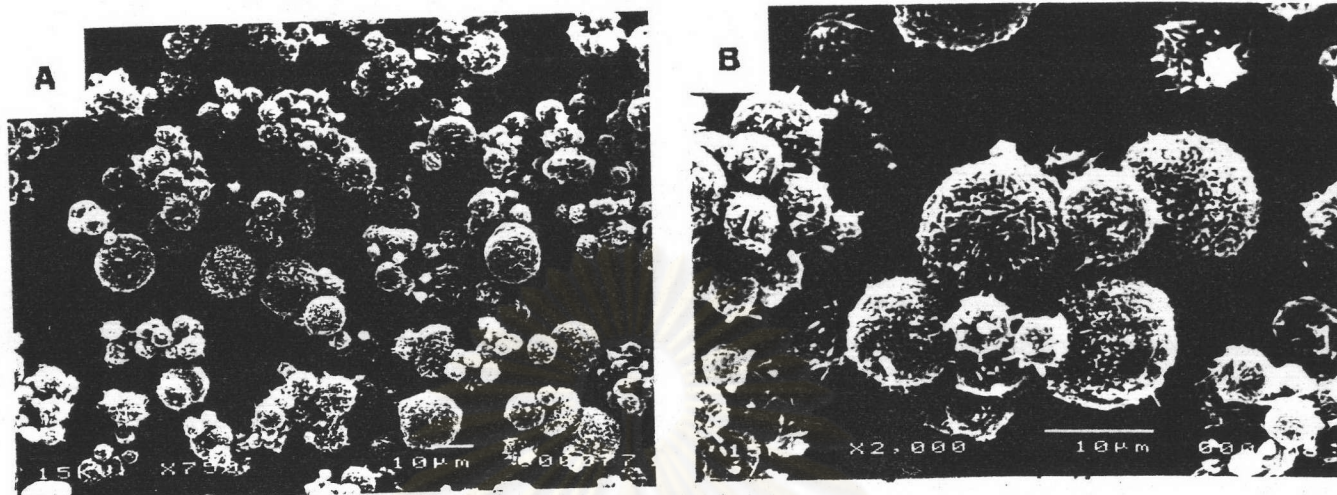


Figure 21. Photomicrographs of Co-Spray Dried Formulation XVI

(Key: A $\times 750$, B $\times 2,000$)

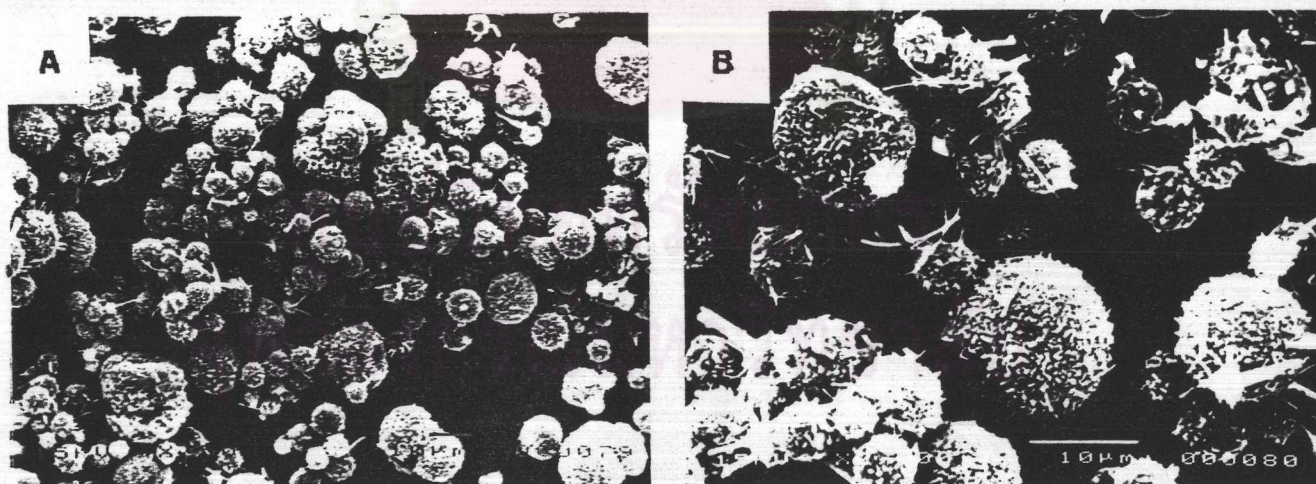


Figure 22. Photomicrographs of Co-Spray Dried Formulation XVII

(Key: A $\times 750$, B $\times 2,000$)

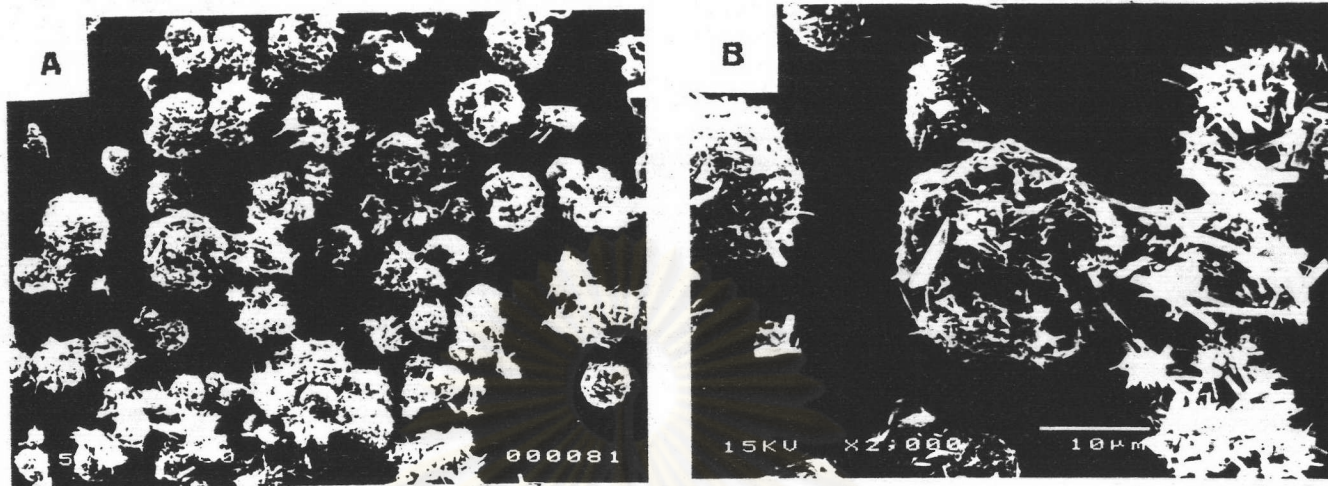


Figure 23. Photomicrographs of Co-Spray Dried Formulation XVIII

(Key: A x 750 , B x 2,000)

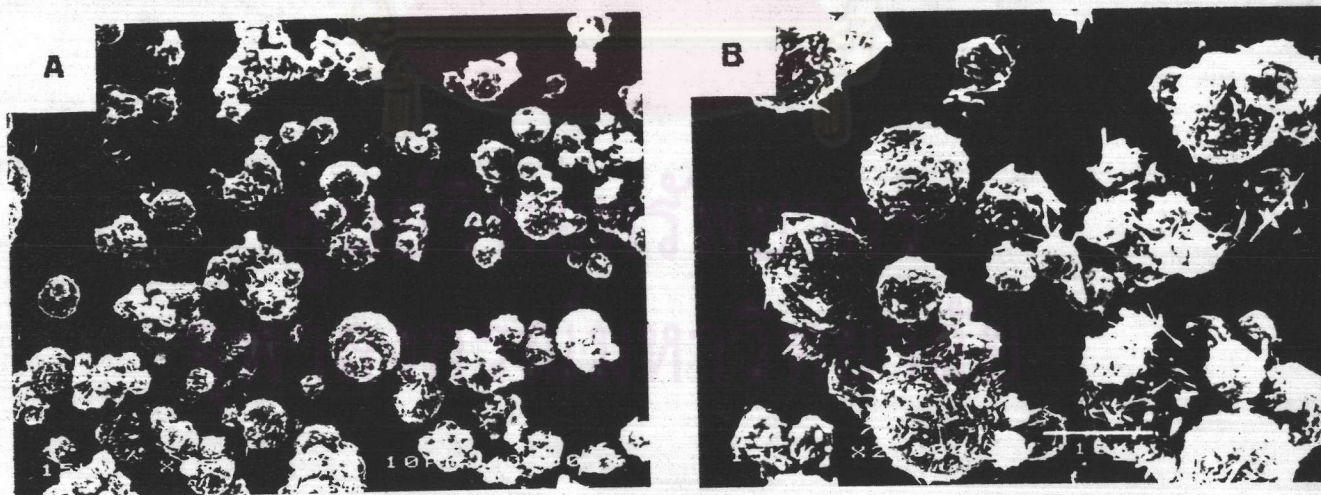


Figure 24. Photomicrographs of Co-Spray Dried Formulation XIX

(Key: A x 750 , B x 2,000)

Table 16. The percentage of drug content and the percentage of moisture content.

Formulation	% Drug Content(\pm SD)**		% Moisture Content in Collector(\pm SD)*
	Collector	Chamber	
I	96.03(0.59)	88.46(0.19)	0.42(0.07)
II	91.23(0.61)	76.70(0.12)	0.96(0.04)
III	88.36(0.43)	71.14(0.38)	1.02(0.05)
IV	83.27(0.94)	66.31(0.09)	1.00(0.06)
V	86.40(0.44)	98.10(0.87)	1.06(0.03)
VI	84.90(0.68)	90.44(0.78)	1.05(0.00)
VII	70.99(1.16)	82.61(0.72)	2.00(0.06)
VIII	65.99(0.26)	75.26(0.31)	2.04(0.05)
IX	91.30(0.46)	90.85(0.41)	1.02(0.03)
X	87.13(0.58)	87.35(0.47)	1.02(0.01)
XI	81.86(0.41)	81.67(0.59)	1.00(0.02)
XII	77.41(0.47)	77.58(0.44)	1.02(0.06)
XIII	87.55(0.11)	87.98(0.32)	1.92(0.05)
XIV	82.62(0.27)	82.24(0.38)	2.00(0.02)
XV	86.80(0.78)	86.52(0.69)	2.04(0.01)
XVI	76.90(0.18)	76.78(0.24)	4.00(0.02)
XVII	76.88(0.60)	76.32(0.52)	3.02(0.02)
XVIII	69.80(0.17)	69.27(0.22)	2.60(0.02)
XIX	69.73(0.27)	69.89(0.32)	2.97(0.01)

* Standard deviation from two determinations

** Standard deviation from three determinations

4. Particles Size Distribution.

The particle size distribution of the powder were shown in Table 17. The particle size distribution was depicted in Figures 89-93(Appendix D). It was apparent that particle size of theophylline-HPMC powders(Formulations V-VIII) were relatively larger than those than of the other formulations. Higher percents of fine powder were attained for the formulations with HPMCP(Formulations IX-XII) and ethylcellulose-channeling agents(Formulations XIII-XIX).

Table 17. Particle size distribution of co-spray dried powder.

% Weight Retained of Preparation	Sieve Size (μm)					
	212	150	90	75	45	Pan
I	3.45	1.44	58.34	6.89	11.12	8.75
II	10.43	3.50	6.44	16.72	50.21	12.70
III	14.99	4.26	8.30	14.88	38.84	18.82
IV	12.63	3.51	6.67	6.98	28.39	41.81
V	0.28	2.38	10.48	8.41	39.35	39.10
VI	0.30	2.86	24.18	16.43	40.03	16.20
VII	0.27	6.84	68.82	6.66	11.10	6.31
VIII	0.61	13.68	66.11	5.63	10.92	3.04
IX	1.98	1.77	4.39	5.70	13.33	56.85
X	1.60	1.44	5.49	20.54	9.95	60.97
XI	2.26	2.22	13.70	17.50	19.96	44.23
XII	4.54	1.88	7.27	17.16	26.91	42.23
XIII	3.71	5.65	7.43	12.50	34.08	36.63
XIV	5.00	4.15	6.05	10.64	21.10	53.06
XV	3.17	1.41	3.30	4.39	12.21	75.51
XVI	3.40	5.39	4.00	4.04	25.80	57.36
XVII	2.47	1.39	2.68	2.64	6.26	84.56
XVIII	3.55	4.41	8.15	8.23	8.10	67.55
XIX	6.72	8.13	6.07	4.64	7.73	66.66

5. IR Spectra.

The IR spectrum of theophylline alone was shown in Figure 25. The peak of theophylline at 2.90μ resulted from N-H stretching. The IR absorption bands at 5.86 and 5.98μ were resulted from C=O stretching. The peaks at 6.20 and 6.40μ were resulted from C=C and C=N stretching, respectively. The C-H bending was observed at 6.92μ . The peaks at 7.7 and 8.0μ resulted from C-N and C-O vibration, respectively.

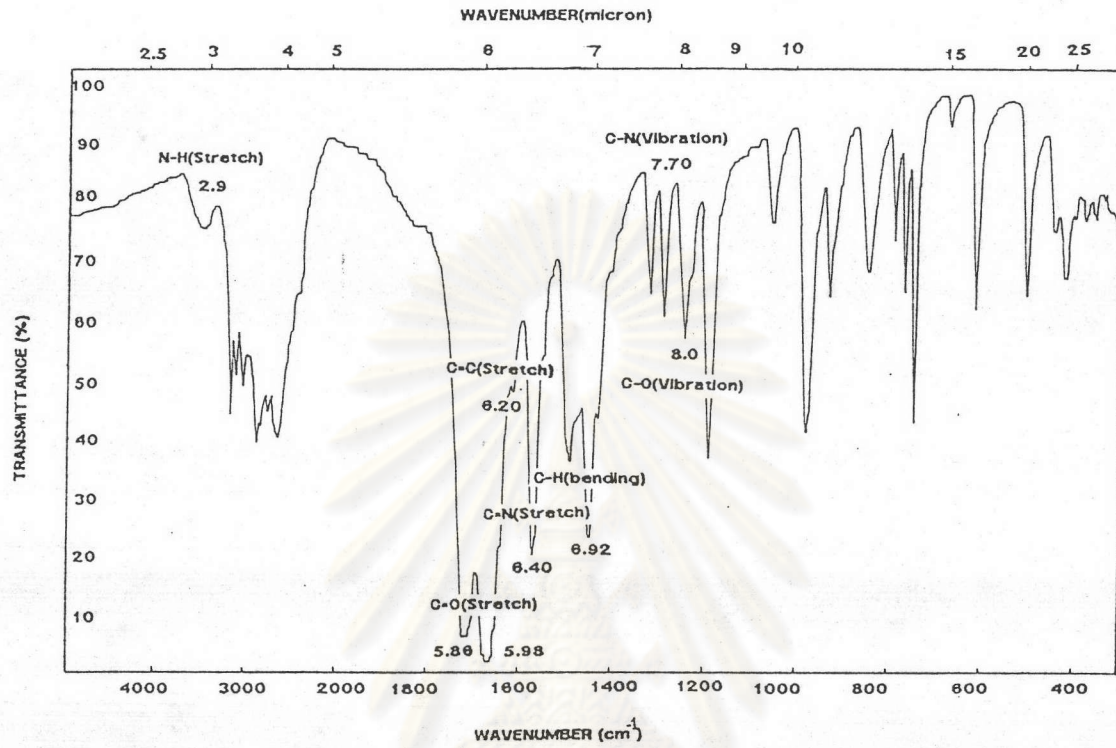


Figure 25. Infrared Spectrum of Theophylline

ศูนย์วิทยทรัพยากร
จุฬาลงกรณ์มหาวิทยาลัย

The co-spray dried powder of theophylline and ethylcellulose showed the spectra of theophylline and ethylcellulose as shown in Figure 26. The spectrum of ethylcellulose had a peak of carbonyl group that did not exist in the structure of ethylcellulose, however, the plasticizer of this latex dispersion was oleic acid that had a carbonyl group. The interaction between drug and ethylcellulose was scarce and the peak of spectra did not shifted. From this result, it could be concluded that these formulation were only simple mixing. The IR-spectra of co-spray dried powder of theophylline-HPMC were displayed in Figure 27. When comparison between theophylline and theophylline-HPMC, the peak at about 2.9μ or 3550 cm^{-1} was shifted slightly to high frequency and the peak intensity was stronger. This was affected by OH group of HPMC and indicated that it might have the diminutive interaction between drug and polymer. When concentration of HPMC was increased, this peak shifted slightly to low frequency and the peak intensity was weaker. This result might be due to the intramolecular H-bond of HPMC was broken down. The IR-spectra of co-spray dried powder of theophylline-HPMCP and of co-spray dried theophylline-ethylcellulose-PVP K30 were depicted in Figure 28 and 29, respectively. This revealed that no interaction or slight interaction occurred, it could be suggested that the co-spray dried theophylline-HPMCP and co-spray dried theophylline-ethylcellulose-PVP K30 were simple mixtures. The IR-spectra of co-spray dried powder of theophylline-ethylcellulose-lactose were depicted in Figure 31. The peak of free OH at 2.8μ or 3571 cm^{-1} in lactose spectrum as shown in Figure 30(Pouchert, 1975) disappeared. This result might be due to the H-bond between the three components.

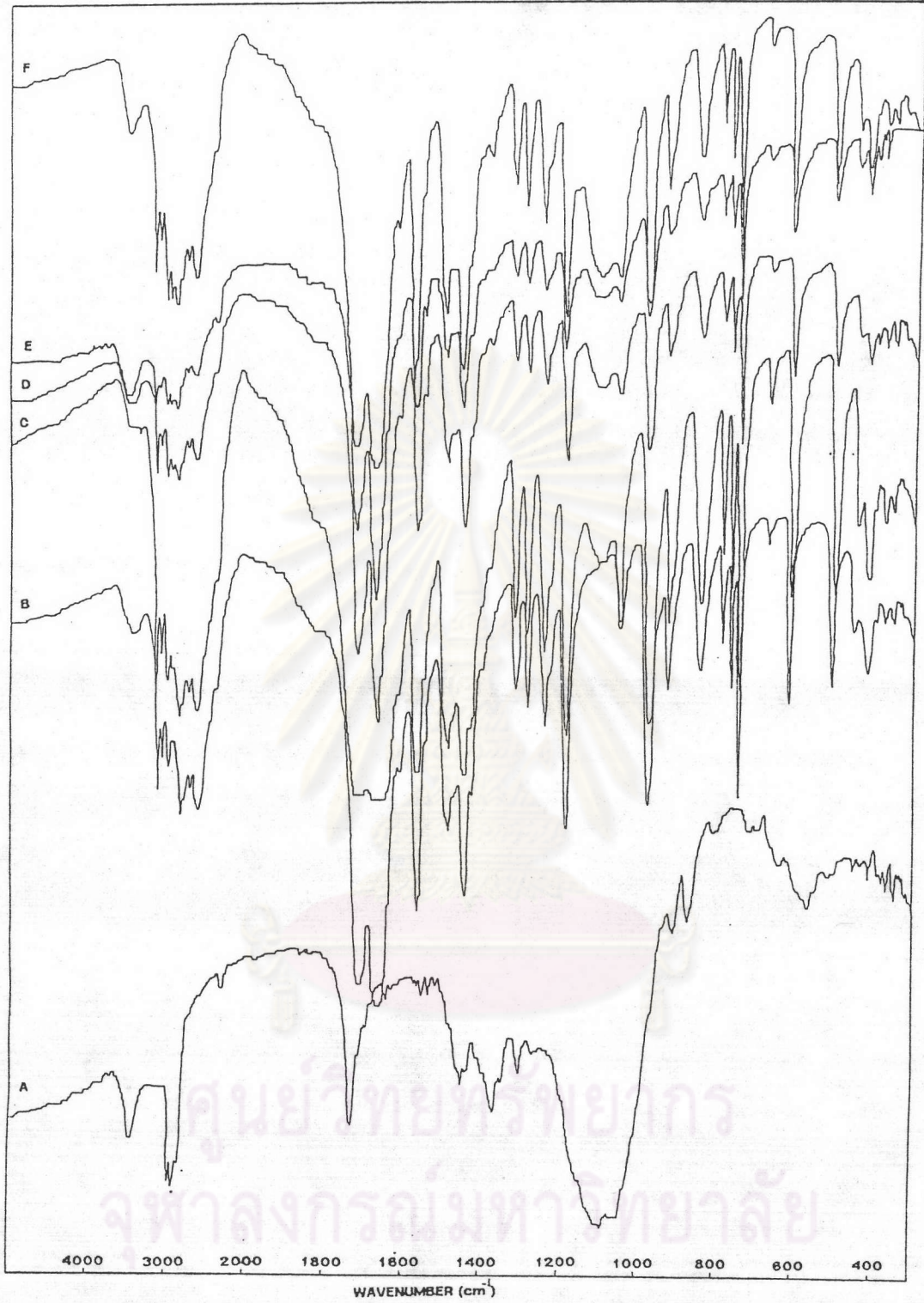


Figure 26. IR Spectra of Theophylline-Ethylcellulose Systems

- Key : A - Ethylcellulose
B - Theophylline
C - Theophylline-5%Ethylcellulose
D - Theophylline-10%Ethylcellulose
E - Theophylline-15%Ethylcellulose
F - Theophylline-20%Ethylcellulose

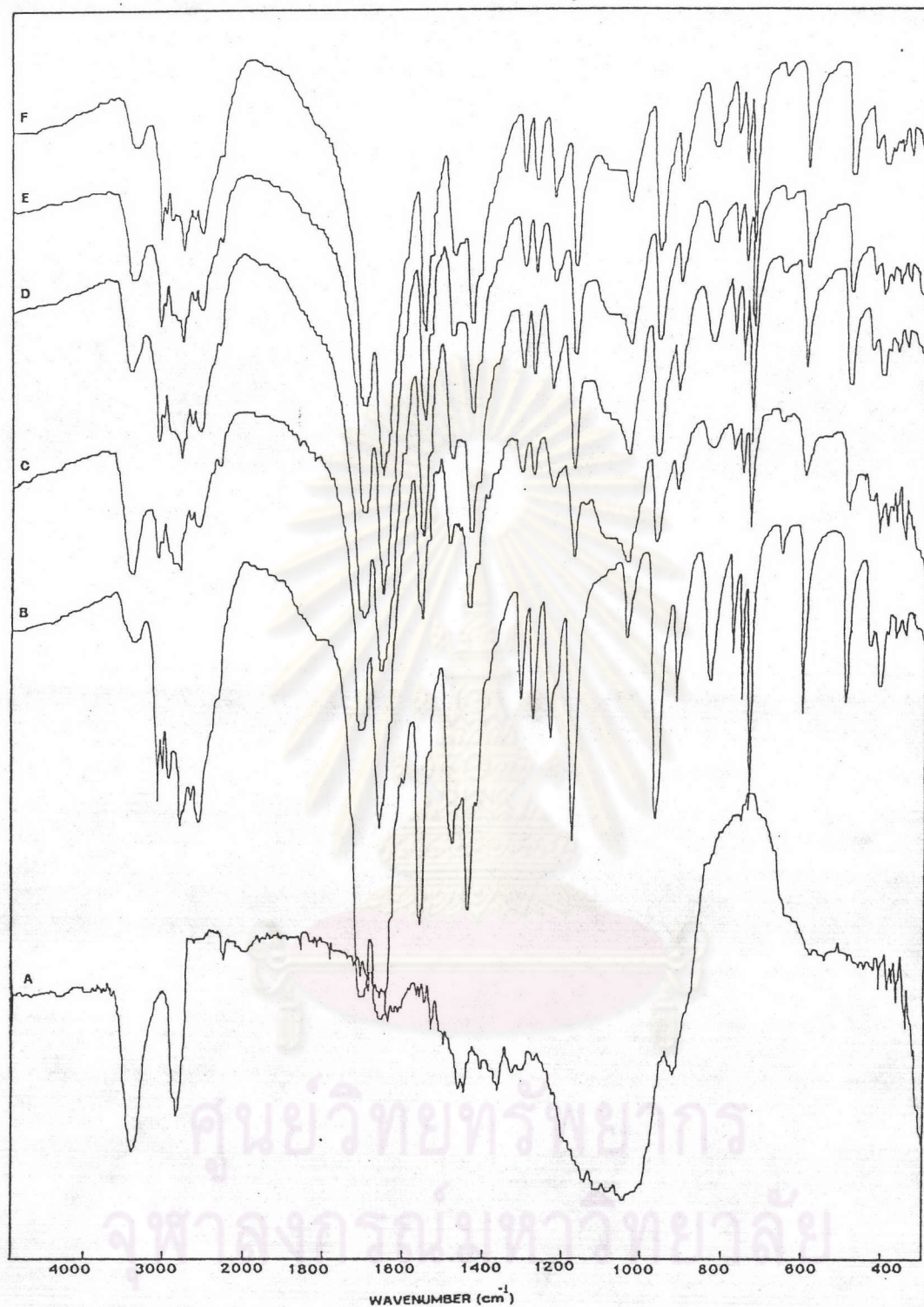


Figure 27. IR Spectra of Theophylline-HPMC Systems

Key : A - HPMC
B - Theophylline
C - Theophylline-5%HPMC
D - Theophylline-10%HPMC
E - Theophylline-15%HPMC
F - Theophylline-20%HPMC

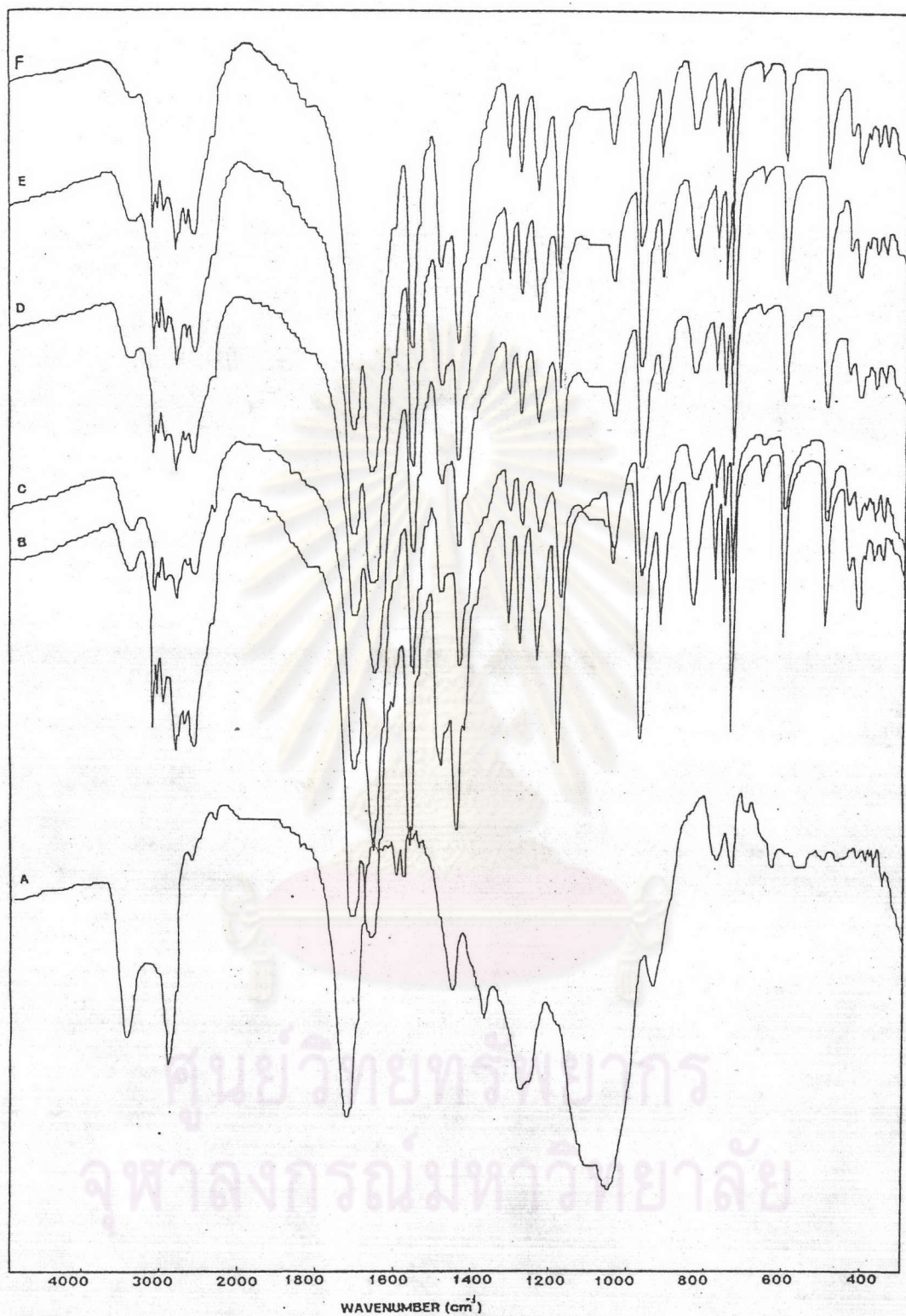


Figure 28. IR Spectra of Theophylline-HPMCP Systems

- Key : A - HPMCP
B - Theophylline
C - Theophylline-5%HPMCP
D - Theophylline-10%HPMCP
E - Theophylline-15%HPMCP
F - Theophylline-20%HPMCP

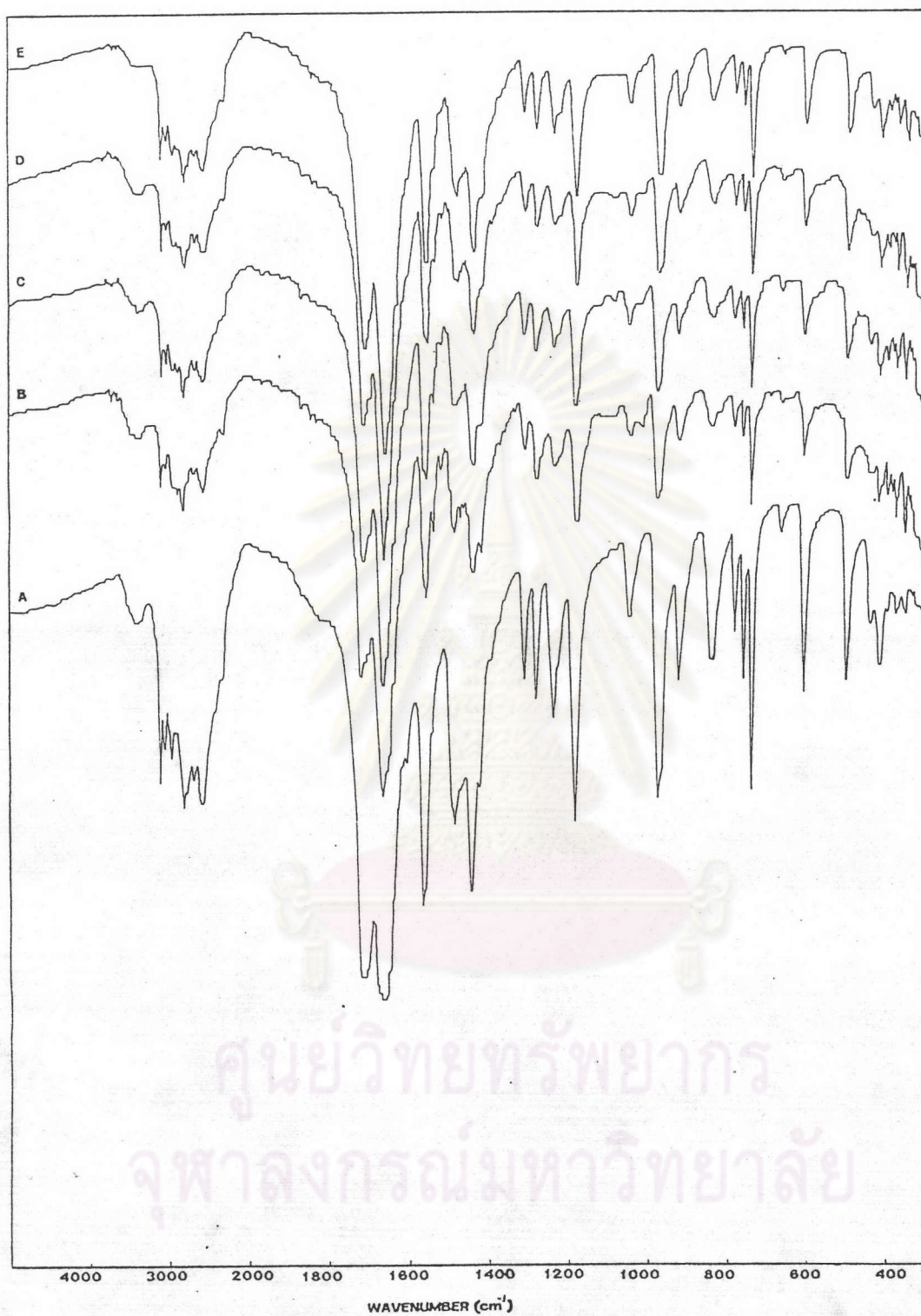


Figure 29. IR Spectra of Theophylline-Ethylcellulose-PVP K30 Systems

- Key : A - Theophylline
B - Theophylline-1%Ethylcellulose-10%PVP K30
C - Theophylline-1%Ethylcellulose-20%PVP K30
D - Theophylline-5%Ethylcellulose-10%PVP K30
E - Theophylline-5%Ethylcellulose-5%PVP K30

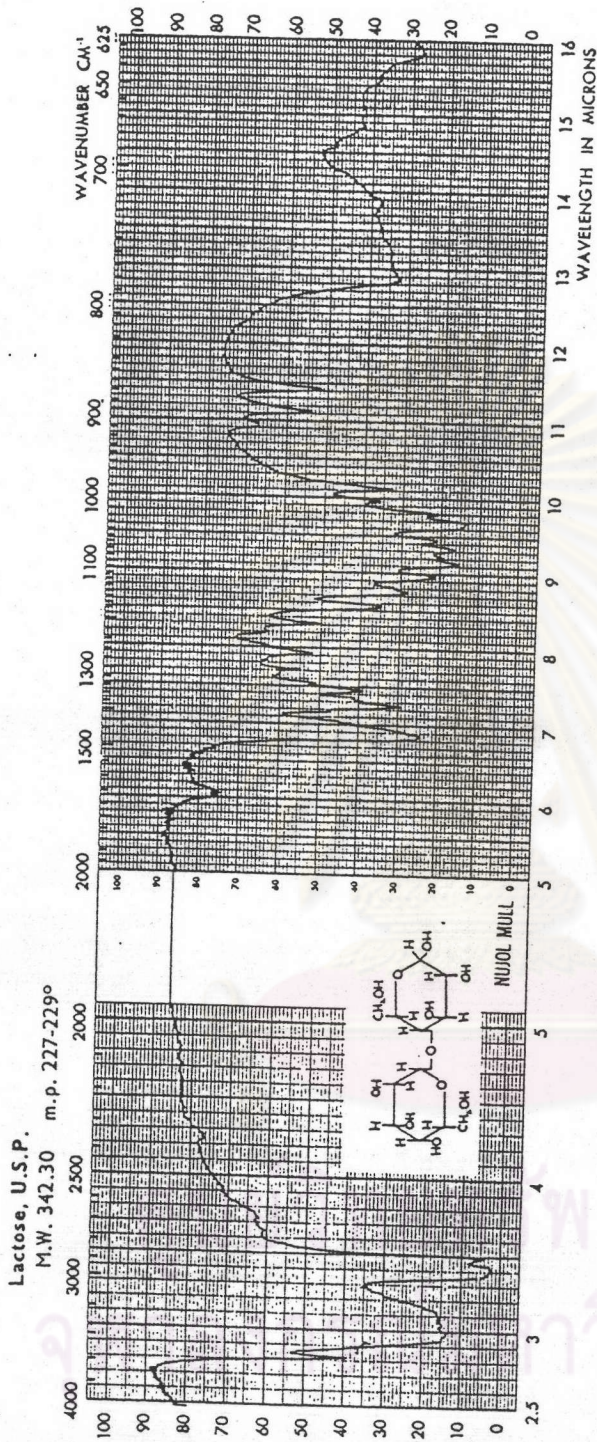


Figure 30. Infrared Spectrum of Lactose

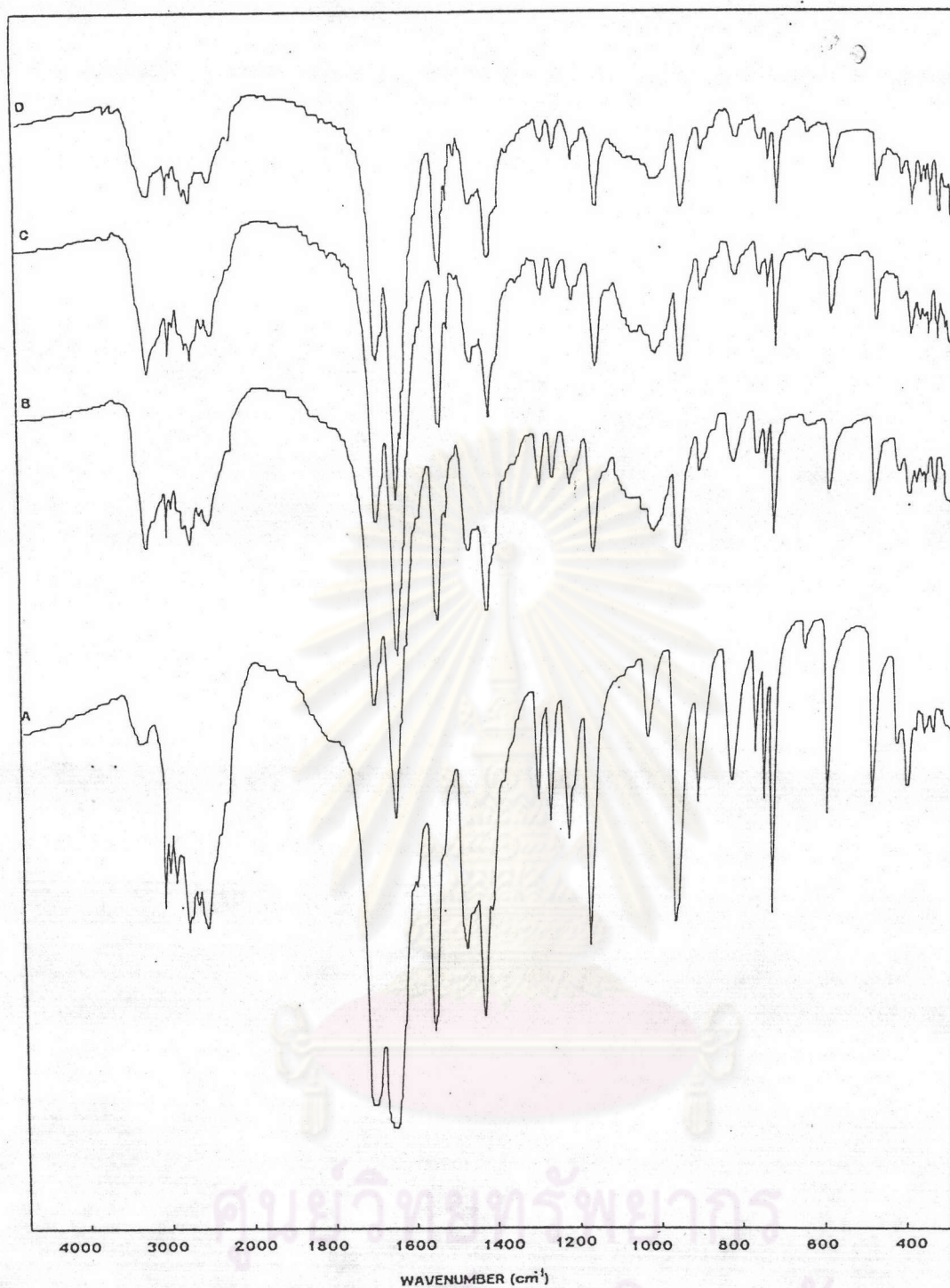


Figure 31. IR Spectra of Theophylline-Ethylcellulose-Lactose Systems

Key : A - Theophylline

B - Theophylline-3%Ethylcellulose-25%Lactose

C - Theophylline-5%Ethylcellulose-25%Lactose

D - Theophylline-5%Ethylcellulose-15%Lactose

6. Thermogram.

Thermograms of theophylline alone, co-spray dried of theophylline and various polymers and channeling agent were shown in Figure 32. The thermogram of pure theophylline gave the characteristic melting endotherm at 268 °C and at 335 °C. While in theophylline -5%ethylcellulose(Formulation I) and theophylline-20% ethylcellulose(Formulation IV) had an exothermic peak at 198 °C and exhibited the characteristic melting endotherm of theophylline. Theophylline-HPMC(Formulation V and VIII) and theophylline-HPMCP (Formulation IX and XII) had endothermic peaks rather same as pure theophylline. No change was observed in thermal analytical profiles indicating absence of any interaction between theophylline and HPMCP. Theophylline-3%ethylcellulose-25%lactose(Formulation XIX) had not exothermic peak of ethylcellulose at 198 °C, but it had endothermic peaks at 59 °C and 203 °C and exhibited the characteristic melting endothermic of theophylline with slightly shifted to 257 °C. This might be due to the interaction between the three components.

7. X-ray Powder Diffraction.

The X-ray diffraction patterns of theophylline and theophylline-ethylcellulose(Formulation I and IV) were shown in Figure 33. The diffraction of the original drug showed sharp peaks. No difference was observed between theophylline alone and co-spray dried theophylline-ethylcellulose. The X-ray diffraction patterns of theophylline and theophylline-HPMC (Formulation V and VIII) were shown in Figure 34. In the co-spray dried theophylline-5%HPMC, some of theophylline was in the form of amorphous. But in the case of co-

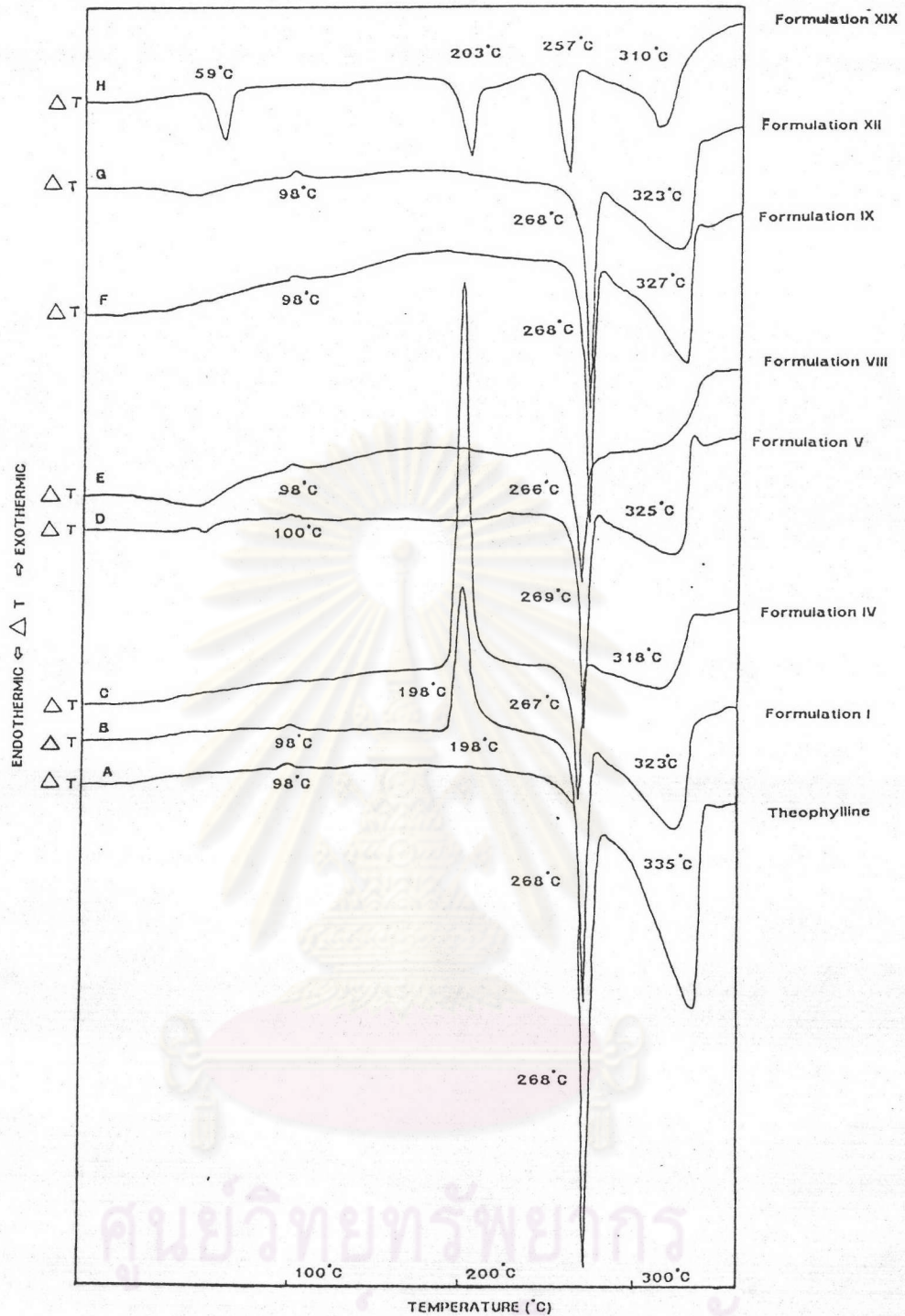


Figure 32. DTA Thermograms of Theophylline, Theophylline-Polymer and Theophylline-Polymer-Channeling Agent

- Key :
- A - Theophylline
 - B - Theophylline-5%Ethylcellulose
 - C - Theophylline-20%Ethylcellulose
 - D - Theophylline-5%HPMC
 - E - Theophylline-20%HPMC
 - F - Theophylline-5%HPMCP
 - G - Theophylline-20%HPMCP
 - H - Theophylline-3%Ethylcellulose-25%Lactose

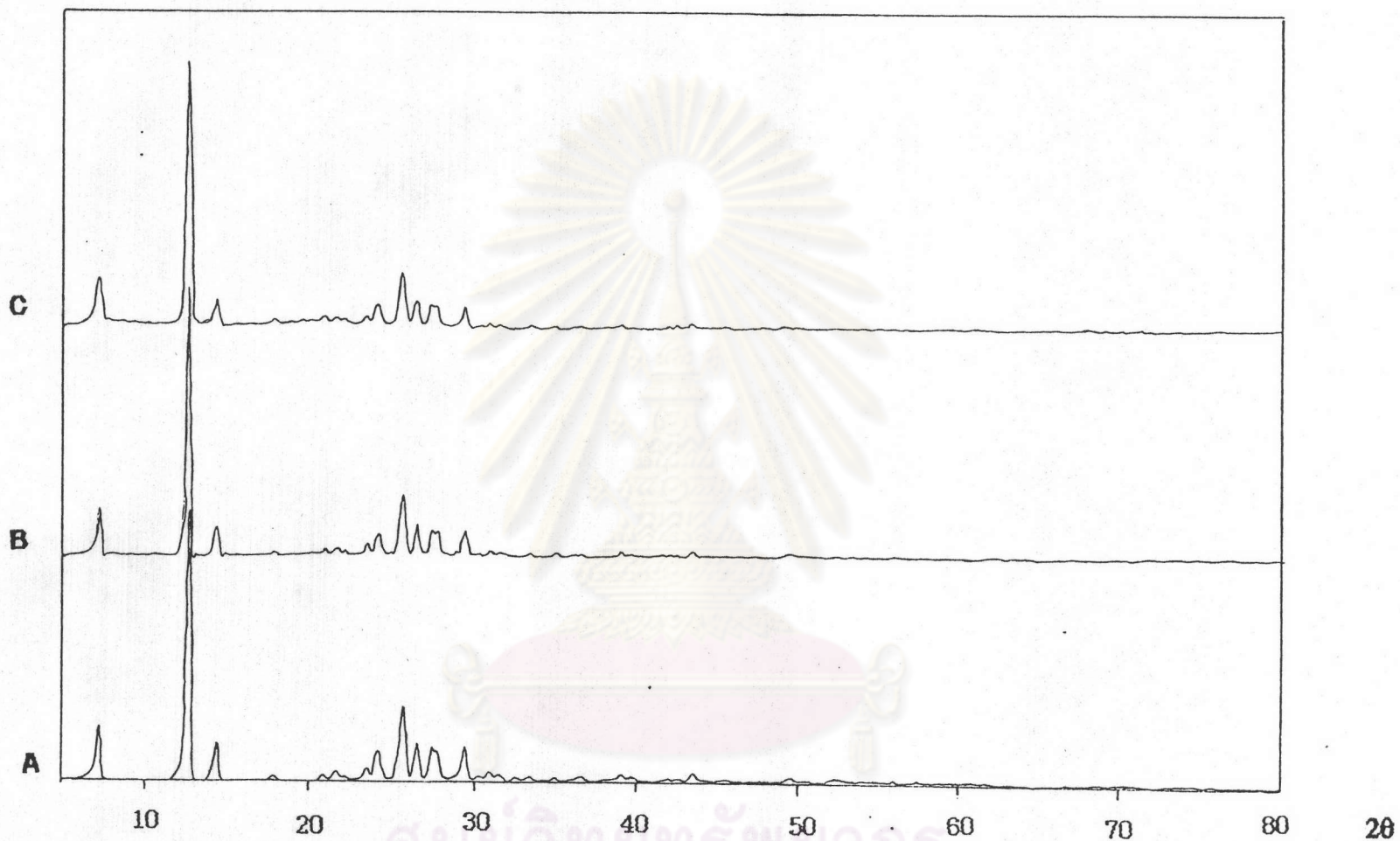


Figure 33. X-ray Diffraction Spectra of Theophylline and Theophylline-Ethylcellulose Systems

Key : A - Theophylline
 B - Theophylline-5%Ethylcellulose
 C - Theophylline-20%Ethylcellulose

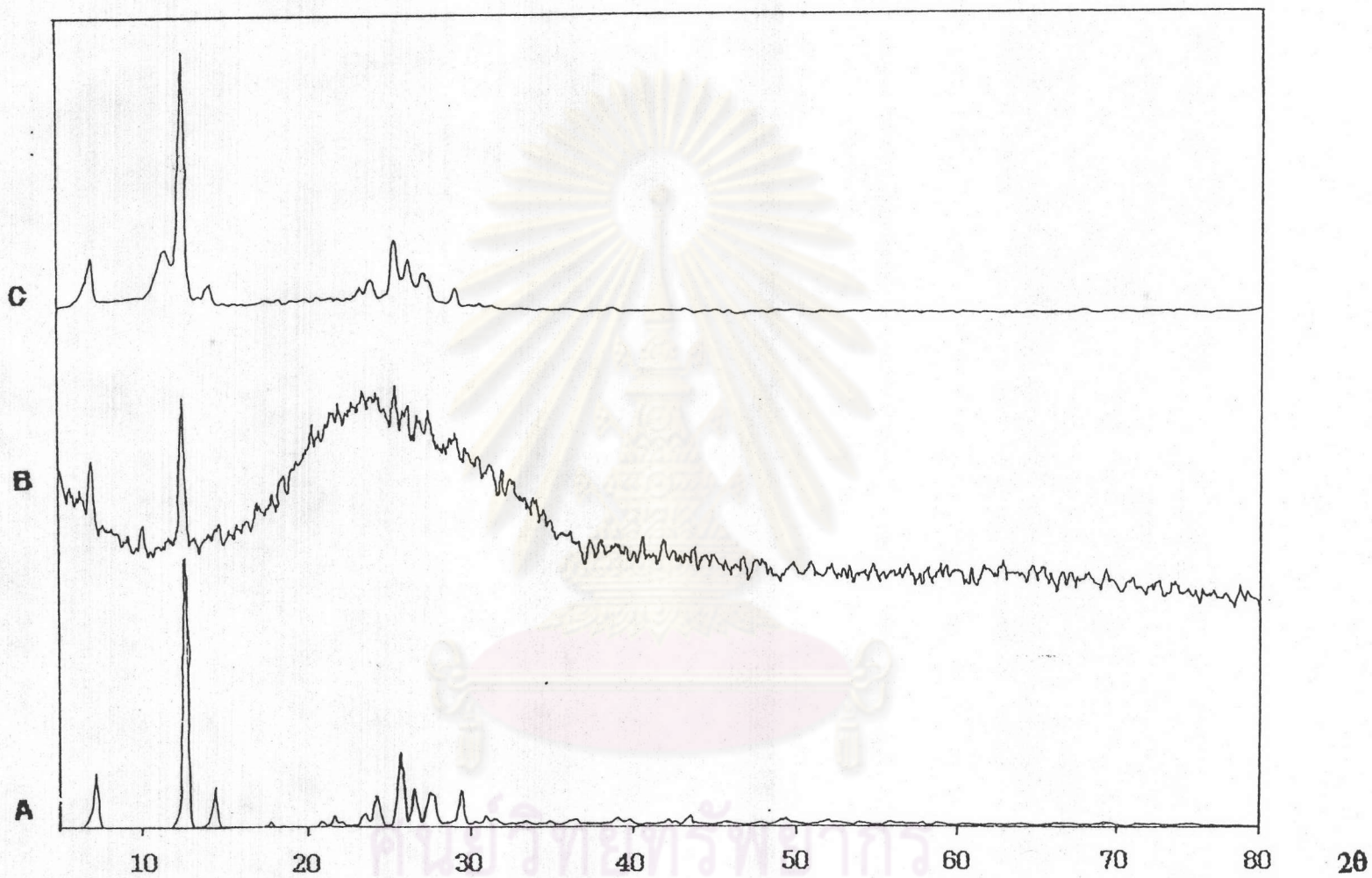



Figure 34. X-ray Diffraction Spectra of Theophylline and Theophylline-HPMC System

Key : A - Theophylline
 B - Theophylline-5%HPMC
 C - Theophylline-20%HPMC

spray dried theophylline-20%HPMC, theophylline was in the form of crystal. The X-ray diffraction patterns of theophylline and theophylline-HPMCP (Formulation IX and XII) were shown in Figure 35. The X-ray diffraction spectra of theophylline alone and theophylline-HPMCP showed identically. The X-ray diffraction patterns of theophylline and theophylline-ethylcellulose-lactose (Formulation XIX) were shown in Figure 36. This spectra of co-spray dried of theophylline-ethylcellulose-lactose showed the peak that identical to theophylline crystal.



ศูนย์วิทยทรัพยากร
จุฬาลงกรณ์มหาวิทยาลัย

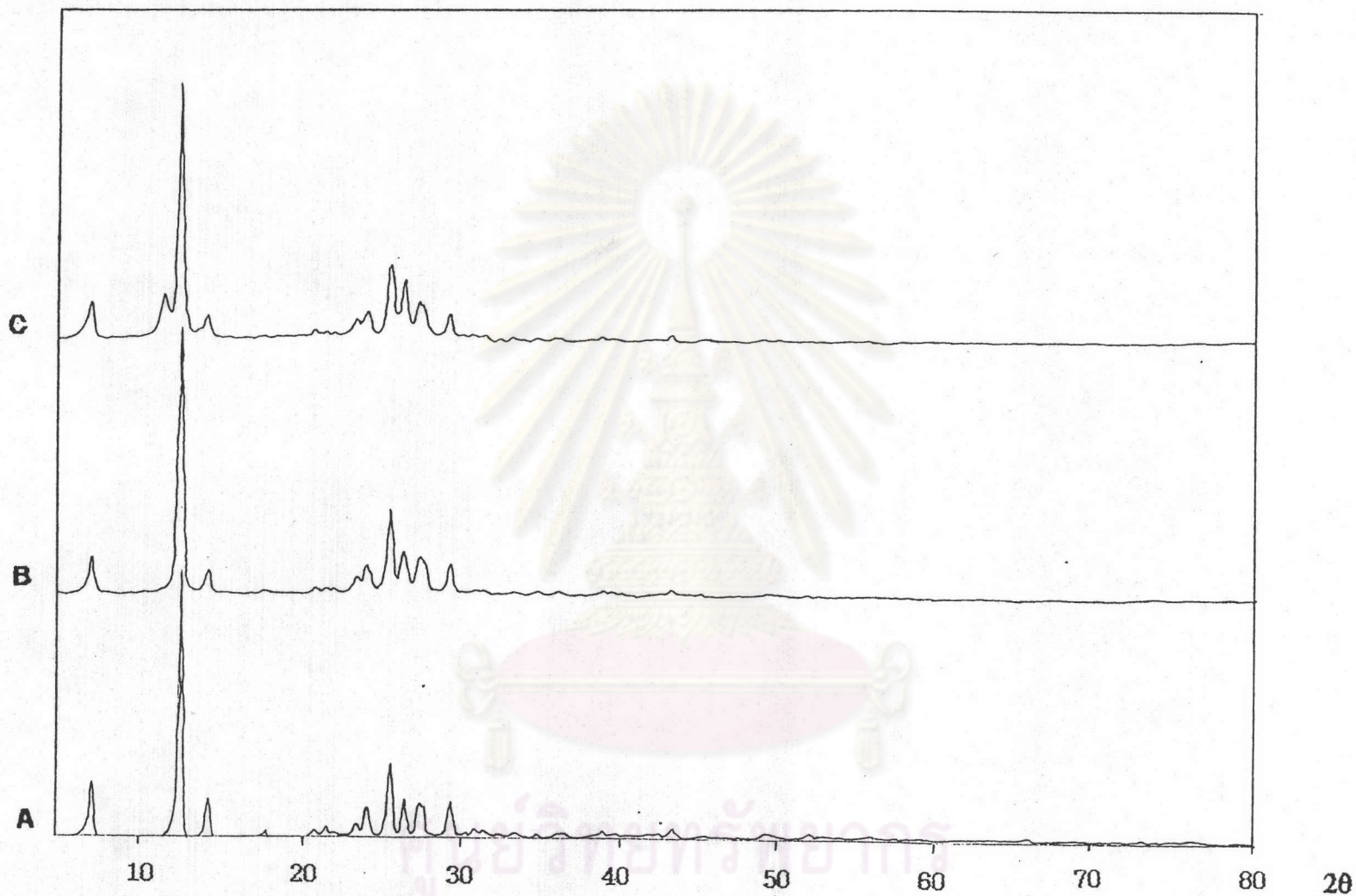


Figure 35. X-ray Diffraction Spectra of Theophylline and Theophylline-HPMCP Systems

Key : A - Theophylline
 B - Theophylline-5%HPMCP
 C - Theophylline-20%HPMCP

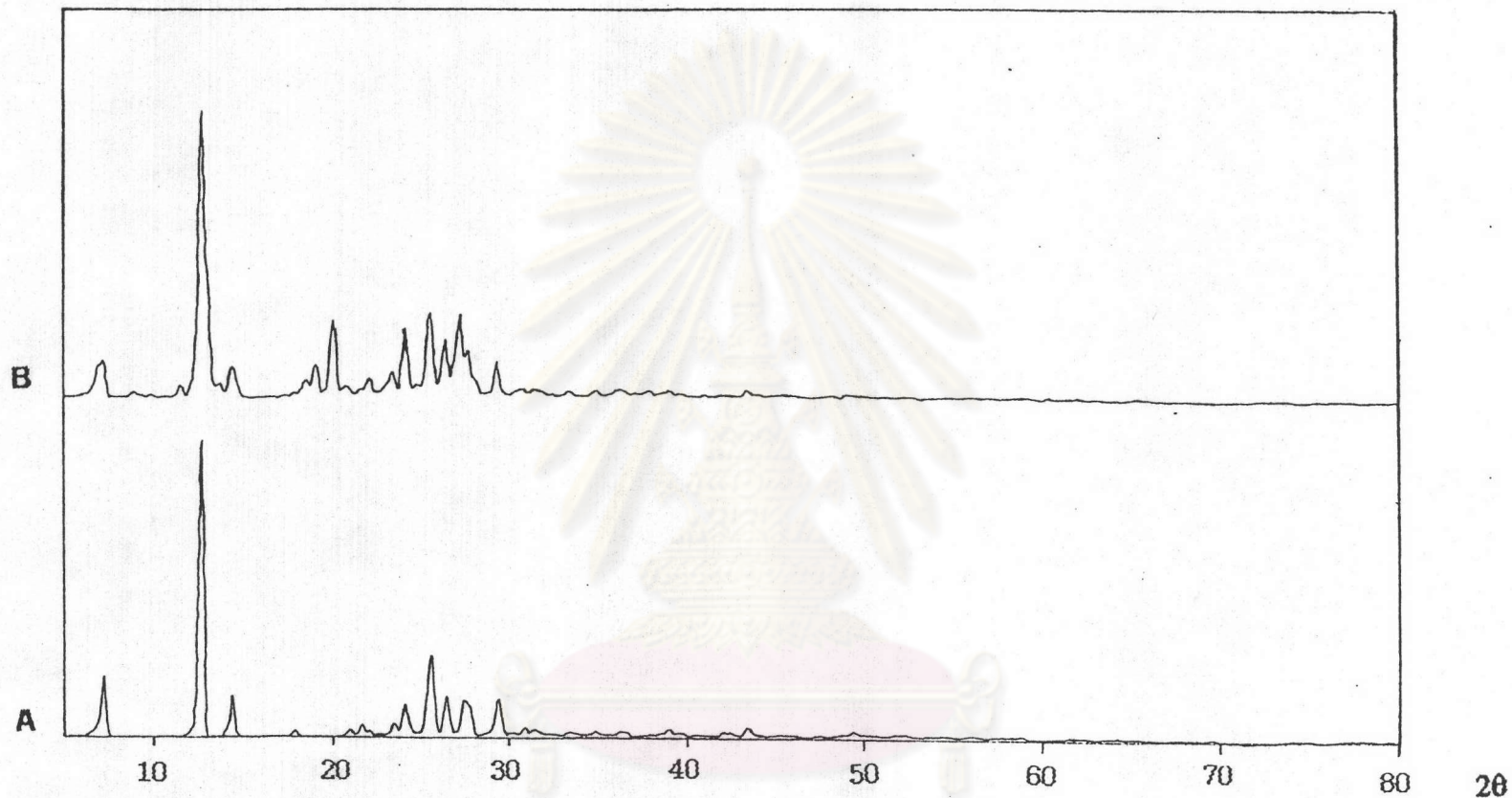


Figure 36. X-ray Diffraction Spectra of Theophylline and Theophylline-Ethycellulose-Lactose System
 Key : A - Theophylline
 B - Theophylline-3%Ethylcellulose-25%Lactose

The Evaluation of the Matrix.

1. Thickness of Matrices

Although the thickness of matrix tablet was not official in quality control of tablet, but the uniformity of tablet thickness could predict the uniformity of compressional force. The mean and standard deviation of tablet thickness were presented in Table 18. The standard deviation obtained were not exceed ± 0.02 for all tested matrices.

2. Matrix Tablet Hardness

The mean and standard deviation of tablet hardness were displayed in Table 18. Figure 37 depicted the relationship between polymer concentration and tablet hardness. Generally, it was found that the increase in polymer concentration caused increase in hardness values except of HPMCF matrices, a little increase of hardness was observed. The increase in lactose caused decrease in hardness values as in Formulation XVII and XVIII.

3. Disintegration Study

Most of the preparations had disintegration time that was longer than two hours. But Formulation X-XII and Formulation XVI had disintegration time that was shorter than two hours. Among three commercial products, only Theodur^(R) had disintegration time that was longer than two hours. All detail data were presented in the Table 18.

Table 18. Physical properties of the commercial products and the matrices prepared from various polymers and concentrations.

Formulation	Physical Properties of Matrices		
	Thickness* [mm±(SD)]	Hardness* [Kp±(SD)]	Disintegration time** [minut±(SD)]
I	4.14(0.01)	10.67(0.63)	>120
II	4.24(0.01)	12.89(0.66)	>120
III	4.43(0.01)	15.34(0.50)	>120
IV	4.78(0.01)	16.94(0.50)	>120
V	4.77(0.01)	9.59(0.26)	>120
VI	4.99(0.01)	12.70(1.27)	>120
VII	5.97(0.02)	>20	>120
VIII	6.45(0.01)	>20	>120
IX	4.74(0.02)	8.07(0.74)	>120
X	5.00(0.02)	8.87(1.01)	80(7)
XI	5.37(0.02)	9.14(0.54)	64(5)
XII	5.47(0.02)	9.18(0.78)	73(12)
XIII	4.33(0.01)	10.91(0.95)	>120
XIV	4.61(0.01)	15.79(2.58)	>120
XV	4.65(0.01)	13.10(1.37)	>120
XVI	5.18(0.01)	10.30(3.37)	86(7)
XVII	4.97(0.02)	12.60(1.24)	>120
XVIII	5.45(0.01)	10.44(0.98)	>120
XIX	5.53(0.01)	9.95(1.20)	>120
Nuelin ^(R)	4.69(0.01)	4.30(0.39)	77(7)
Quibron ^(R)	2.43(0.01)	>20	71(5)
Theodur ^(R)	6.54(0.05)	12.38(0.94)	>120

* = Averaged from ten determinations

** = Averaged from six determinations

จุฬาลงกรณ์มหาวิทยาลัย

HARDNESS

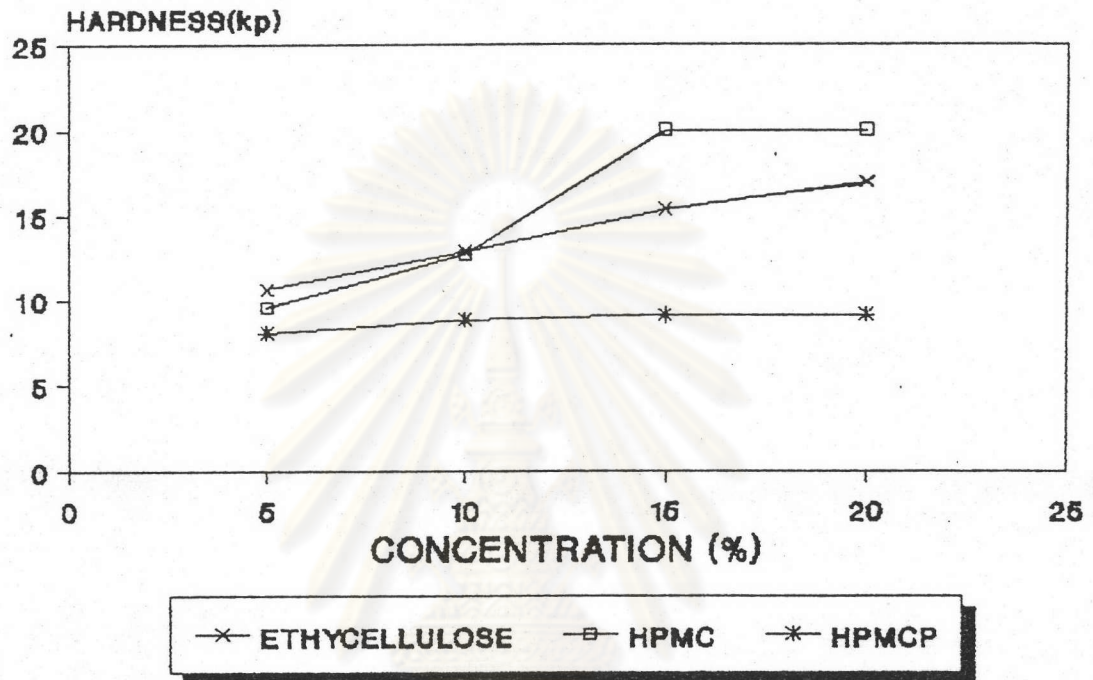


Figure 37 The Hardness Profiles of Three Polymers Matrices.

ศูนย์วิทยทรัพยากร
จุฬาลงกรณ์มหาวิทยาลัย

4. Dissolution Study

4.1 Dissolution Profiles and Release Rate Profiles

From the experimental data, the dissolution or the release profiles could be plotted between amount percent of drug release against time. Then, the change of release rate profile was constructed from the dissolution profile to elucidate the release rate at various time interval during the course of drug dissolution from the matrices. The dissolution and release rate profiles of each formulation were described in Table 33-54(Appendix E).

The release rate was calculated by dividing the different of percent drug release at various time interval with the time utilized to release that certain amount of the drug(see data in Table 41-54, Appendix E). The rate, then, was plotted with the average time interval. It was shown that the rate of release decreased with the time.

4.1.1 The Blank Theophylline Matrix

Theophylline itself could be compressed and the influence of dissolution medium on theophylline release and release rate at various time intervals from this blank matrix were depicted in Figure 38-39. The release rate of theophylline in 0.1 N. HCl was faster than in phosphate buffer pH 6.8 as illustrated in Figure 38. This result indicated that theophylline may be more soluble in 0.1 N. HCl than in phosphate buffer pH 6.8. In 0.1 N. HCl and in phosphate buffer pH 6.8, the entire matrix dissolved in approximately five and six hours, respectively. The release rate

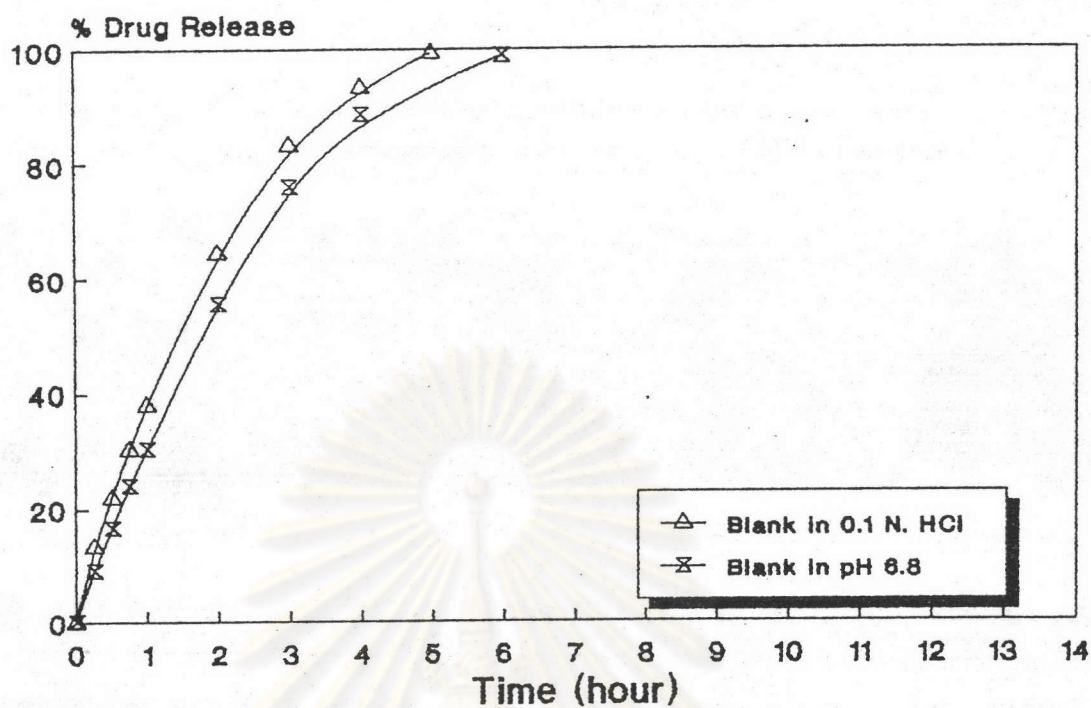


Figure 38. The Release Profiles of Theophylline Matrices without Additives

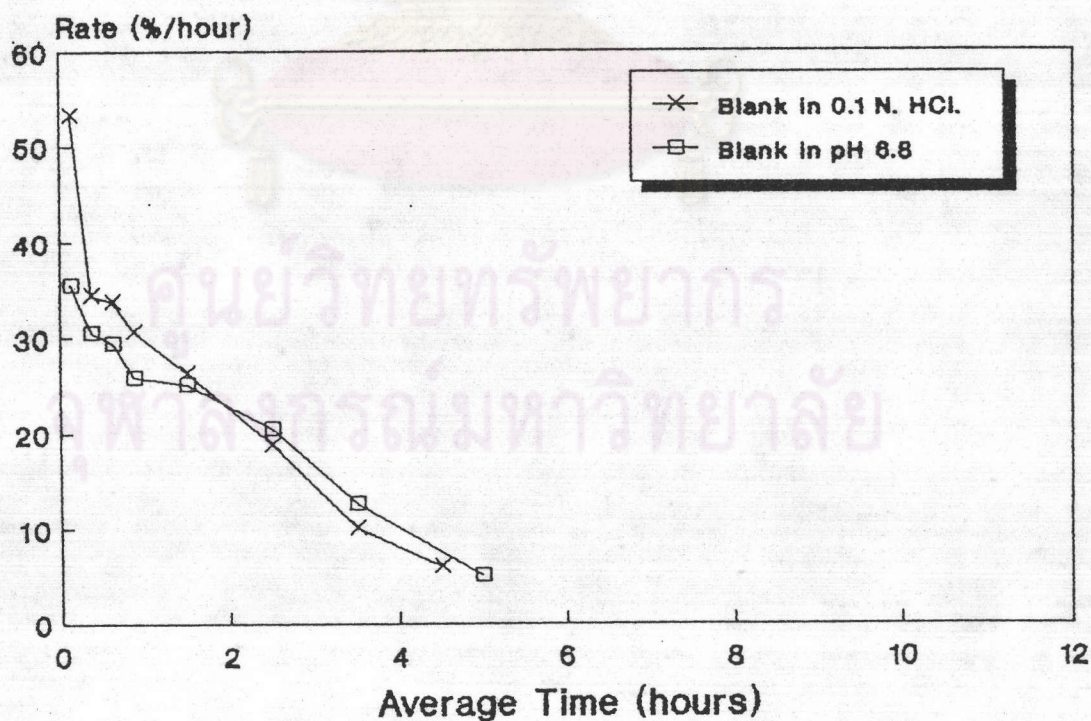


Figure 39. The Release Rate Profiles of Theophylline Matrices without Additives

profile was shown in Figure 39, this release rate was faster than other theophylline-polymer matrices.

4.1.2 The Formulations I-IV Matrices

The dissolution profiles of theophylline from theophylline-ethylcellulose matrices with various ethylcellulose ratios in 0.1 N. HCl and phosphate buffer pH 6.8 were shown in Figure 40 (Table 34, Appendix E). Each point represents the average value obtained from three determinations at the given sampling time. The convex curves were turned to the X axis. The release rate was decreased with time as shown in Figure 41 and this might be due to an increase in diffusional path length for the drug.

Increasing the weight fraction of ethylcellulose resulted in a corresponding decrease of the dissolution rate. The concentration of ethylcellulose in the formulation was the determining factor in controlling release rate of drug.

The release of drug from this matrices containing various levels of ethylcellulose were affected by dissolution medium as shown in Figures 40(A) and 40(B). The amount of theophylline released in 0.1 N.HCl was higher than in phosphate buffer pH 6.8. This result may be affected by an increase in theophylline solubility as previous mentioned in section 4.1.1.

4.1.3 The Formulations V-VIII Matrices

These matrices hydrated quickly and formed a protective gelatinous layer. Both diffusion and erosion could be

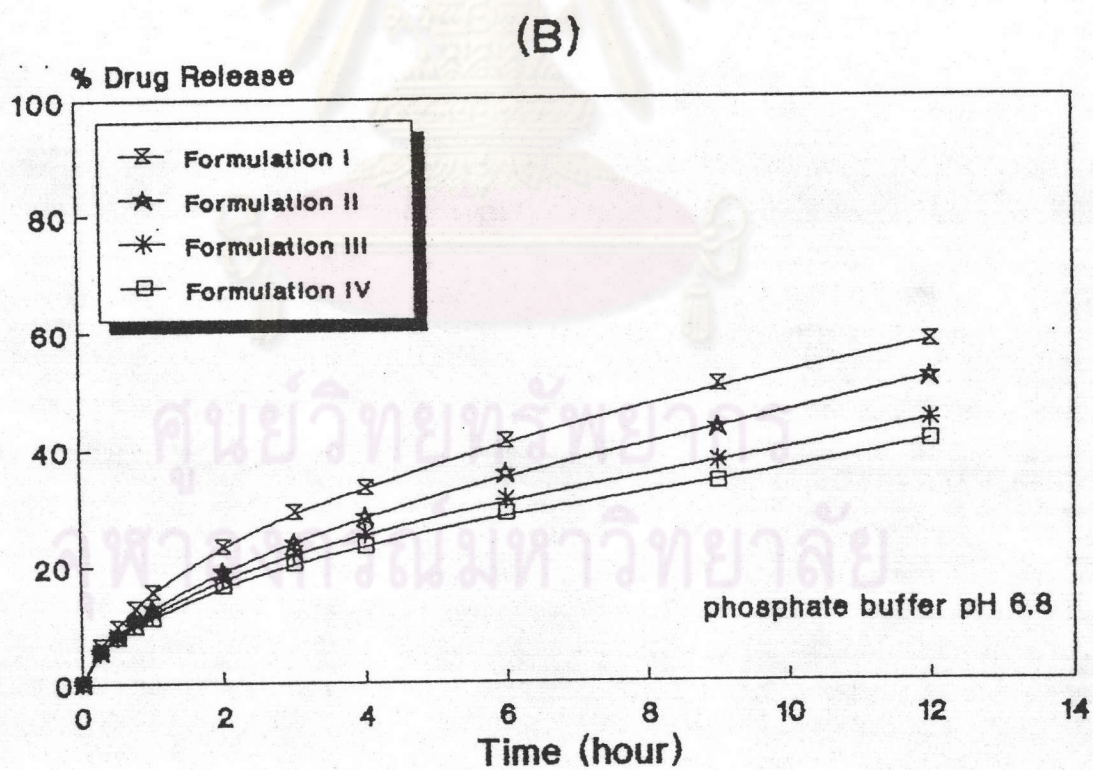
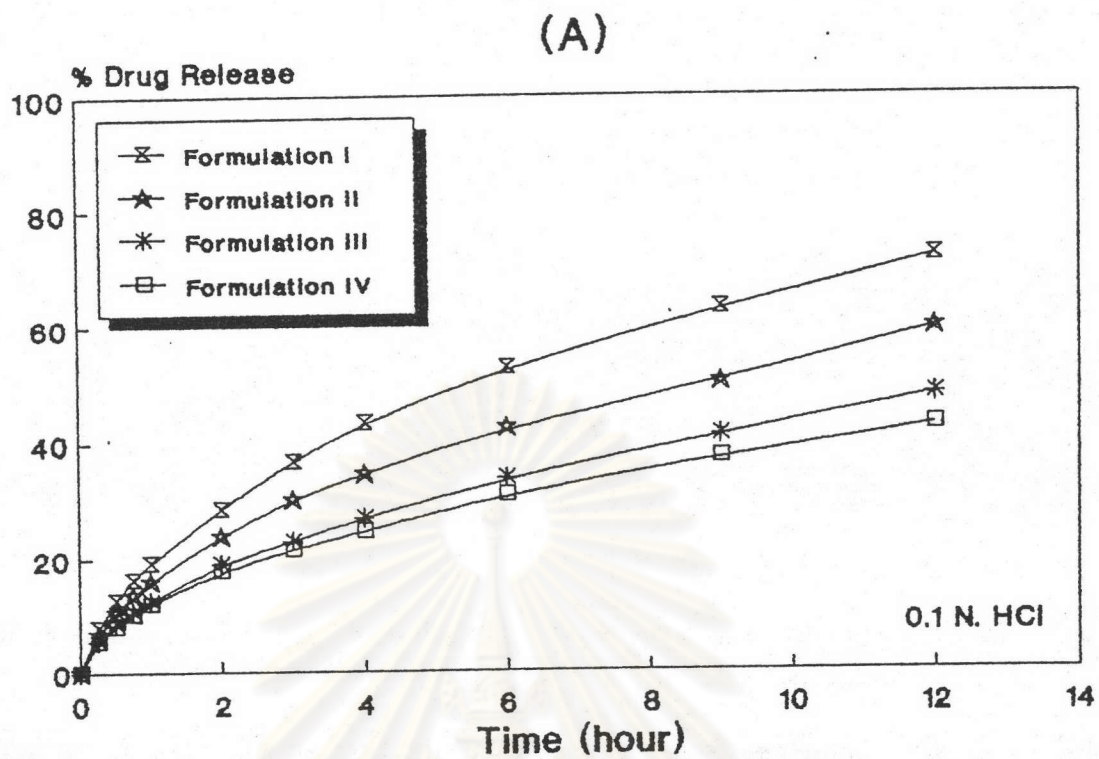


Figure 40. The Release Profiles of Theophylline-Ethylcellulose Matrices in
 A) 0.1 N.HCl
 B) Buffer pH 6.8

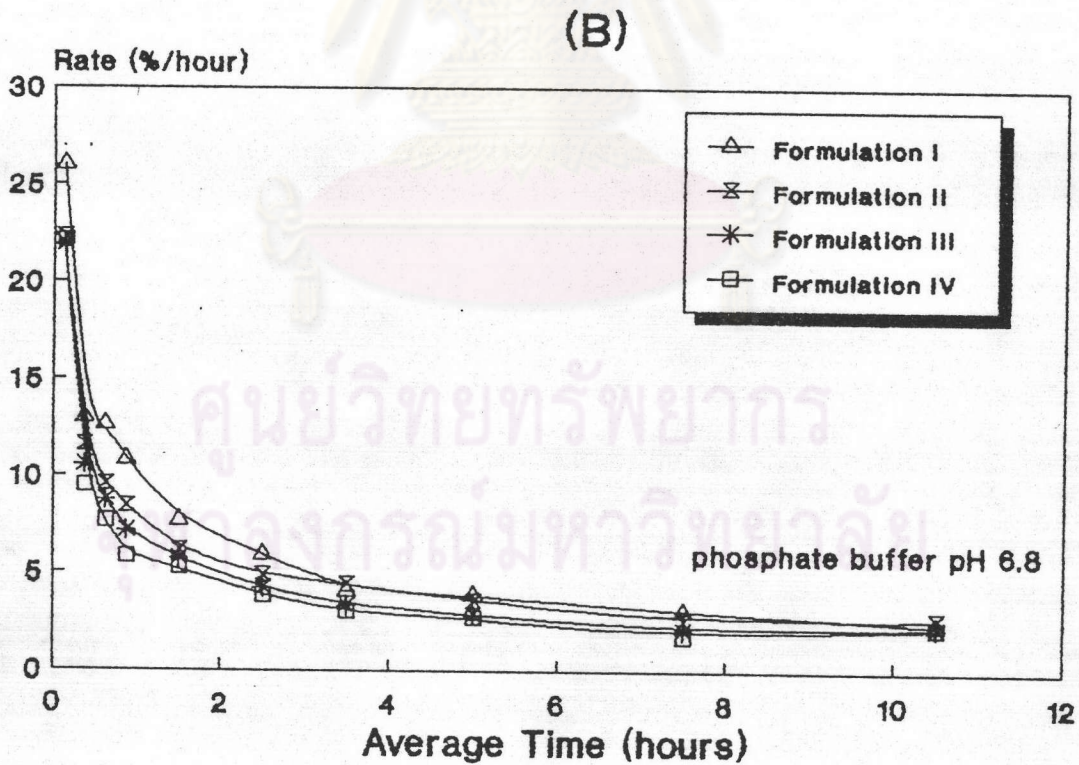
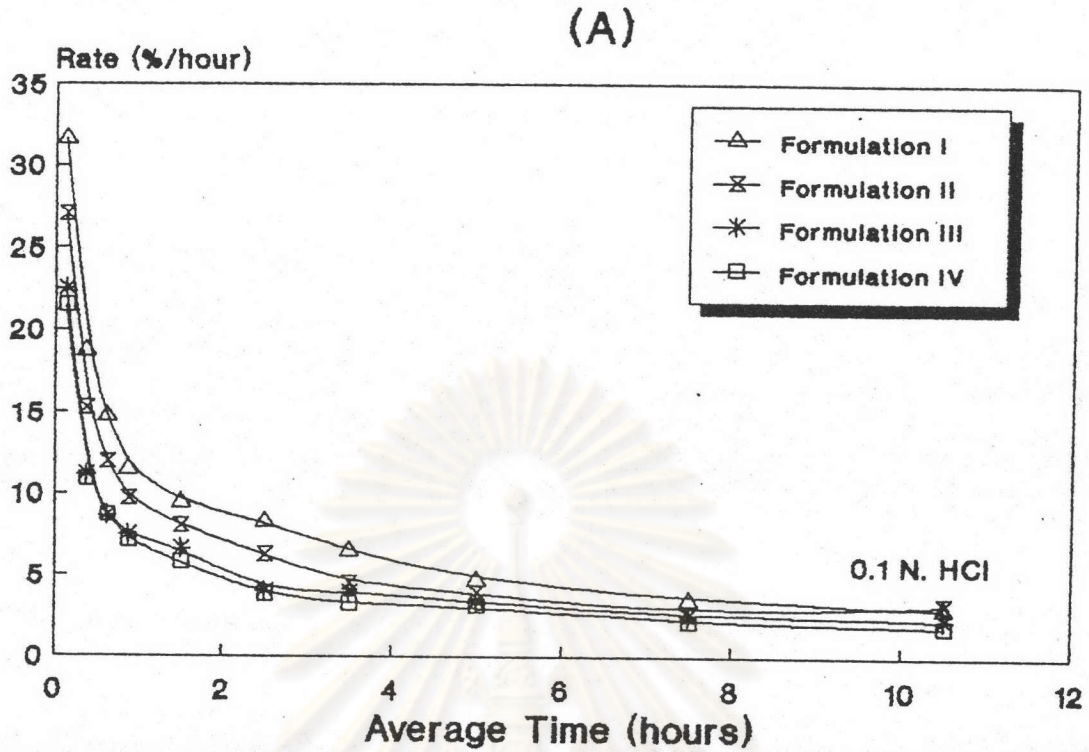


Figure 41. The Release Rate Profiles of Theophylline-Ethylcellulose Matrices in
 A) 0.1 N.HCl
 B) Buffer pH 6.8

important in controlling the release of drug from a hydrophilic matrices. But this gel-matrix had good durability, soluble drug may diffuse out of the gel before erosion occurred.

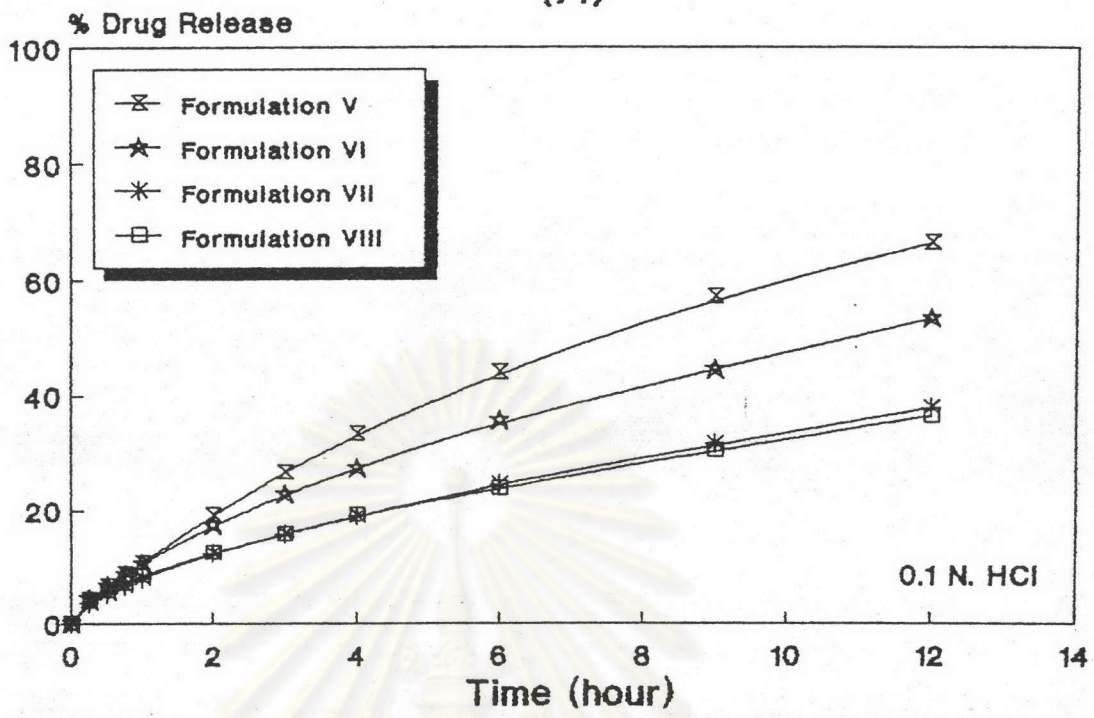
The release of theophylline from matrices containing all levels of HPMC were affected by dissolution medium as displayed in Figure 42. The dissolution medium affected the release rate but did not affect the pattern of drug release. The release rate of these formulations decrease with the time increase as shown in Figure 43 and this may be due to an increase in diffusional path length for drug which in turn may be due to slower erosion rate of the rubbery layer (gel at the tablet periphery) and faster advancement of swelling front into the glassy polymer. The release rate in 0.1 N.HCl was faster than the release rate in buffer pH 6.8.

The higher HPMC ratios affected the slower release rate of drug. As the concentration of HPMC was increased in the matrix tablet, the resulting was gelatinous diffusion more than erosion. Therefore, increase in HPMC concentration would generally reduced drug release.

4.1.4 The Formulations IX-XII Matrices

The theophylline-HPMCP matrix was ruptured but did not disintegrate into particle during dissolution studied in 0.1 N.HCl. However it was completely dissolved within 5 hours in buffer pH 6.8. Thus, these formulations would be evaluated in two parts.

(A)



(B)

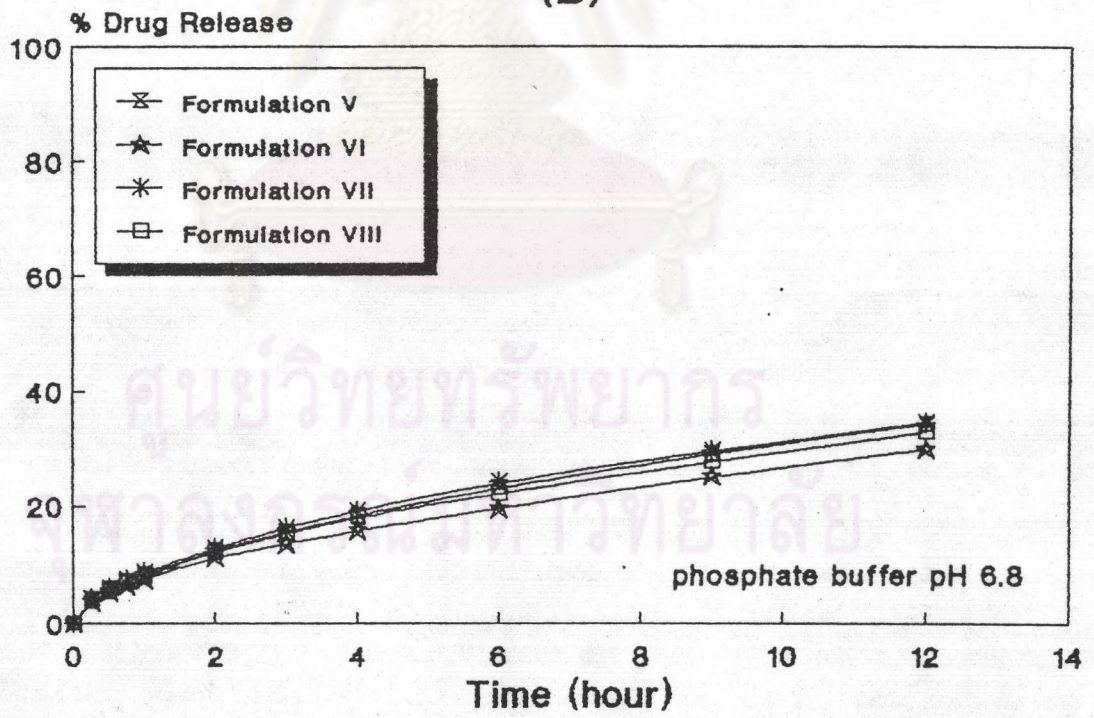


Figure 42. The Release Profiles of Theophylline-HPMC Matrices in
A) 0.1 N.HCl
B) Buffer pH 6.8

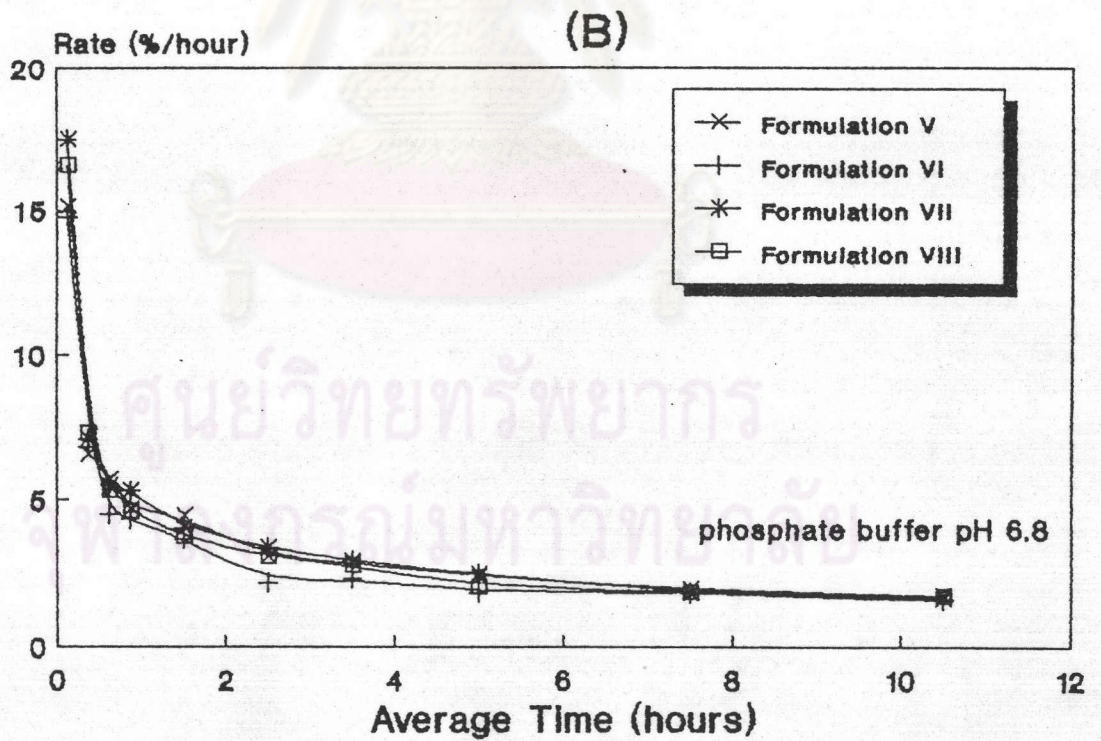
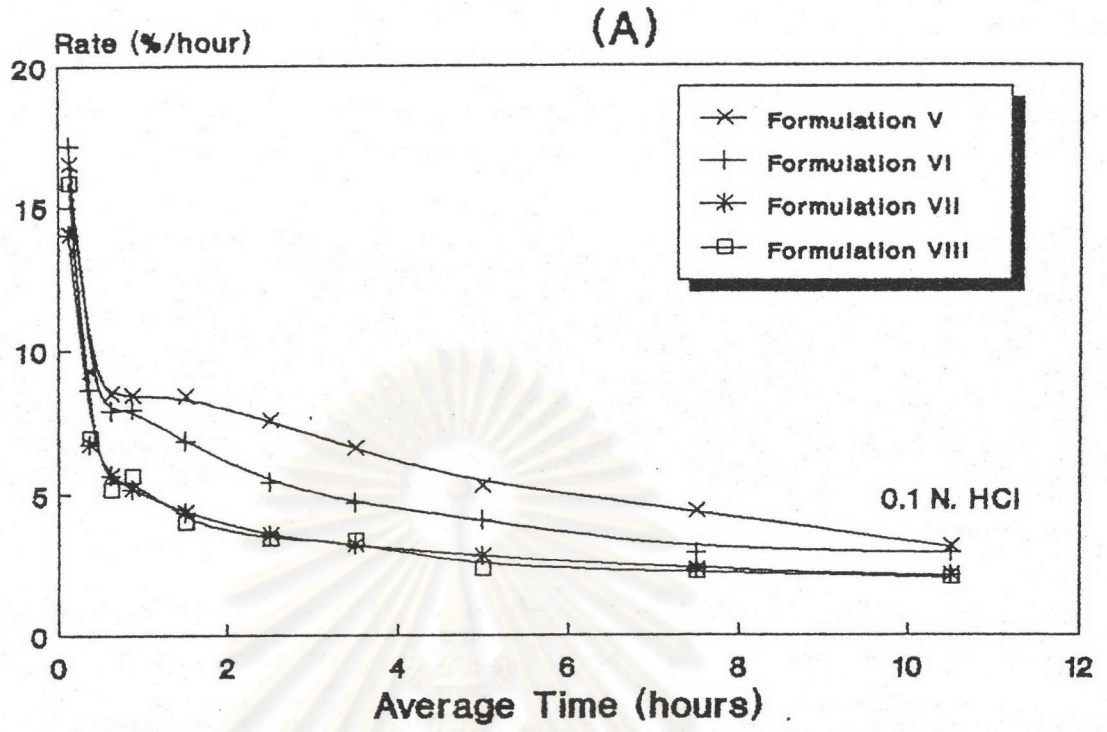


Figure 43. The Release Rate Profiles of Theophylline-HPMC Matrices in
A) 0.1 N.HCl
B) Buffer pH 6.8

In 0.1 N.HCl, the dissolution profiles of theophylline from theophylline-HPMCP matrices with various HPMCP ratios were shown in Figure 44(A)(data in Table 36, Appendix E). The highest amount of theophylline in 12 hours obtained from formulation X that had 10% w/w of HPMCP. The release rate of this formulation also faster than others as shown in Figure 45(A)(data in Table 46, Appendix E). This result may be affected from this concentration was an optimum for disintegration property.

In buffer pH 6.8, the dissolution profiles of formulations IX-XII were shown in Figure 44(B)(data in Table 36, Appendix E). These matrices were completely dissolved within five hours. The release rate profiles were depicted in Figure 45(B)(data in Table 47, Appendix E).

As these results, it was indicated that the concentration of the polymer obviously affected the percentage of drug released. The different polymers produced the different drug released-time profiles. The pH of medium had an effect on the release rate profile. Finally, the theophylline-ethylcellulose system was chosen for further study.

4.1.5 The Formulations XIII-XVI Matrices

These Formulations contained theophylline-ethylcellulose-PVP K30 but the amount of polymer and channeling agent in each formulations was adjusted differently in order to modify the release rate(see Table 13). The release of theophylline from Formulation XIII and XIV were affected by dissolution medium as depicted in Figure 46. The release rate of these formulations

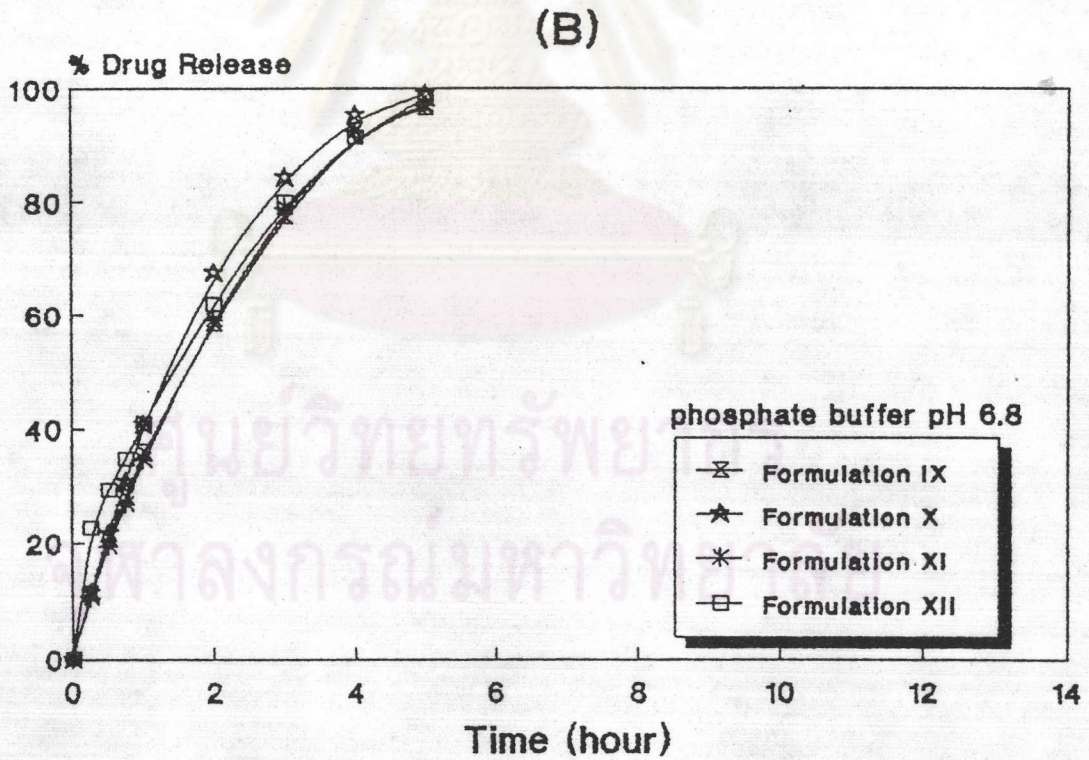
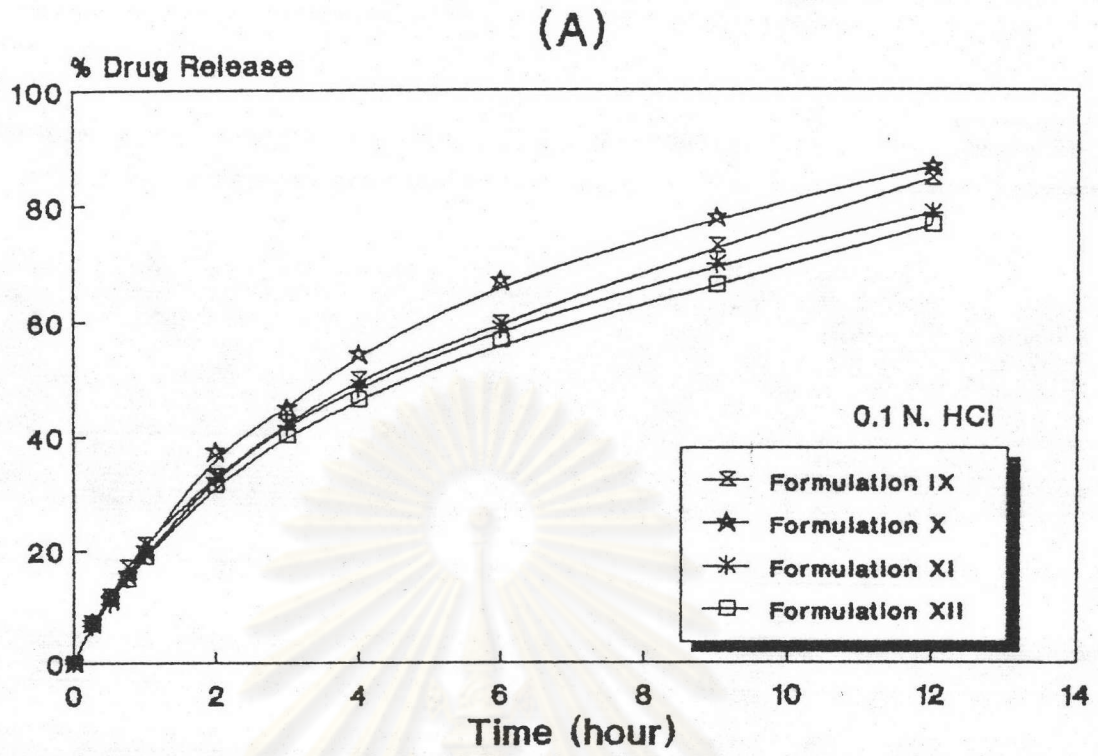


Figure 44. The Release Profiles of Theophylline-HPMCP Matrices in
 A) 0.1 N.HCl
 B) Buffer pH 6.8

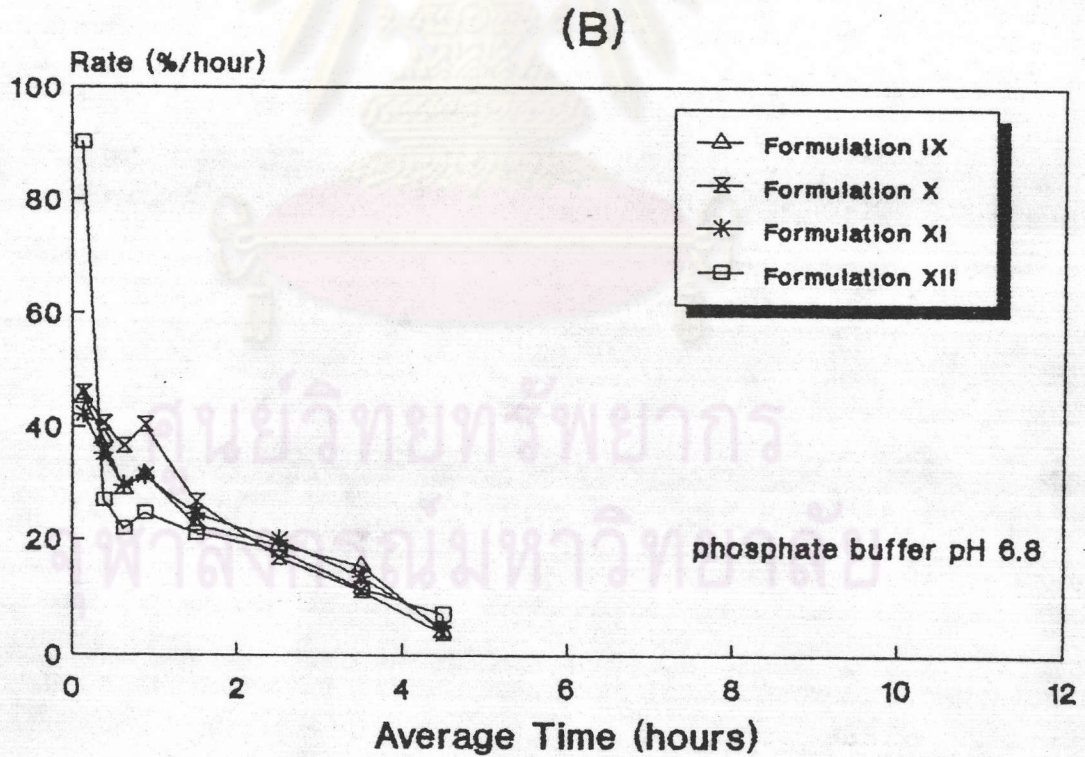
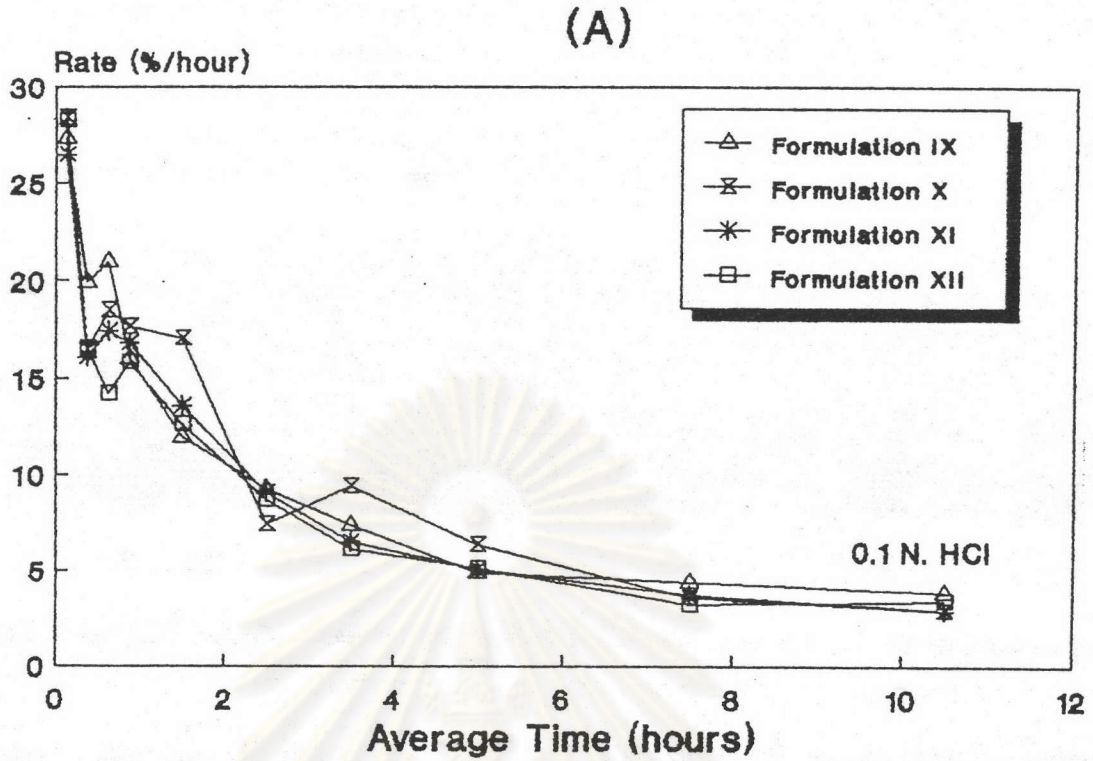


Figure 45. The Release Rate Profiles of Theophylline-HPMCP Matrices in
 A) 0.1 N.HCl
 B) Buffer pH 6.8

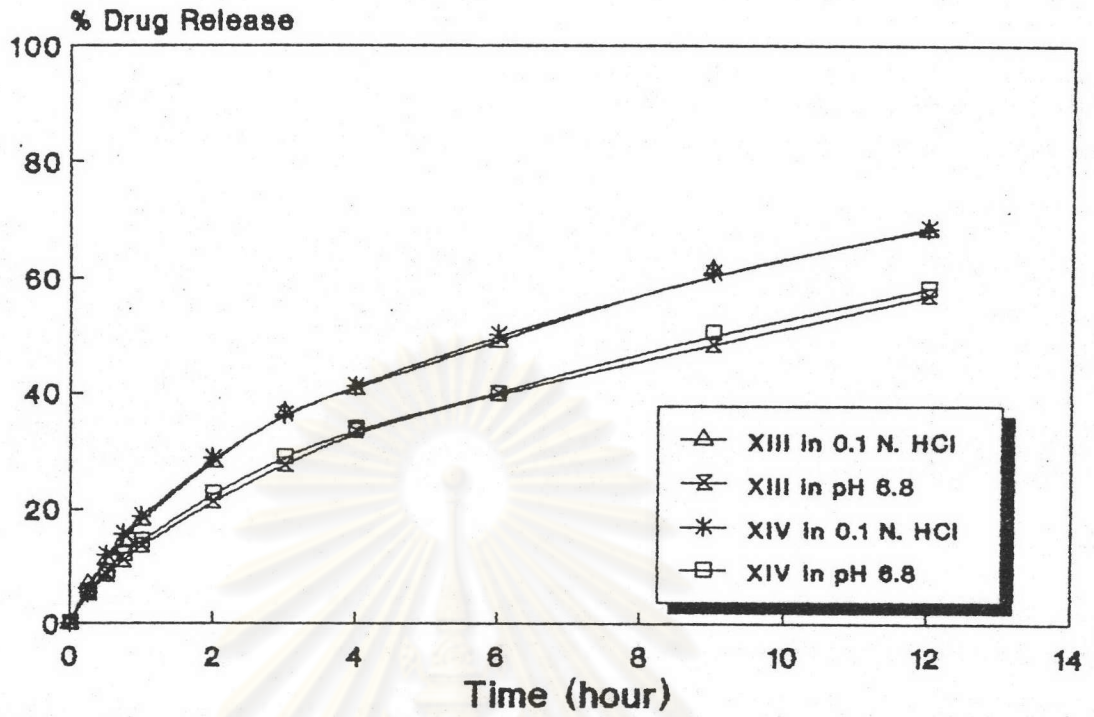


Figure 46. The Release Profiles of Formulations XIII and XIV Matrices

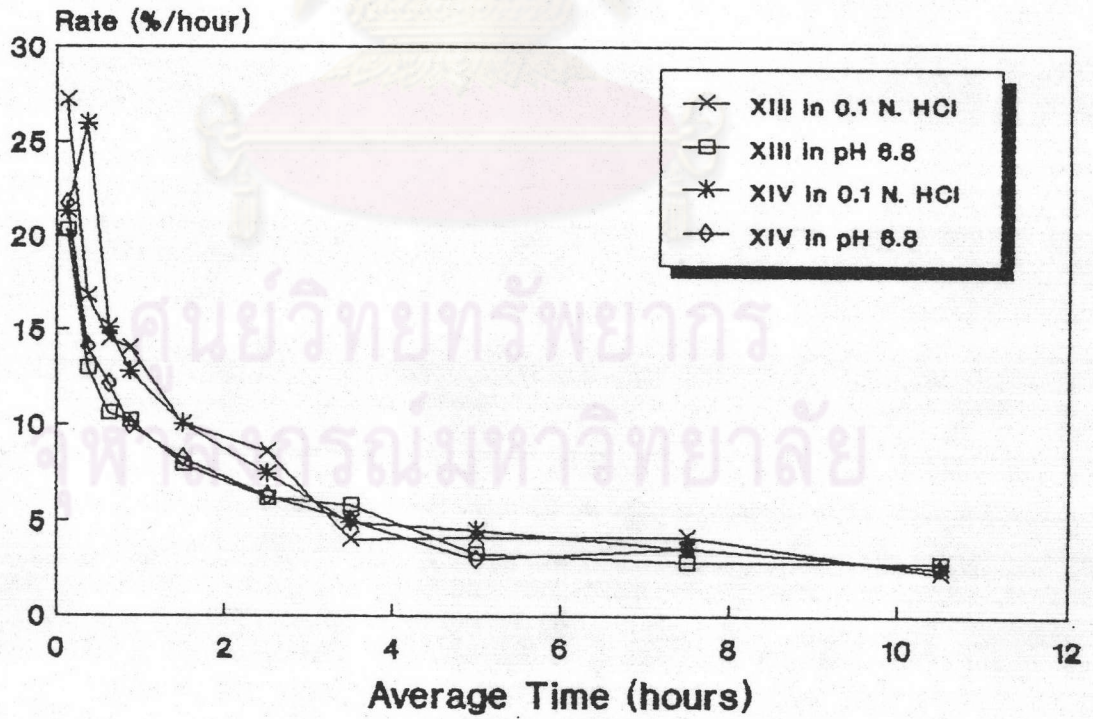


Figure 47. The Release Rate Profiles of Formulation XIII and XIV Matrices

decreased with the time increased as displayed in Figure 47. For the first three hours, the release rate in 0.1 N.HCl was faster than the rate in buffer pH 6.8. Increasing PVP K30 from 5% to 10% did not affect the dissolution profile and the dissolution rate.

The release of theophylline from Formulation XV and XVI were affected by dissolution medium as shown in Figure 48. The release rate of these formulations decreased with the time increased as depicted in Figure 49. The release rate in buffer pH 6.8 was faster than the release rate in 0.1 N.HCl. This result may be affected by high erosion of matrix in buffer pH 6.8 and completely dispersed within 9 hours. Increasing PVP K30 from 10 to 20% did not affect the dissolution profile and dissolution rate.

4.1.6 The Formulations XVII-XIX Matrices

These formulations contained theophylline-ethylcellulose-lactose but the amount of polymer and channeling agent in each formulations was adjusted differently in order to modify the release rate(see Table 13). The release of theophylline from Formulations XVII and XVIII were affected by dissolution medium as displayed in Figure 50. The release rate of these formulations decreased with the time increased as depicted in Figure 51. The release rate in 0.1 N.HCl was slightly faster than the release rate in buffer pH 6.8. An increase in lactose from 15 to 25% resulted in decrease of an initial release rate as shown in Figure 51.

The release of theophylline from Formulation XIX was affected by pH of dissolution medium as depicted in Figure 52. The release rate of this formulation decreased with the time

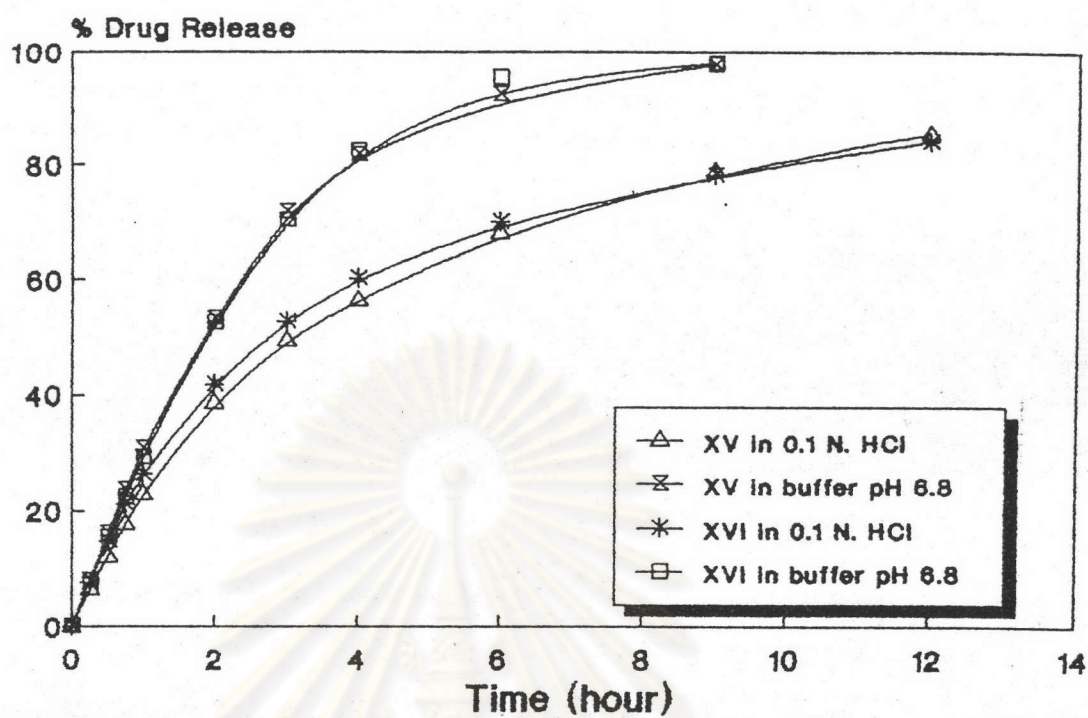


Figure 48. The Release Profiles of Formulation XV and XVI Matrices

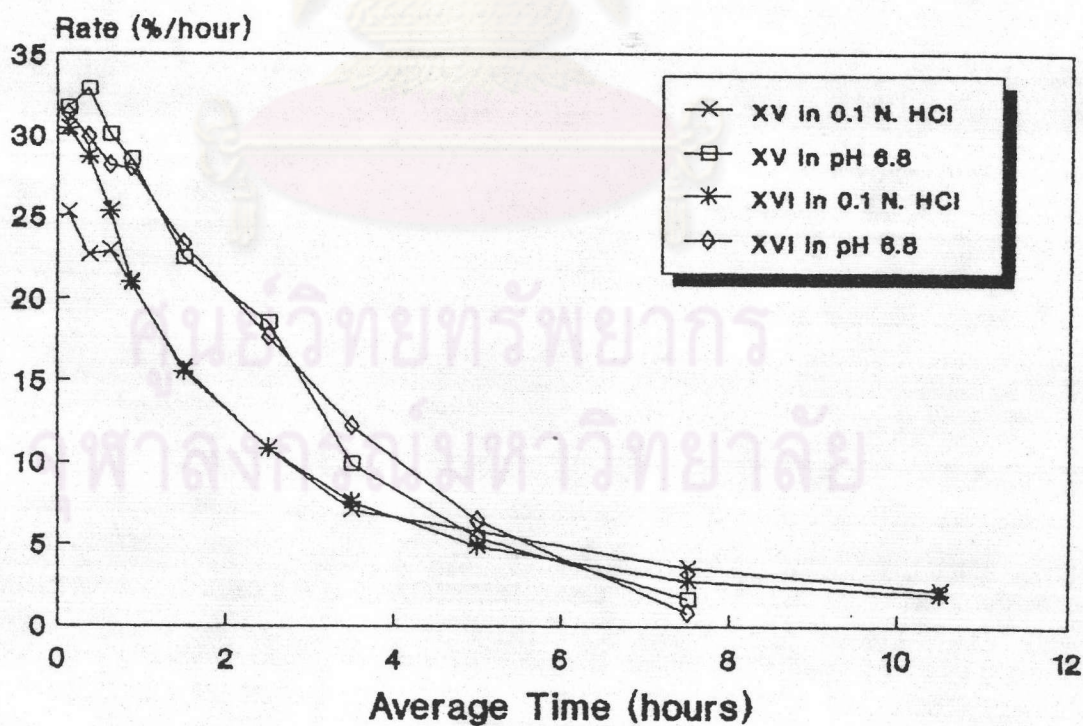


Figure 49. The Release Rate Profiles of Formulation XV and XVI Matrices

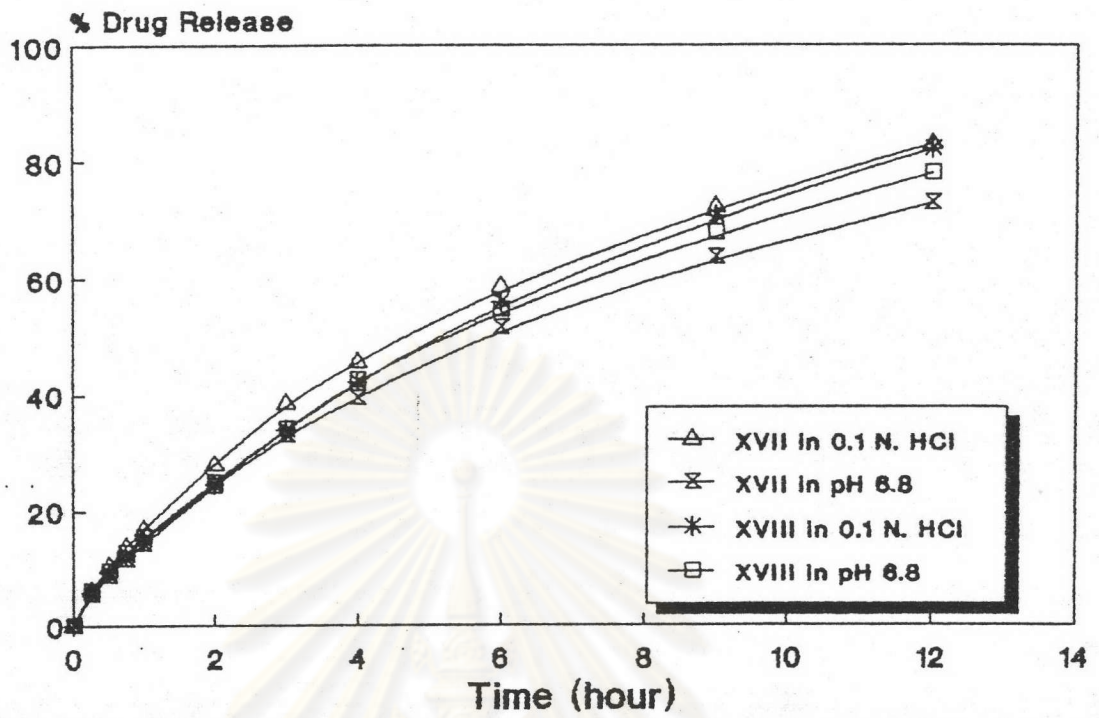


Figure 50. The Release Profiles of Formulation XVII and XVIII Matrices

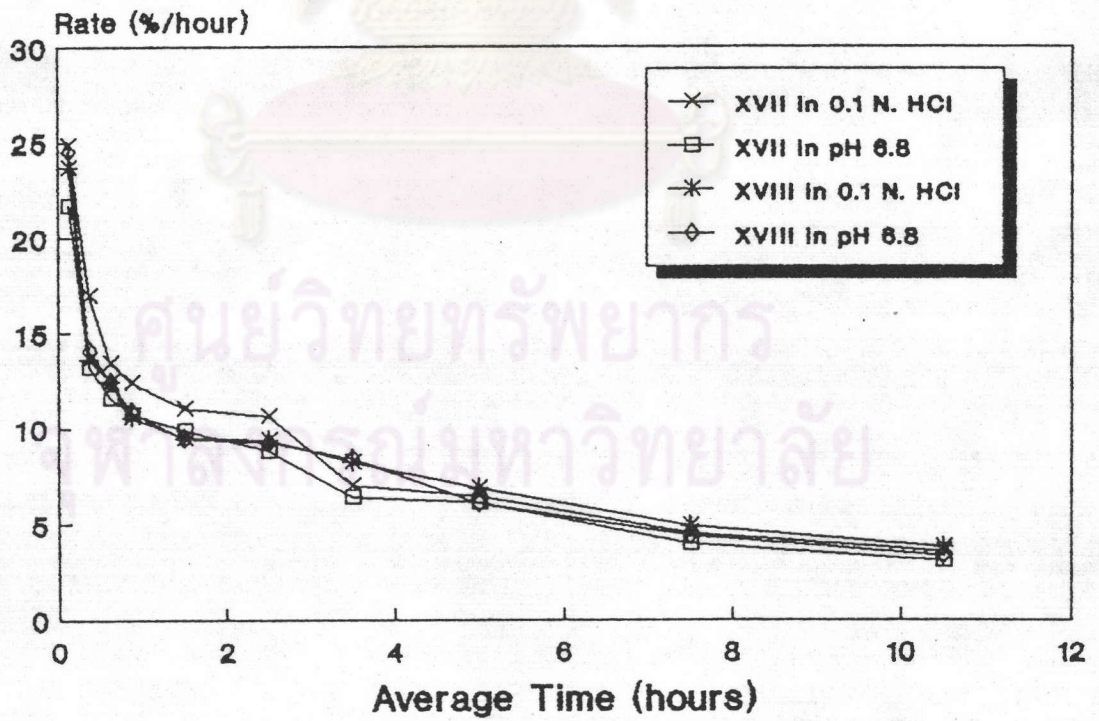


Figure 51. The Release Rate Profiles of Formulation XVII and XVIII Matrices

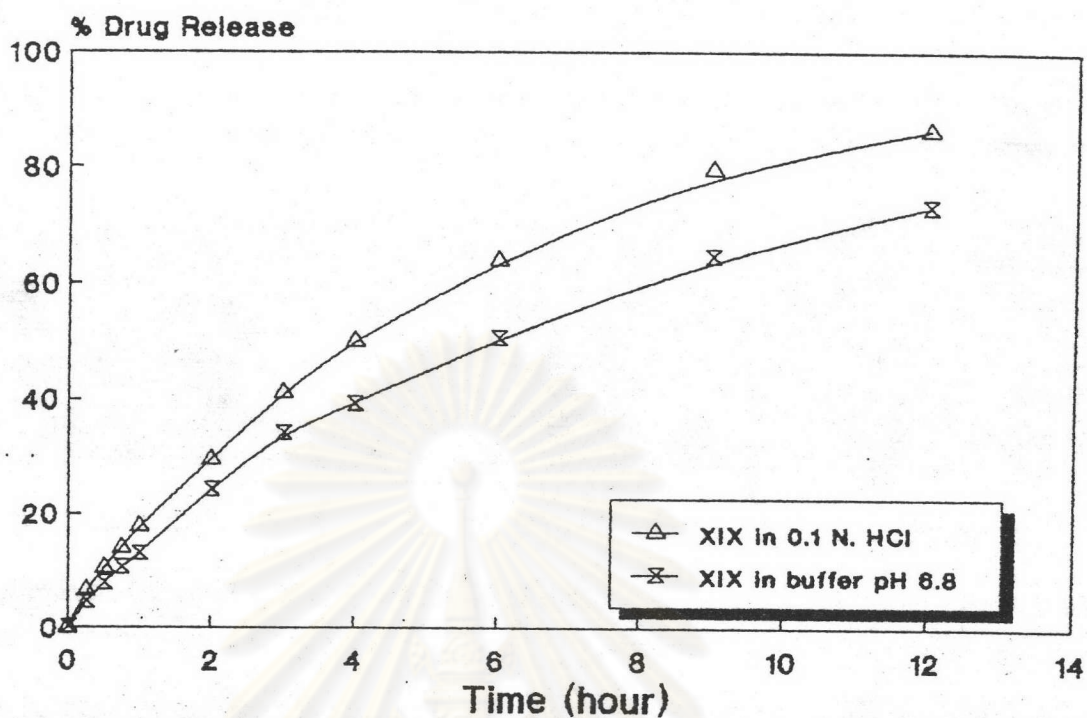


Figure 52. The Release Profiles of Formulation XIX Matrices

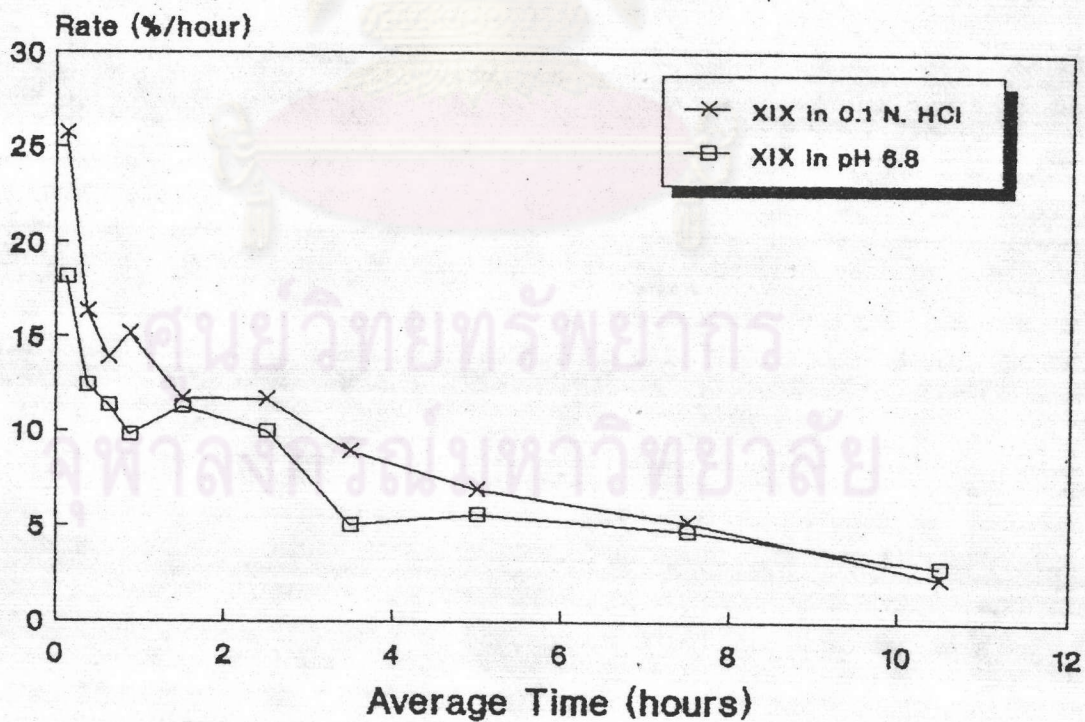


Figure 53. The Release Rate Profiles of Formulation XIX Matrices

increased as shown in Figure 53. But the decrease of release rate was fluctuated. The release rate in 0.1 N.HCl was higher than the release rate in buffer pH 6.8.

4.1.7 Quibron^(R)

The release profile was shown in Figure 54. Quibron^(R) dissolved completely within 6 hours in buffer pH 6.8 and in 0.1 N.HCl. The released rate of Quibron^(R) was fastest in comparison with all other formulations and products tested. The release rate in phosphate buffer pH 6.8 was faster than in 0.1 N. HCl as depicted in Figure 55.

4.1.8 Theodur^(R)

The difference of release profiles of Theodur^(R) in acid and alkali medium were detected. The release of theophylline from Theodur^(R) was affected by dissolution medium as illustrated in Figure 56. The observed wave-like appearance was in agreement with previously reported data (Jonkman, et al., 1981; McGinity, Cameron, and Cuff, 1983). The release rate profile of Theodur^(R) in phosphate buffer pH 6.8 was faster than that in 0.1 N. HCl after 5 hours of dissolution as shown in Figure 57.

4.1.9 Nuelin^(R)

Nuelin^(R) was completely dispersed within 9 hours in buffer pH 6.8, but it remained in the matrix form within 12 hours in 0.1 N.HCl. The dissolution profiles of theophylline from Nuelin^(R) were depicted in Figure 58.

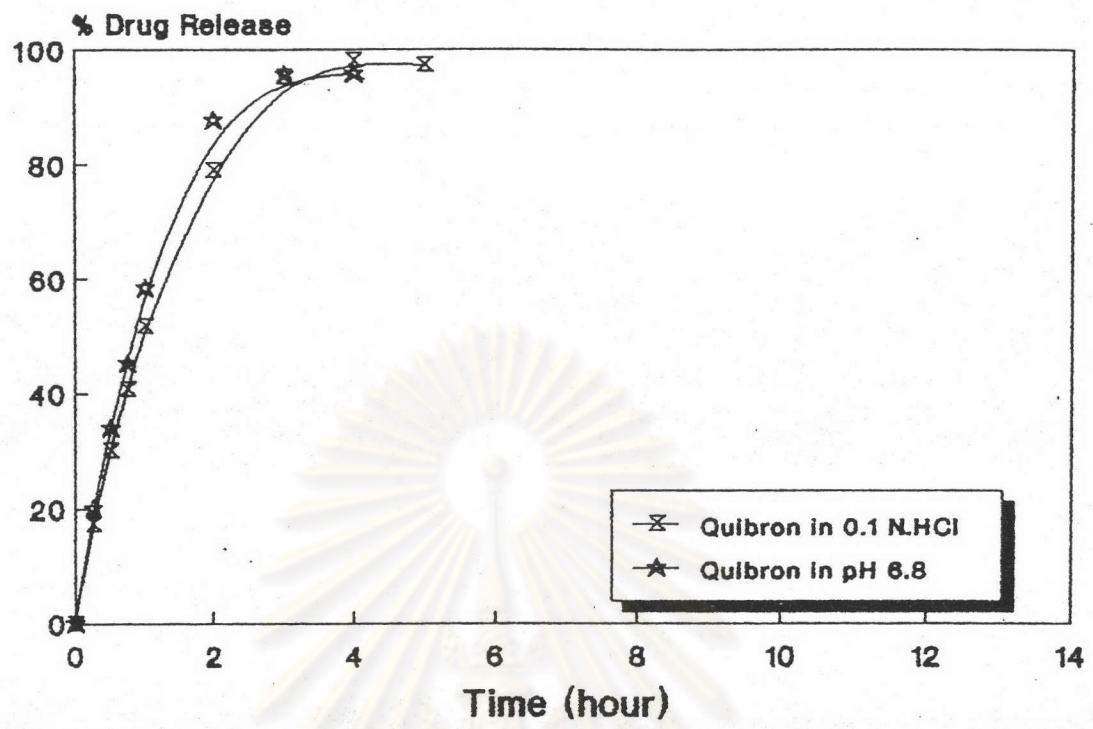


Figure 54. The Release Profiles of Quibron T/SR

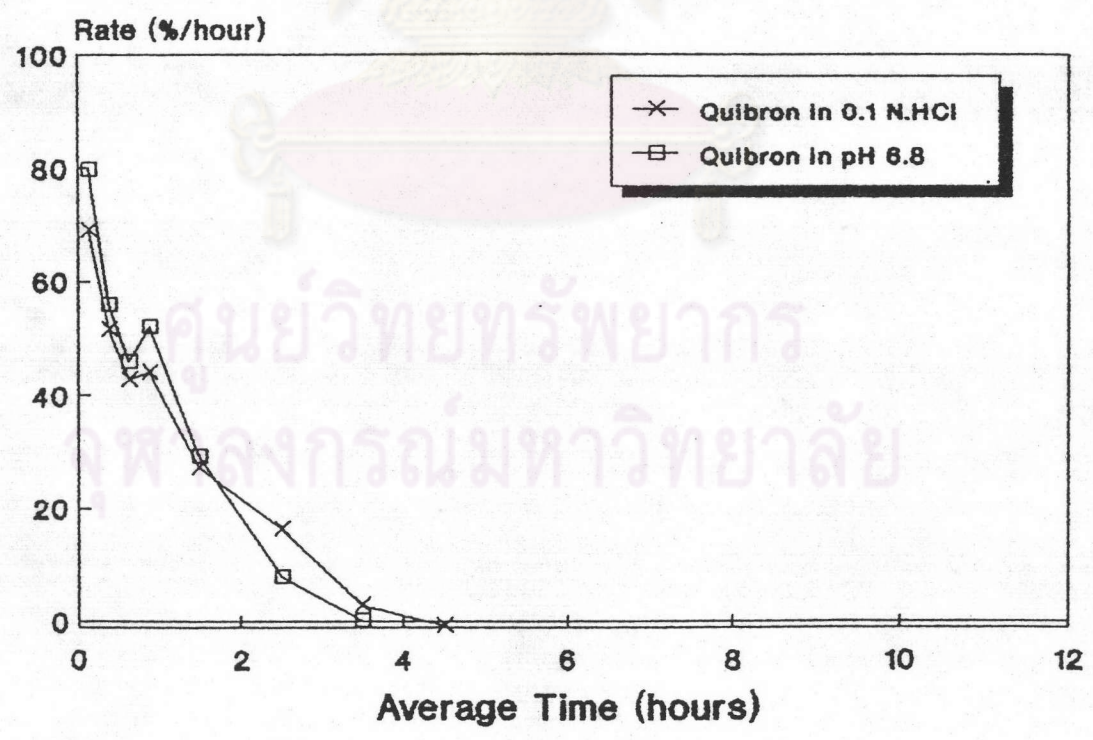


Figure 55. The Release Rate Profiles of Quibron T/SR

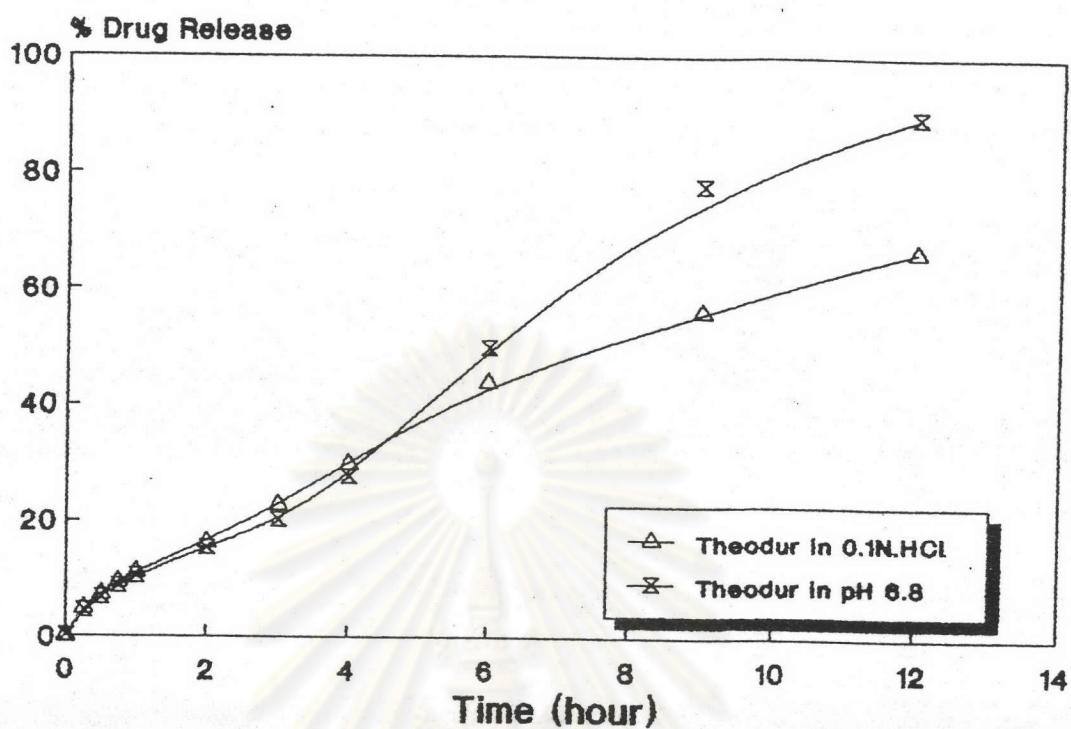


Figure 56. The Release Profiles of Theodur(R)

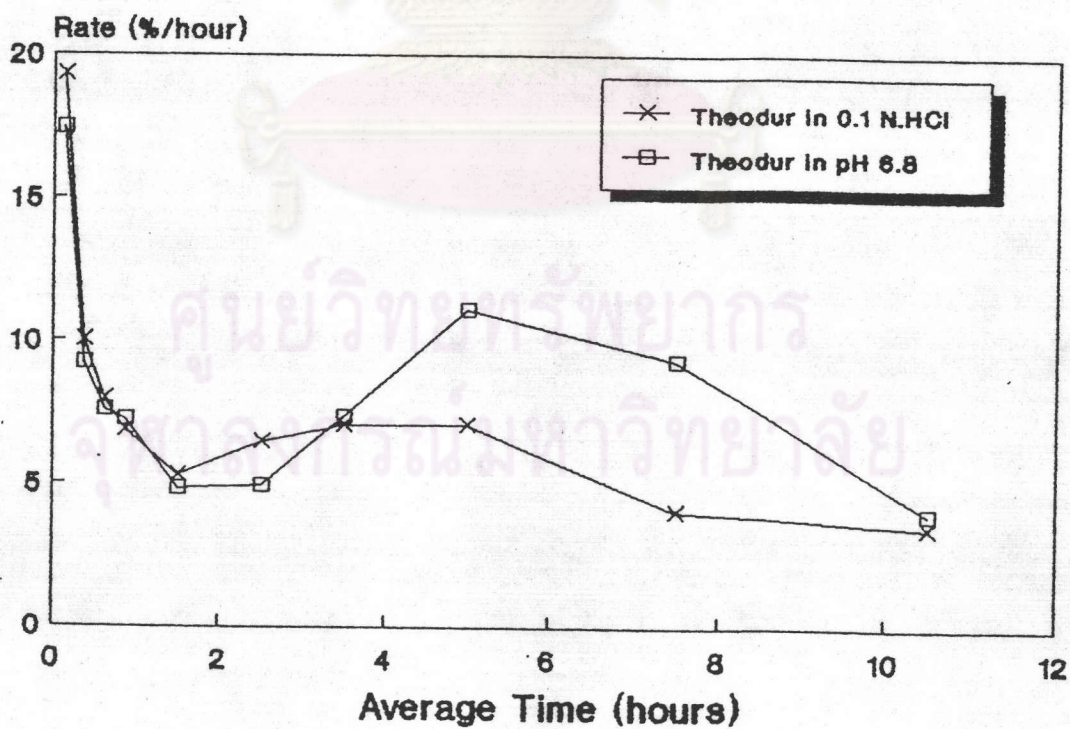


Figure 57. The Release Rate Profiles of Theodur(R)

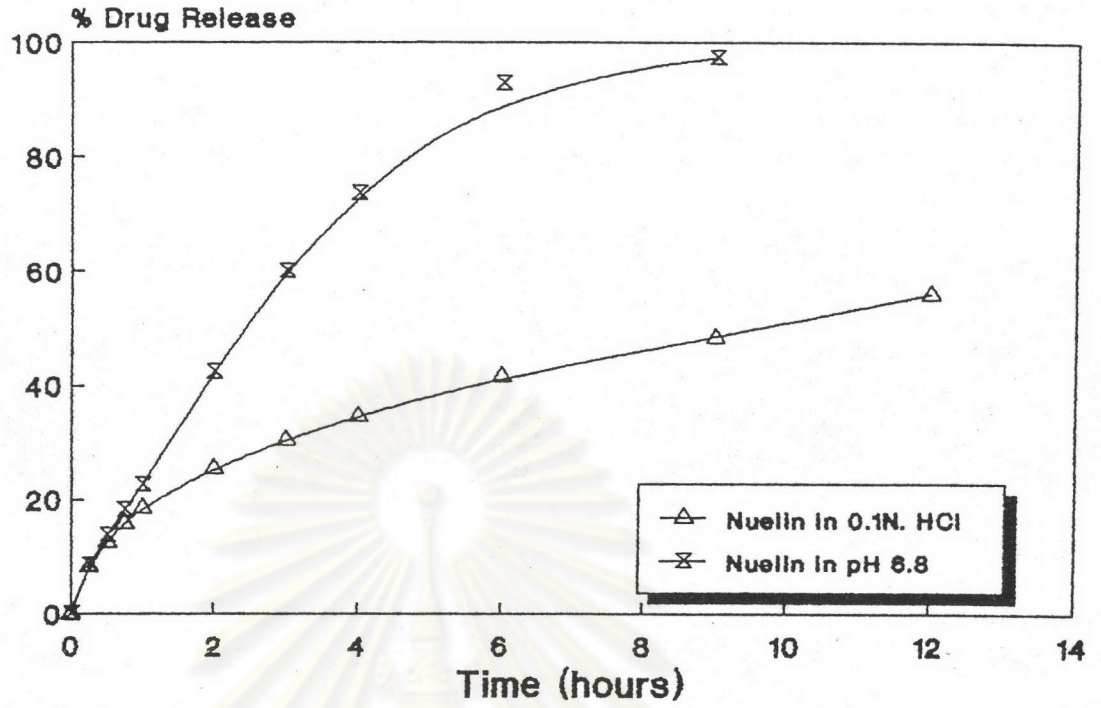


Figure 58. The Release Profiles of Nuelin(R)

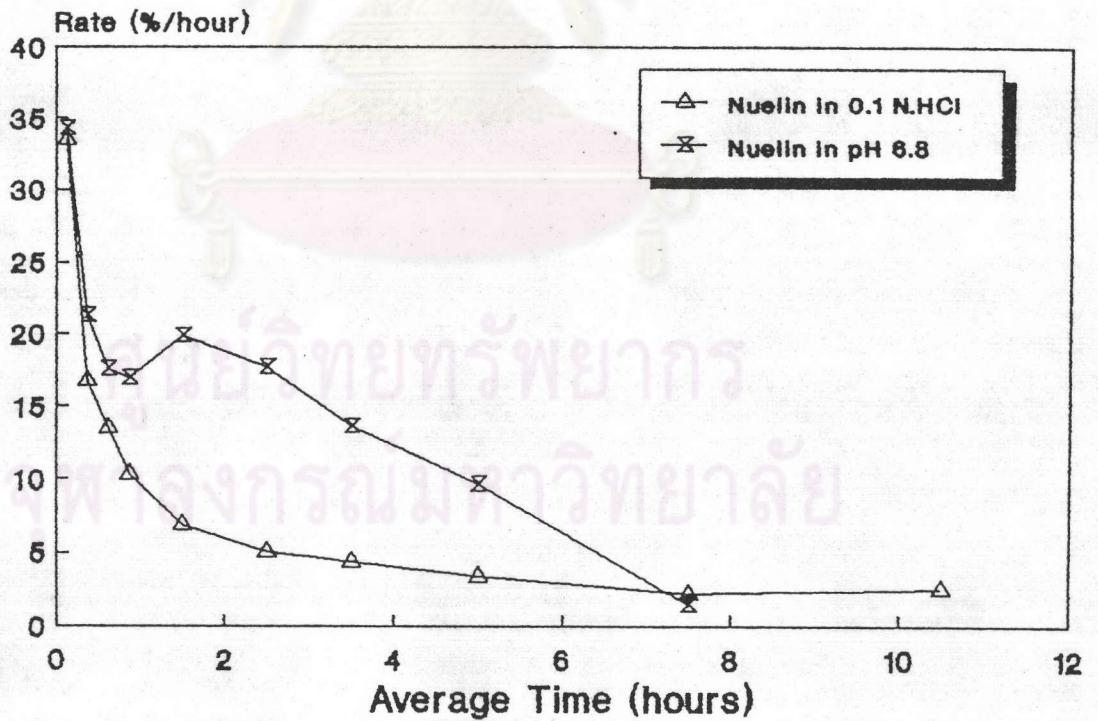


Figure 59. The Release Rate Profiles of Nuelin(R)

The release of drug from this product was affected by pH of the dissolution medium. The release rate of drug in buffer pH 6.8 was much higher than that rate in 0.1 N.HCl as depicted in Figure 59. This result may be affected by polymer solubility in these two pH media.

4.1.10 Release Studies in pH Change Method

From the release study as previously described, the Formulation XIX was seemed superior to the other formulations. Consequently, this formulation was selected to determine the release behavior by pH change method and compared to with the commercial products, Theodur^(R) and Nuelin^(R). Quibron^(R) was excluded from this study as it failed to release the drug for 12 hours in both acid and alkali medium. The release and release rate profiles attained were presented in Figure 60 and 61, respectively. The amount of drug that released in 12 hours were 92.80, 81.46, and 77.94% for Theodur^(R), Formulation XIX Matrices, and Nuelin^(R), respectively. The release rate of Theodur^(R) was lower at first 2 hours in comparing with Formulation XIX and Nuelin^(R) and higher rate was observed after that(Figure 61).

4.2 The Elucidation of Drug Release Model

In order to determine the effect of type of polymer and formulation difference on the model of drug release. Therefore, analysis of all dissolution data were carried out to elucidate what model(zero order, first order, and Higuchi model) could be fitted by the data. The plots between percentage of drug against time (zero order), log percent of drug remained versus time(first order), and

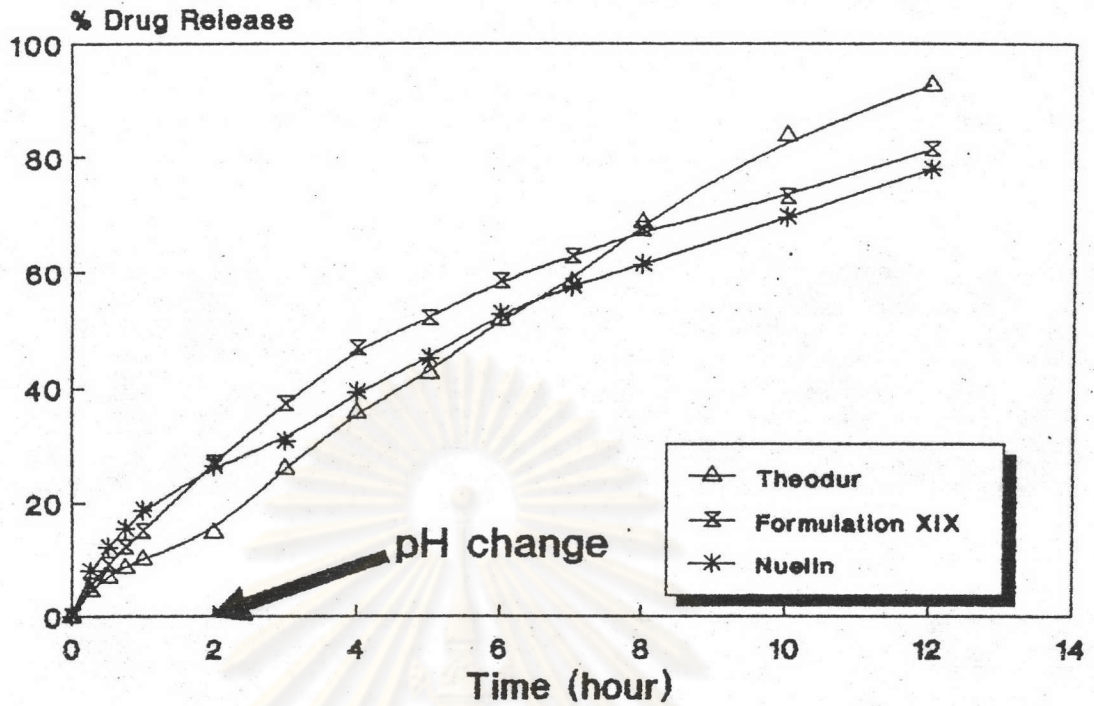


Figure 60. The Release Profiles of Formulation XIX Matrices, Nuelin^(R) and Theodur^(R) in pH Change Method

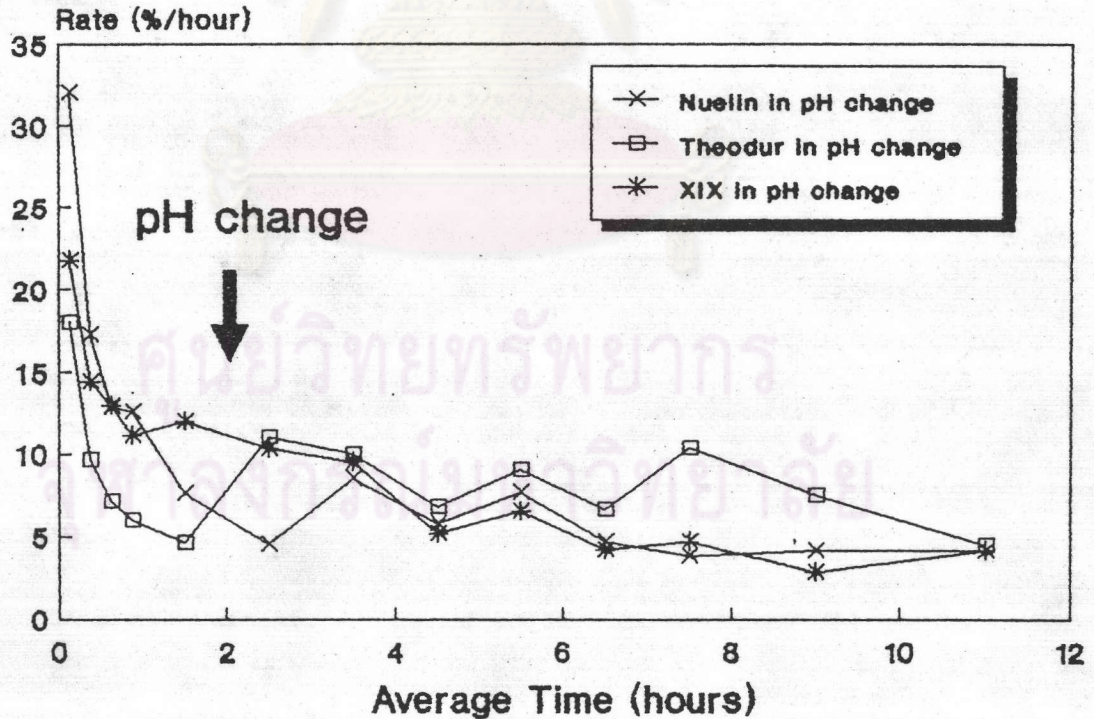


Figure 61. The Release Rate Profiles of Formulation XIX Matrices, Nuelin^(R) and Theodur^(R) in pH Change Method

percentage of drug versus square root of time(Higuchi model) were, therefore, constructed and determined the one which was the most linear as the accepted model of drug release.

4.2.1 The Blank Theophylline Matrix

The Higuchi plot and first-order plot of the blank formulation were illustrated in Figure 62-63, respectively. The correlation coefficient was obtained as tabulated in Table 19. Since both the Higuchi plot and the first order plot were rather linear, it was necessary to distinguish between the models. The treatment was based upon use of the differential forms of the first-order and Higuchi equations(data in Table 55-62, Appendix E). The correlation coefficient of rates of release versus Q were higher than those of rates versus $1/Q$ as exhibited in Table 20-21 and the statistical significance difference was found as presented in Table 66(Appendix F), these indicated that the trend of theophylline release from the matrices without additives, first order model would probably be operative.

4.2.2 The Formulations I-IV Matrices

From the graphs showed in Figures 64-65 and the values of correlation coefficient of the relationship shown in Table 19 indicated that the first-order model and the Higuchi model were interested. The further treatment was based upon use of the differential forms of the first-order and Higuchi equations. The correlation coefficient of rates of release versus $1/Q$ were higher than those of rates versus Q as exhibited in Table 20-21. This was true for all the matrices having different drug-polymer ratios and

Table 19. Correlation coefficient of the relationships between percent drug released versus time (A), percent drug released versus square root time (B), and log percent drug remained versus time (C).

Formulation	Dissolution Medium					
	0.1 N. HCl			Phosphate buffer pH 6.8		
	A	B	C	A	B	C
Blank	0.9403	0.9828	0.9203	0.9280	0.9702	0.9529
I	0.9179	0.9974	0.9853	0.9247	0.9985	0.9748
II	0.9215	0.9981	0.9736	0.9425	0.9980	0.9794
III	0.9340	0.9990	0.9715	0.9286	0.9993	0.9648
IV	0.9217	0.9993	0.9582	0.9265	0.9992	0.9599
V	0.9684	0.9827	0.9987	0.9511	0.9966	0.9730
VI	0.9602	0.9910	0.9900	0.9504	0.9968	0.9696
VII	0.9659	0.9912	0.9853	0.9413	0.9985	0.9658
VIII	0.9595	0.9943	0.9802	0.9452	0.9983	0.9676
IX	0.9230	0.9953	0.9939	0.9548	0.9818	0.9737
X	0.9001	0.9869	0.9950	0.9266	0.9786	0.9629
XI	0.9047	0.9903	0.9875	0.9548	0.9777	0.9740
XII	0.9103	0.9926	0.9861	0.9354	0.9957	0.9445
XIII	0.9130	0.9950	0.9789	0.9301	0.9956	0.9761
XIV	0.9075	0.9947	0.9774	0.9290	0.9967	0.9772
XV	0.8727	0.9808	0.9855	0.8337	0.9565	0.9986
XVI	0.8351	0.9703	0.9642	0.8394	0.9552	0.9851
XVII	0.9446	0.9920	0.9987	0.9476	0.9906	0.9962
XVIII	0.9632	0.9869	0.9983	0.9518	0.9903	0.9989
XIX	0.9332	0.9880	0.9987	0.9474	0.9878	0.9961
Nuelin ^(R)	0.8923	0.9960	0.9530	0.9002	0.9681	0.9842
Quibron ^(R)	0.8450	0.9612	0.9505	0.8368	0.9604	0.9611
Theodur ^(R)	0.9807	0.9704	0.9977	0.9871	0.9103	0.9451

Table 20. Comparison of linearity between plots of rate of release against reciprocal amount ($1/Q$) and amount (Q) of theophylline released from the matrices in 0.1 N. HCl.

Formulation	Correlation coefficient of rate dQ/dt	
	versus Q	versus $1/Q$
Blank	0.8908	0.8497
I	0.7012	0.9895
II	0.6613	0.9863
III	0.5806	0.9490
IV	0.6159	0.9687
V	0.6686	0.8560
VI	0.6181	0.9196
VII	0.5134	0.9220
VIII	0.4731	0.8798
IX	0.8715	0.8614
X	0.8372	0.7803
XI	0.8797	0.8407
XII	0.8014	0.9167

Table 21. Comparison of linearity between plots of rate of release against reciprocal amount ($1/Q$) and amount (Q) of theophylline released from the matrices in phosphate buffer pH 6.8.

Formulation	Correlation coefficient of rate dQ/dt	
	versus Q	versus $1/Q$
Blank	0.9064	0.6033
I	0.6785	0.9665
II	0.6056	0.9736
III	0.5872	0.9556
IV	0.5151	0.8995
V	0.5045	0.8903
VI	0.4657	0.8941
VII	0.4831	0.8833
VIII	0.4764	0.8875
IX	0.9137	0.7678
X	0.9458	0.5865
XI	0.9271	0.7096
XII	0.4477	0.6968

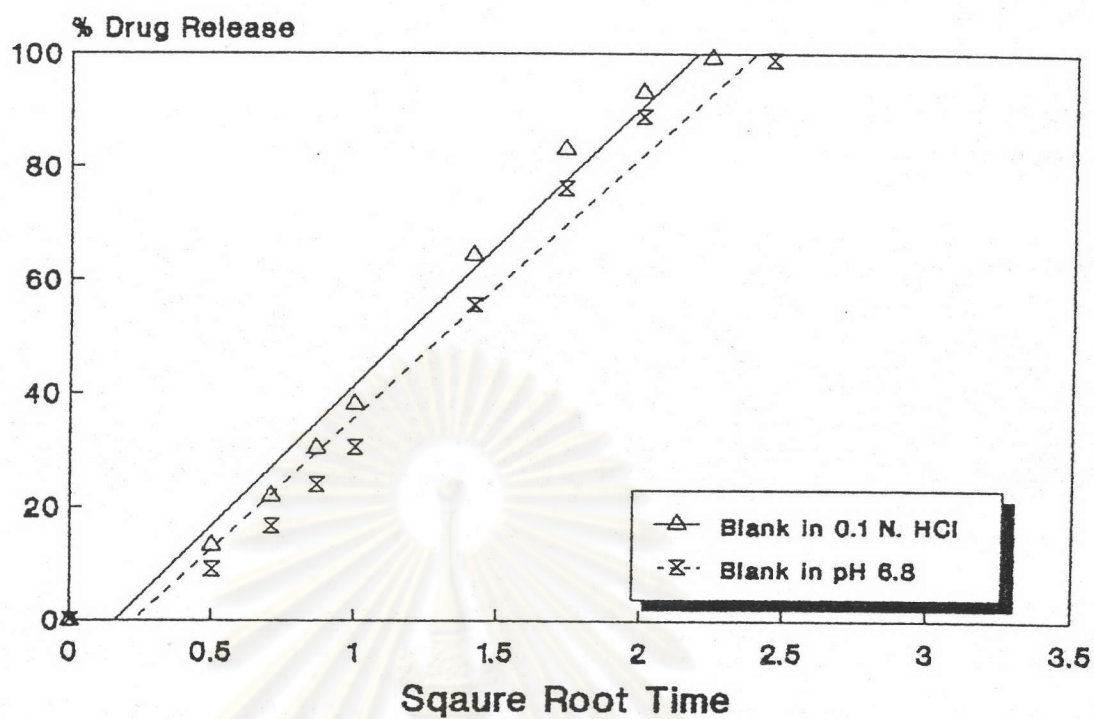


Figure 62. The Higuchi Plot of Theophylline Matrices without Additives

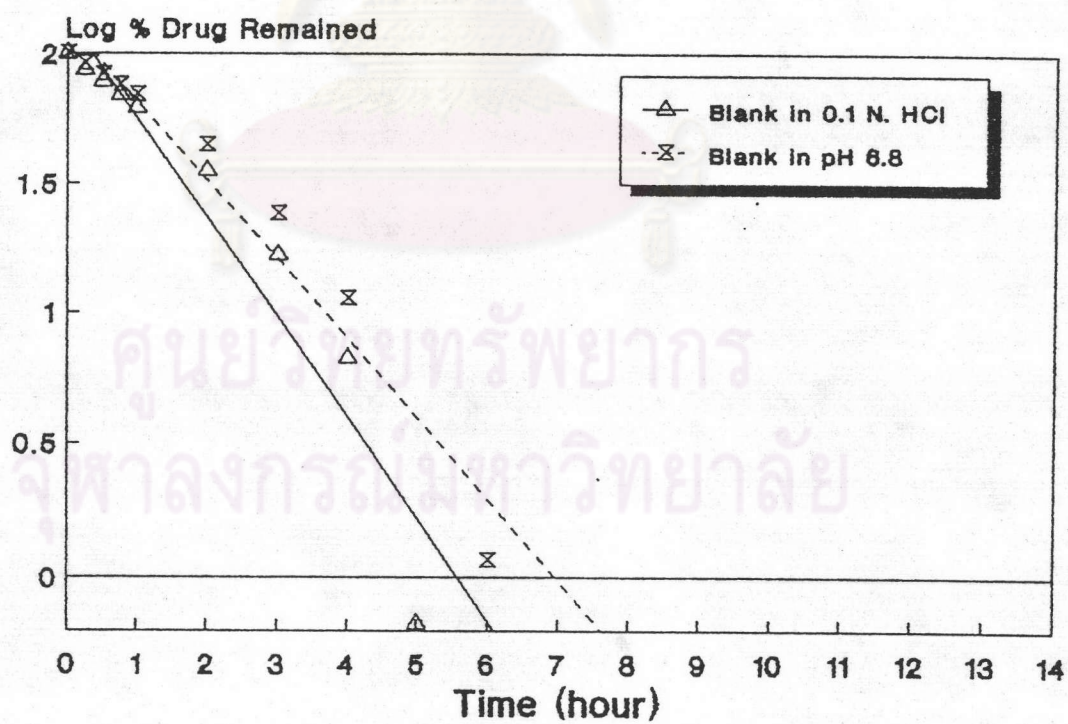


Figure 63. The First-order Plot of Theophylline Matrices without Additives

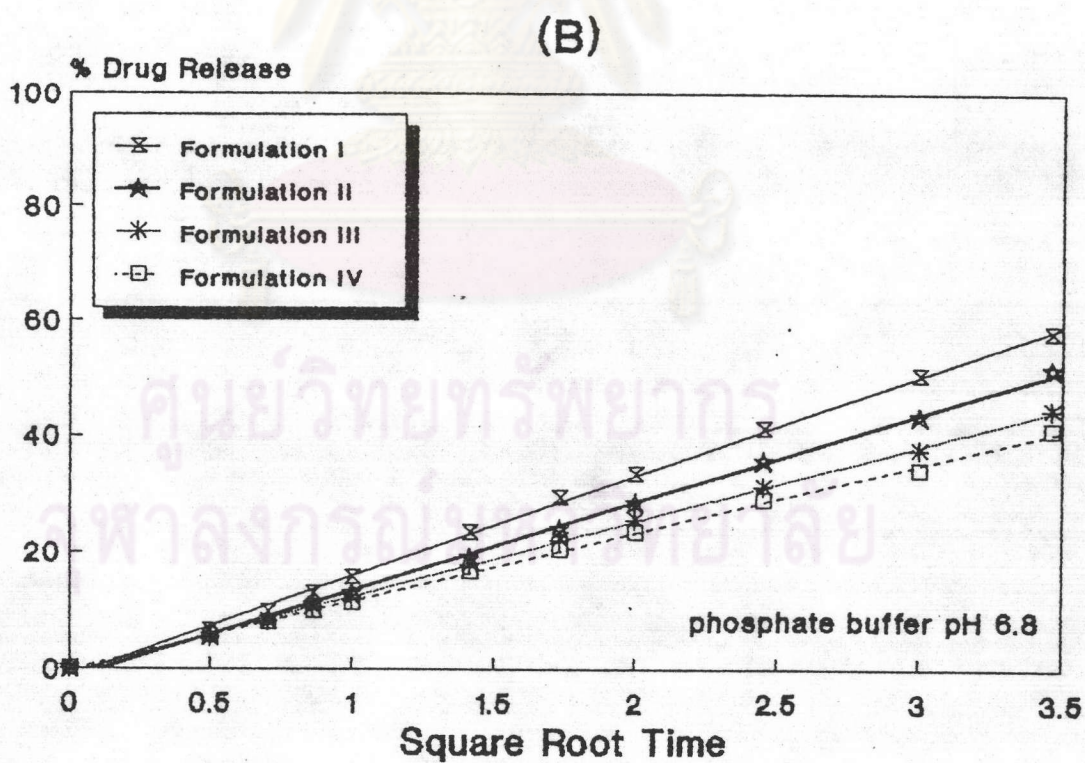
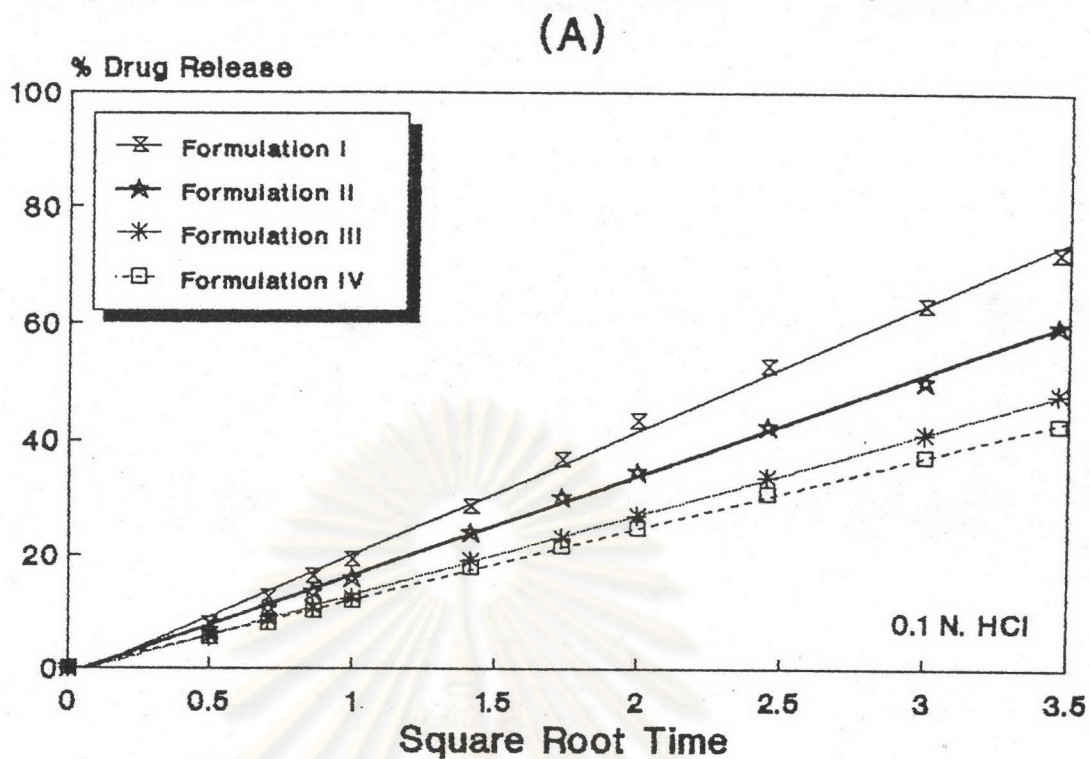


Figure 64. The Higuchi Plot of Theophylline-Ethylcellulose Matrices
in
A) 0.1 N.HCl
B) Buffer pH 6.8

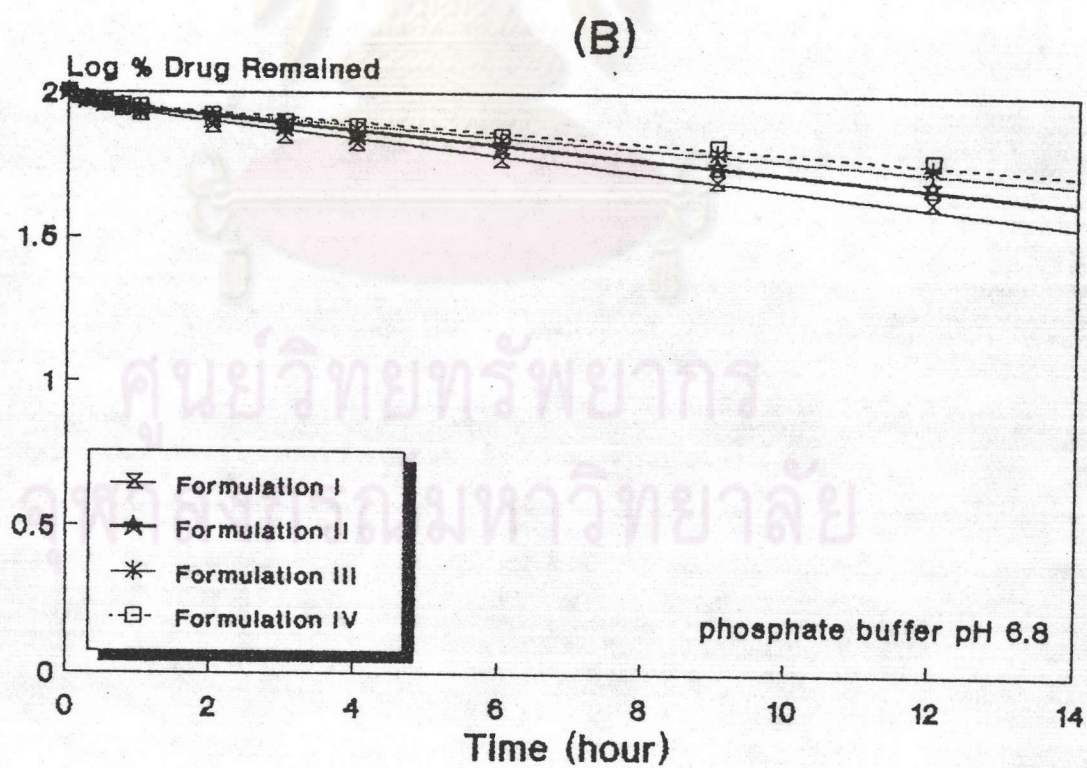
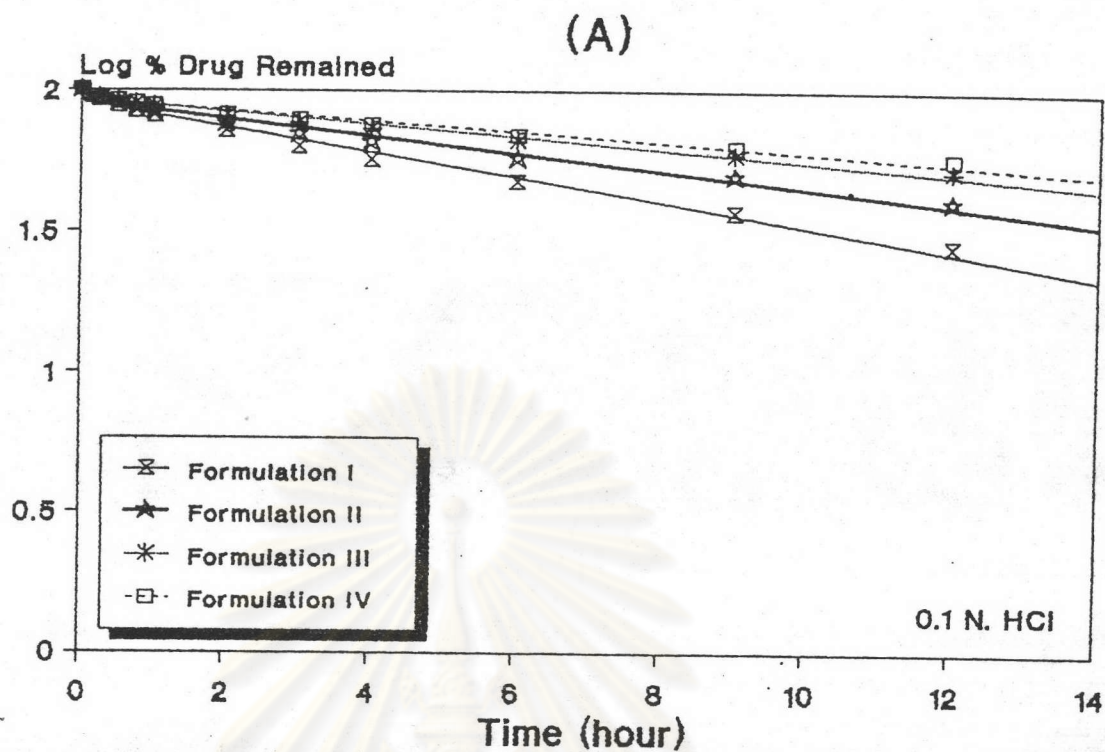


Figure 65. The First-order Plot of Theophylline- Ethylcellulose Matrices in
 A) 0.1 N.HCl
 B) Buffer pH 6.8

indicated that the trend of theophylline release from ethylcellulose matrices, Higuchi model would probably be operative.

4.2.3 The Formulations V-VIII Matrices

All these formulations gave similar release model in both dissolution fluids. Table 19 and Figures 66-67 gave the comparison between the linearizations of release rate data by the two models. Both the Higuchi plot and first-order plot were linearity with the correlation coefficient values greater than 0.96. However, the Higuchi equation gave consistently higher values for the correlation coefficient than that did the first-order equation. Nevertheless, since both models were acceptably linear, a more discriminating test, Equation 17,18 as well, was utilized to distinguish between the two models. The relative validity of the test was obtained by using the differential forms of the rate equations. The result as shown in Table 20-21 indicated that the release data would possibly follow Higuchi model.

4.2.4 The Formulations IX-XII Matrices

For the test in 0.1 N.HCl, the Higuchi plot and first-order plot were shown in Figures 68(A) and 69(A), respectively. From the Figures 68(A)-69(A) and the values of correlation coefficient of the relationship shown in Table 19 pointed out that the first-order model and the Higuchi model were interested. In further treatment, the correlation coefficient of rates of release against Q were higher than those of rates against $1/Q$. This was true for Formulations IX-XI but Formulation XII was opposite as shown in Table 20. The statistical significance difference of Formulations

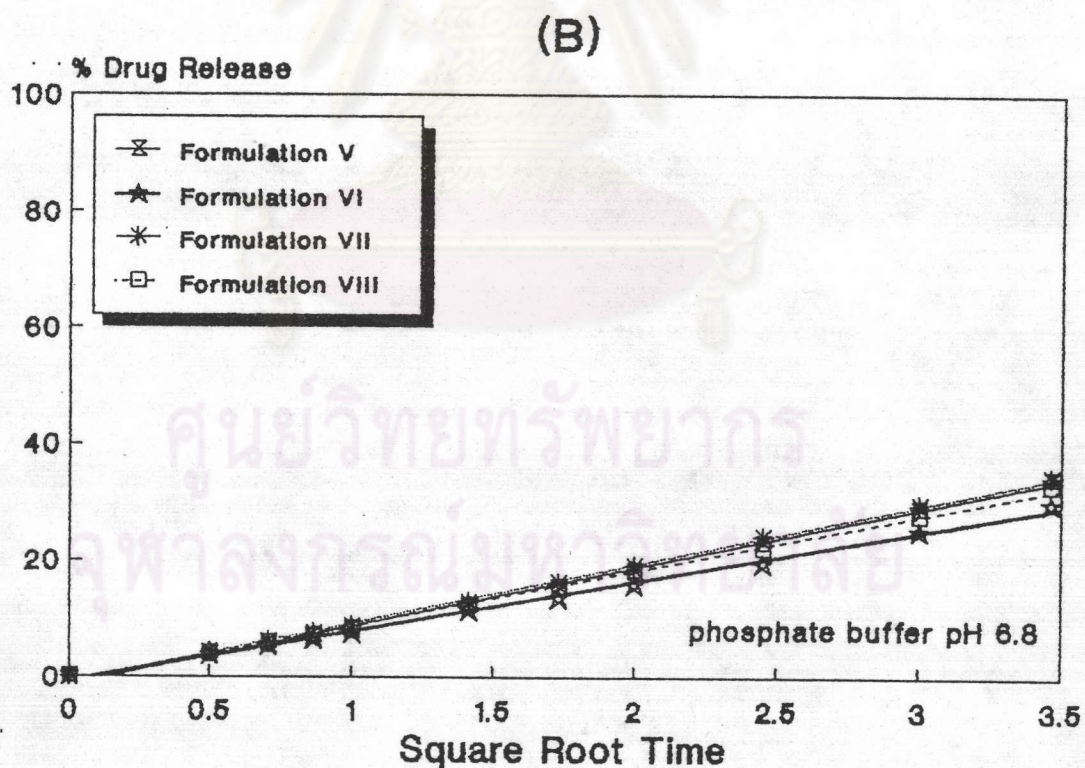
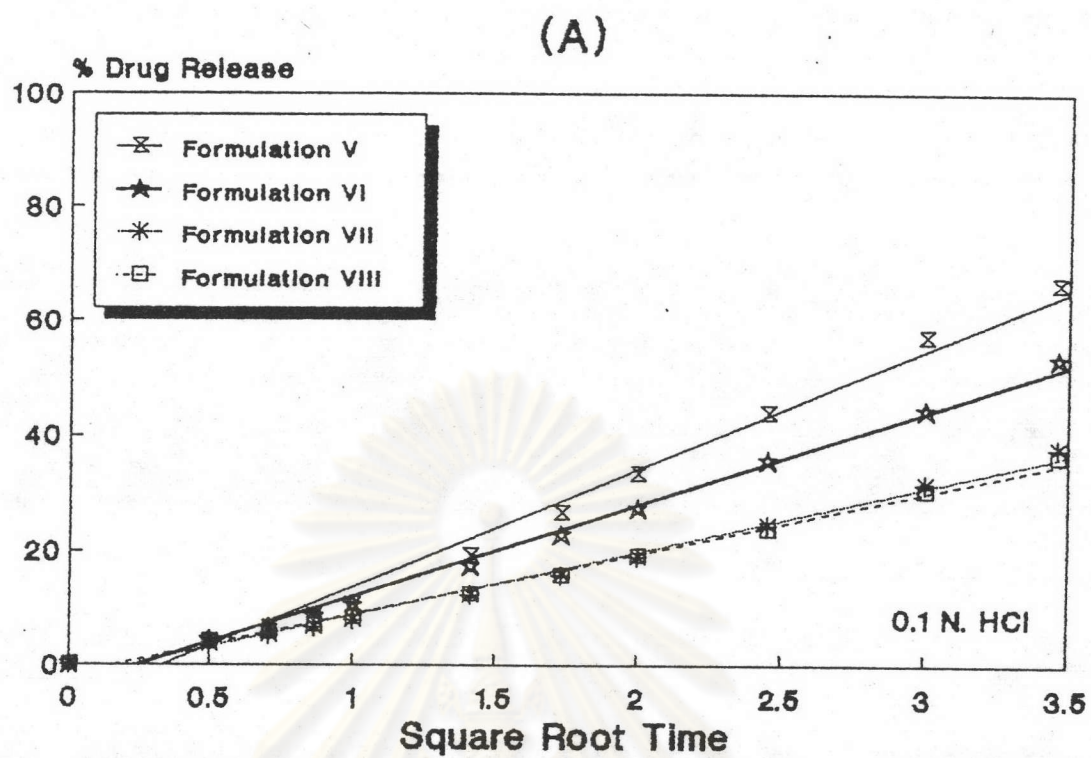


Figure 66. The Higuchi Plot of Theophylline-HPMC Matrices in
 A) 0.1 N.HCl
 B) Buffer pH 6.8

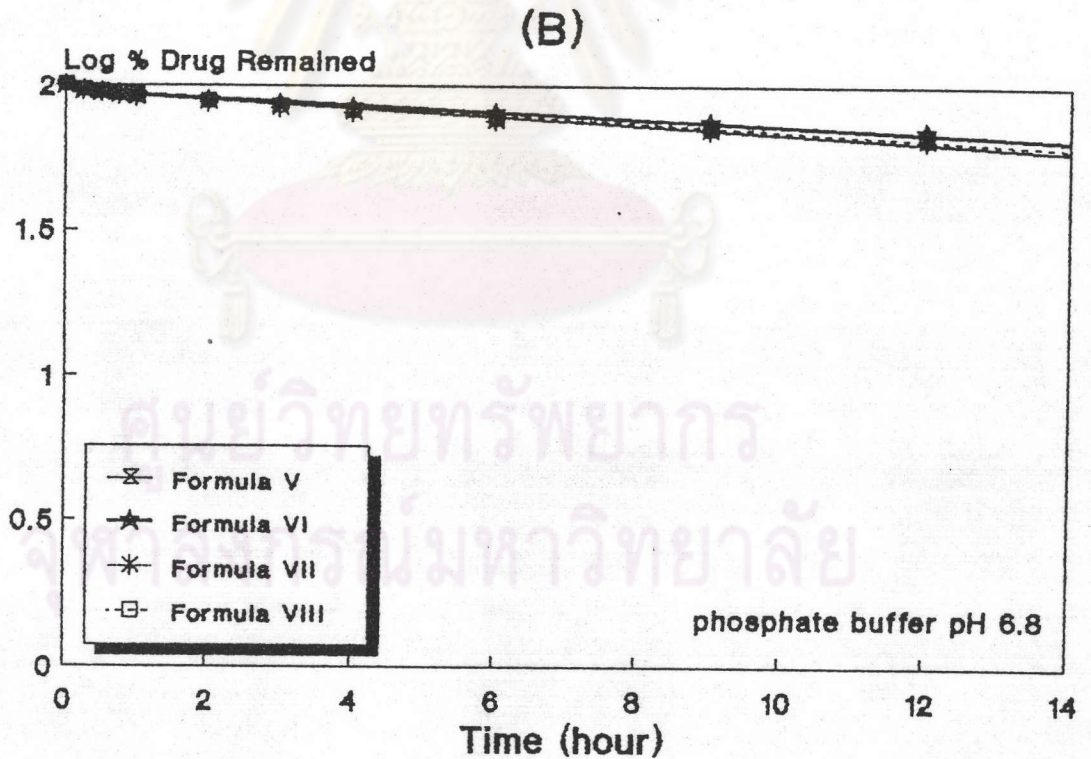
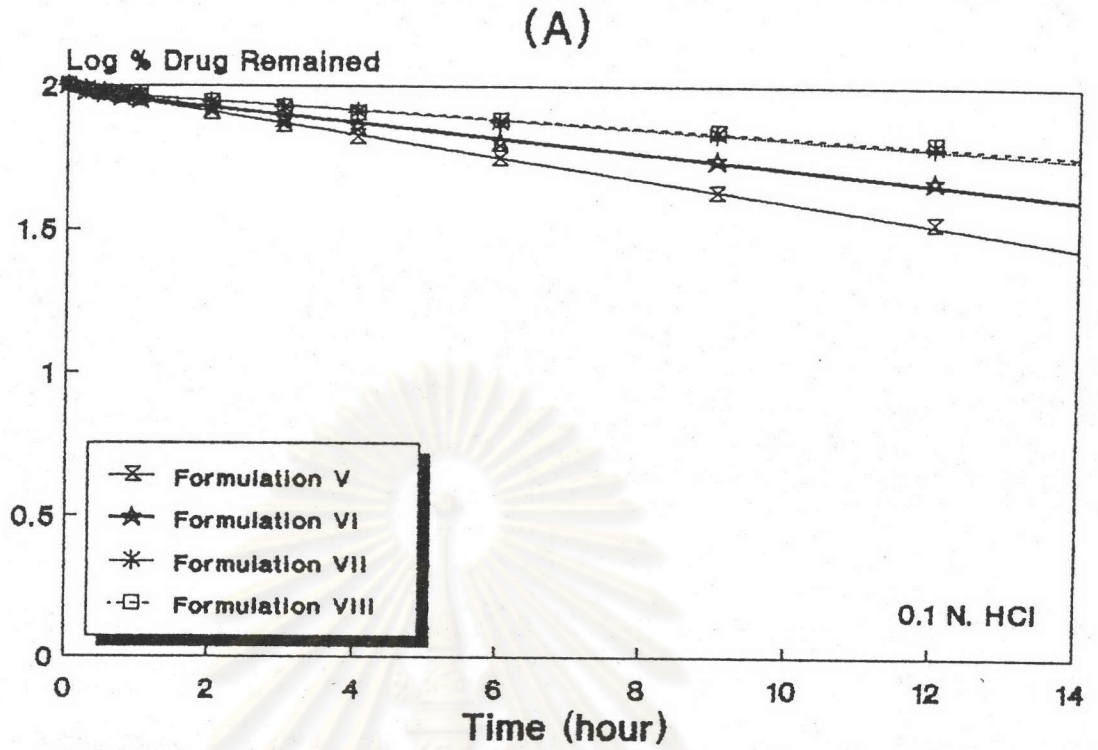


Figure 67. The First-order Plot of Theophylline-HPMC Matrices in
 A) 0.1 N.HCl
 B) Buffer pH 6.8

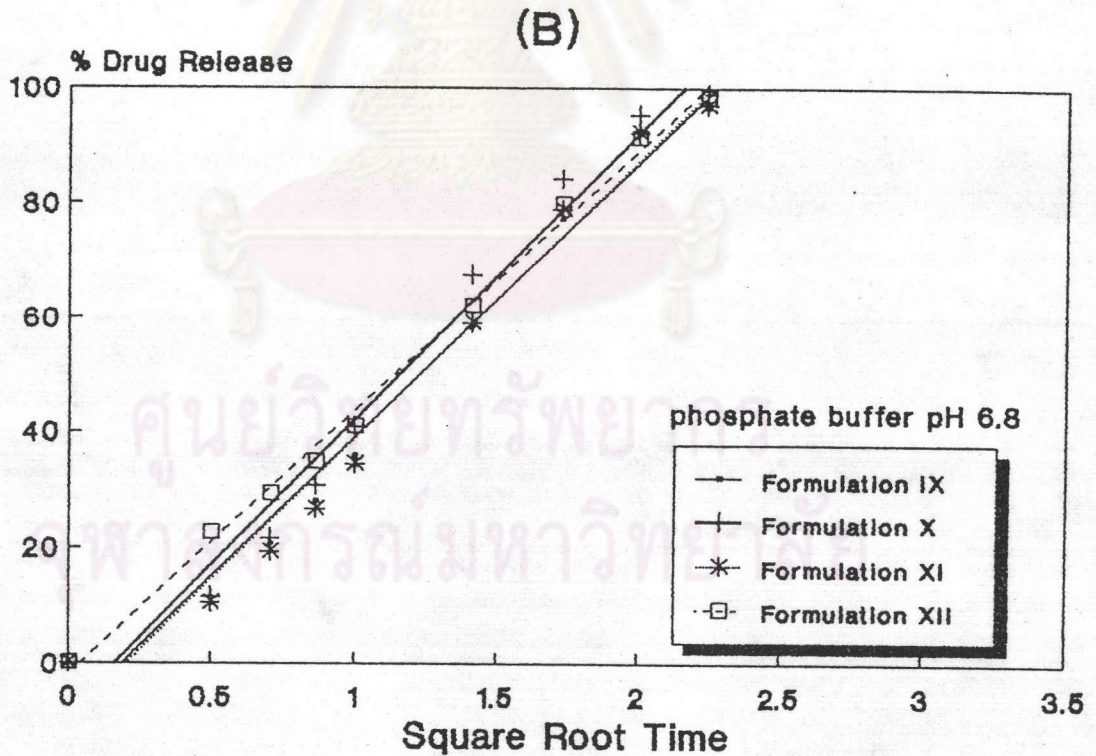
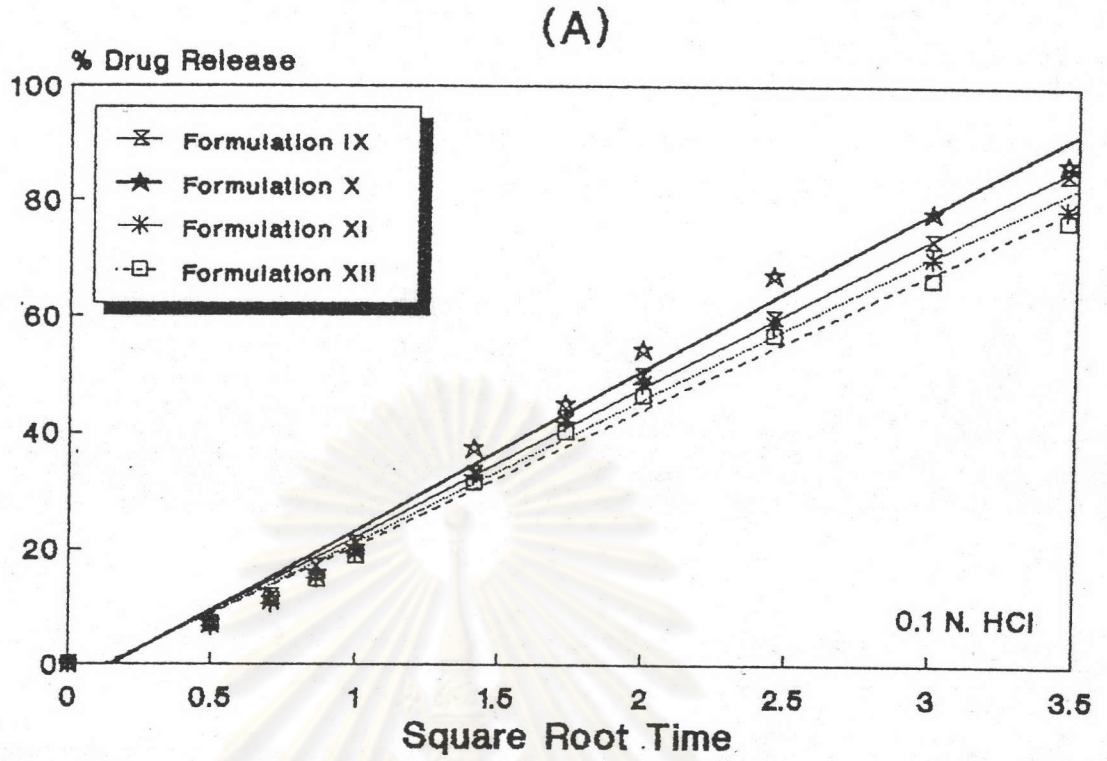


Figure 68. The Higuchi Plot of Theophylline-HPMCP Matrices in
 A) 0.1 N.HCl
 B) Buffer pH 6.8

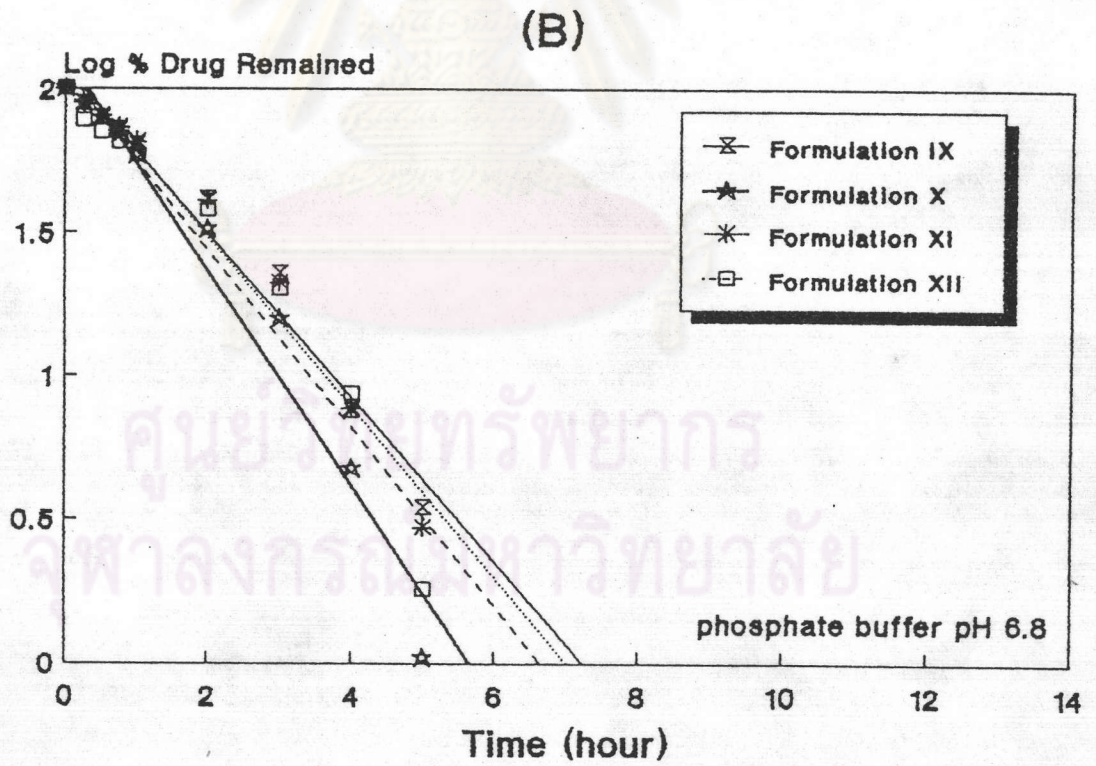
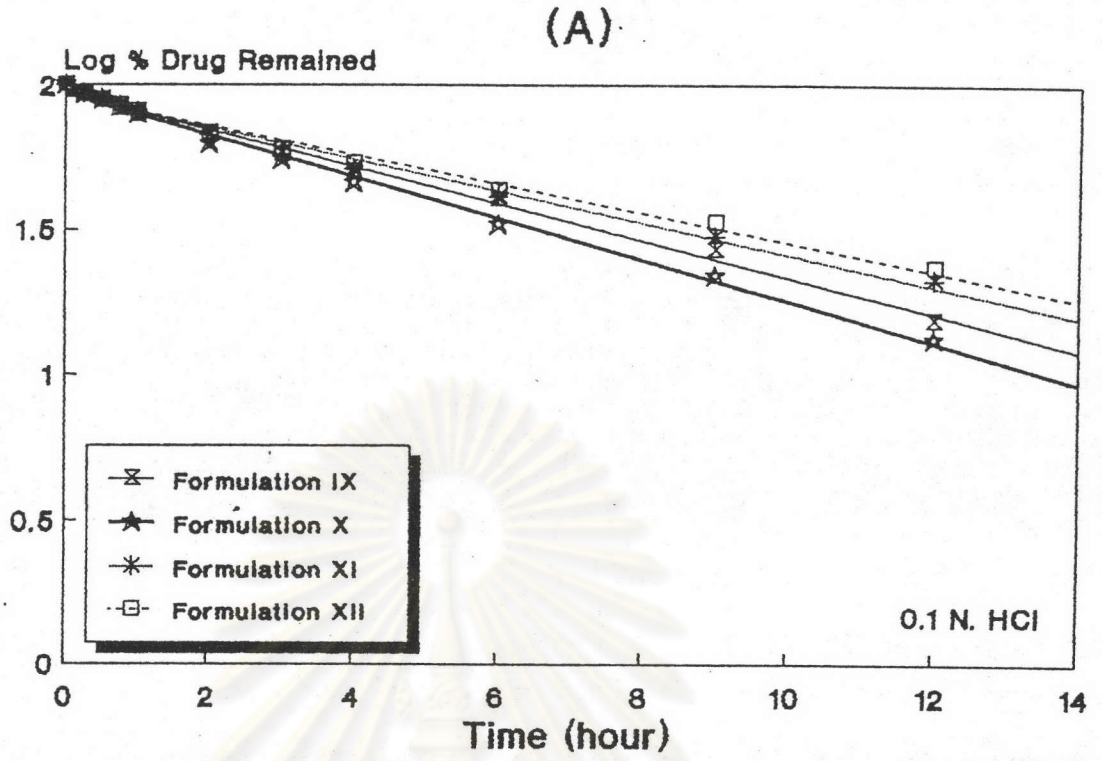


Figure 69. The First-order Plot of Theophylline-HPMCP Matrices in
 A) 0.1 N.HCl
 B) Buffer pH 6.8

X-XII were observed, but the t-value of Formulation IX showed no statistical significance difference (Table 66, Appendix F). Therefore, the release profiles of Formulations X-XI would probably follow first-order model, while Formulation XII would possibly exhibit Higuchi model and the model of Formulation IX was not cleared.

The Higuchi plot and first-order plot of these formulations in buffer pH 6.8 were shown in Figure 68(B) and 69(B), respectively. From the Figure 68(B)-69(B) and the values of correlation coefficient of the relationship shown in Table 19 pointed out that the first-order model and the Higuchi model were interested. In further treatment, the correlation coefficients of rates of release against Q were higher than those of rates against $1/Q$. This was true for Formulations IX-XI but Formulation XII was opposite as presented in Table 21. The t-values of Formulation XII showed no statistical significance difference. The Formulations IX-XI would possibly follow first-order model, but the model of Formulation XII was not cleared.

4.2.5 The Formulations XIII-XVI Matrices

Table 19 and Figures 70-71 gave the comparison between the linearizations of the first-order model and Higuchi model among the Formulations XIII-XIV. The correlation coefficient values of Higuchi plot were higher than that obtained from first-order plot. The further treatment was based upon use of the differential form of first-order and Higuchi equation as tabulated in Table 22-23 indicated that these release profiles would

Table 22. Comparison of linearity between plots of rate of release against reciprocal amount ($1/Q$) and amount (Q) of theophylline release from the Formulations XIII-XIX and commercial products in 0.1 N.HCl.

Products	Correlation Coefficient of Rate dQ/dt	
	versus Q	versus $1/Q$
XIII	0.7912	0.9509
XIV	0.8005	0.6315
XV	0.9799	0.6249
XVI	0.9851	0.7004
XVII	0.7775	0.9422
XVIII	0.6624	0.9368
XIX	0.8205	0.8782
Quibron ^(R)	0.9430	0.7976
Nuelin ^(R)	0.6406	0.9781
Theodur ^(R)	0.3917	0.8156

Table 23. Comparison of linearity between plots of rate of release against reciprocal amount ($1/Q$) and amount (Q) of theophylline release from the Formulations XIII-XIX and commercial products in buffer pH 6.8

Products	Correlation Coefficient of Rate dQ/dt	
	versus Q	versus $1/Q$
XIII	0.7749	0.9682
XIV	0.7669	0.9743
XV	0.9501	0.4750
XVI	0.9389	0.4920
XVII	0.7535	0.9311
XVIII	0.6878	0.9399
XIX	0.7893	0.8011
Quibron ^(R)	0.8984	0.7602
Nuelin ^(R)	0.6864	0.7188
Theodur ^(R)	0.0695	0.4370

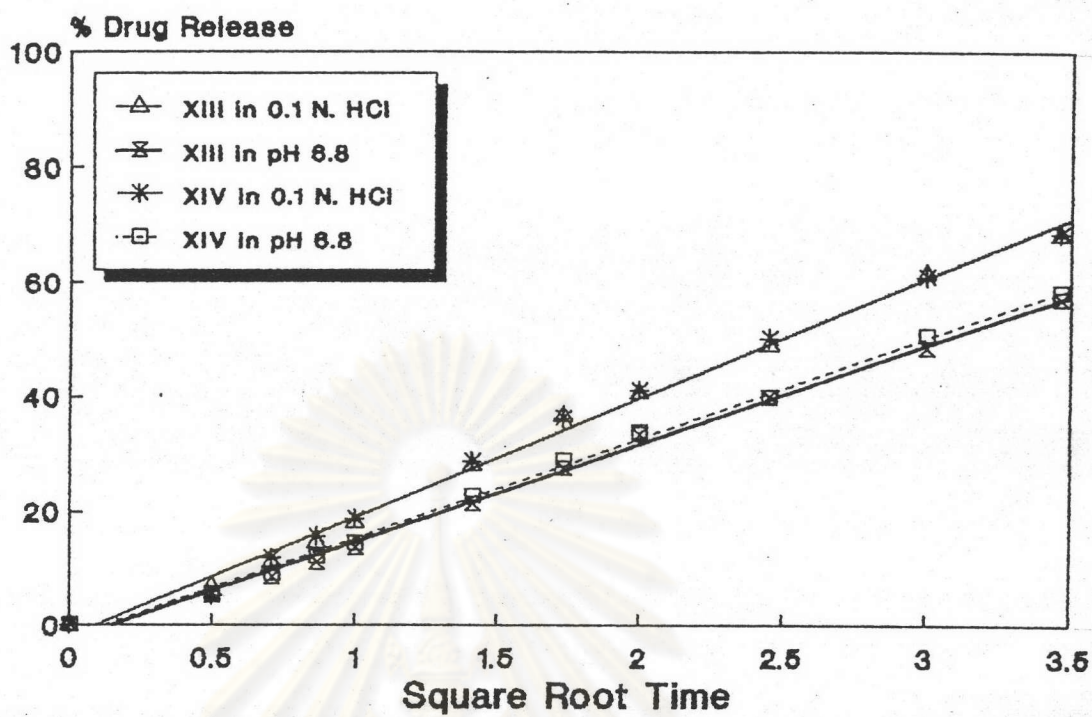


Figure 70. The Higuchi Plot of Formulation XIII and XIV Matrices

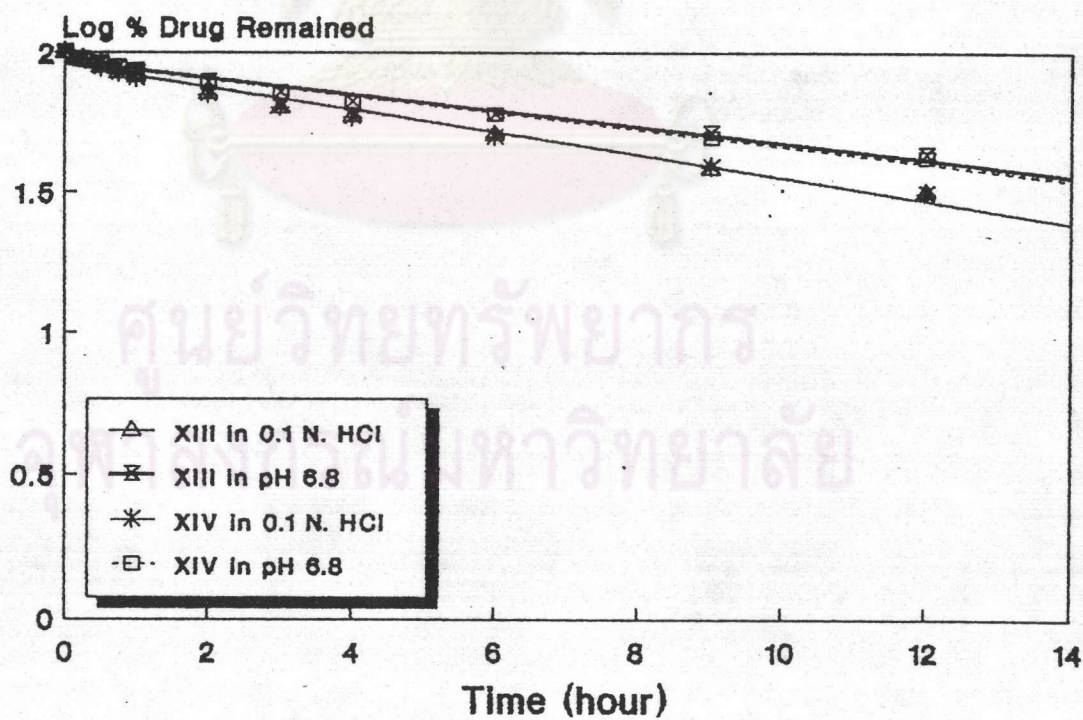


Figure 71. The First-order Plot of Formulation XIII and XIV Matrices

possibly follow Higuchi model, except Formulation XIV in 0.1 N HCl that would possibly follow first-order model.

Table 19 and Figures 72-73 gave the comparison between the linearizations of the first-order model and Higuchi model for Formulations XV-XVI. Both the Higuchi plot and the first-order plot were linear. Then the further treatment was examined, the correlation coefficient of rates of release against Q were higher than those of rates against $1/Q$ as presented in Table 22-23. As a result, the first-order model would probably be operative.

4.2.6 The Formulations XVII-XIX Matrices

Table 19 and Figure 74-75 gave the comparison between linearizations of the first-order model and Higuchi model for Formulations XVII-XVIII. Both models plots were linear, so it was necessary to distinguish between the models. In further treatment, the correlation coefficient of rates of release versus $1/Q$ were higher than those of rates versus Q as presented in Table 22-23 and indicated that the Higuchi model would possibly be better followed.

The comparison between the linearizations of the first-order model and Higuchi model for Formulation XIX presented in Figure 76-77 and Table 19 and indicated that these two models were interested. In further treatment, the correlation coefficient of rates of release versus $1/Q$ were higher than those of rates versus Q as tabulated in Table 22-23 and the statistical significance difference was found as presented in Table 66(Appendix F), these indicated that the Higuchi model would probably be operative.

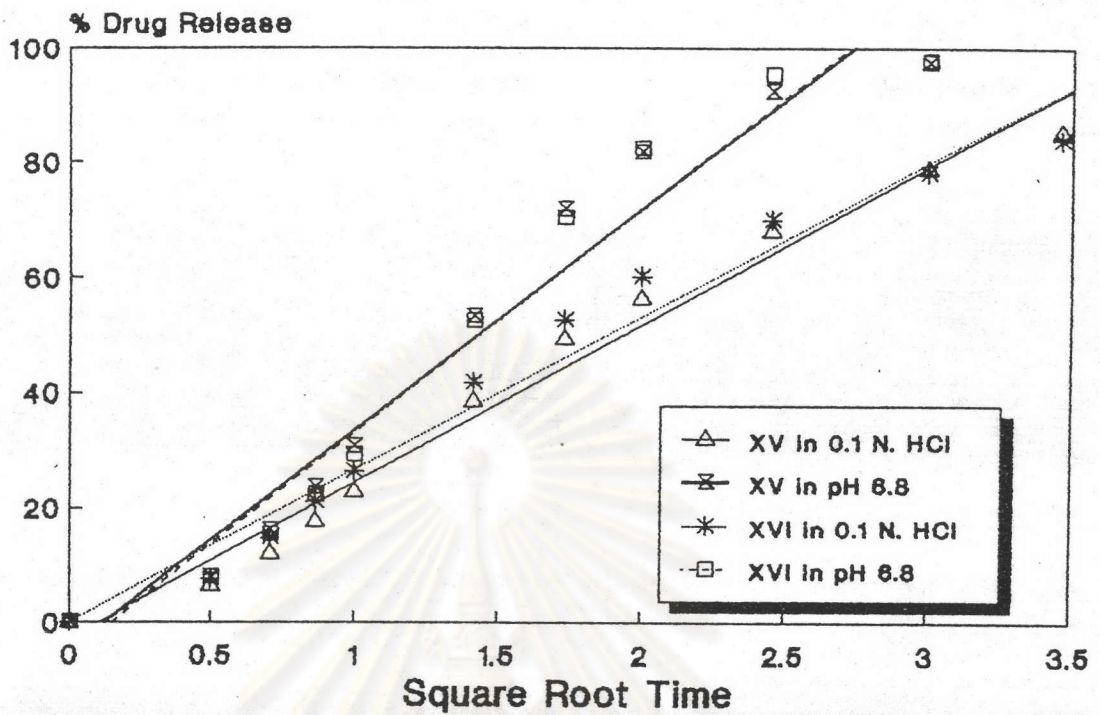


Figure 72. The Higuchi Plot of Formulation XV and XVI Matrices

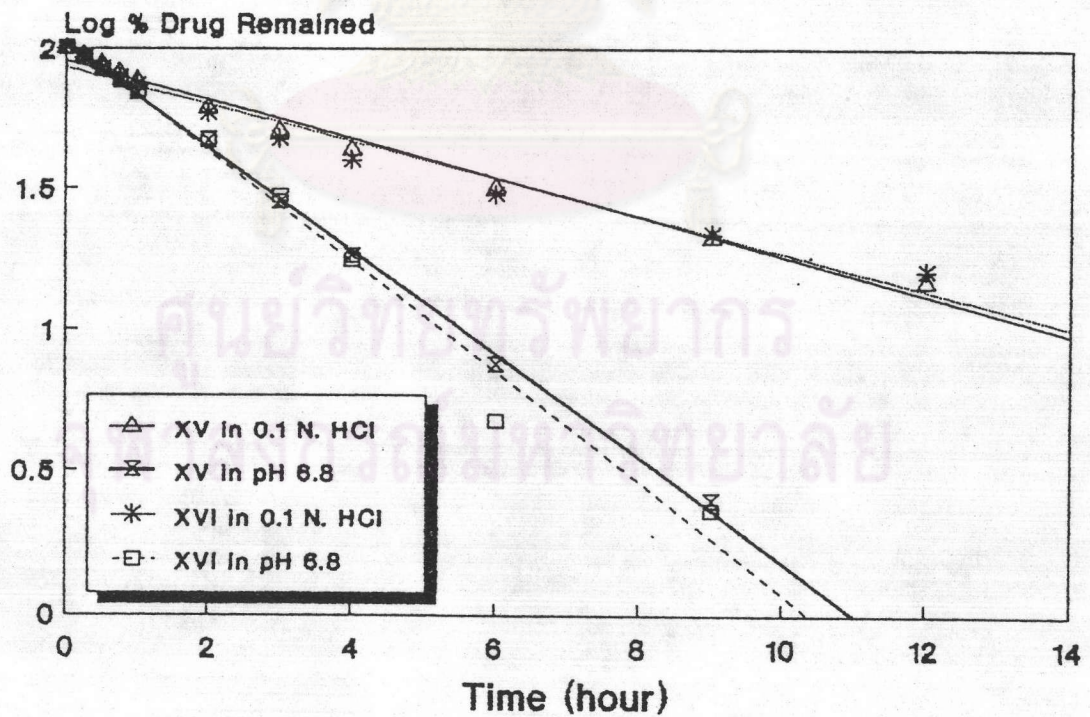


Figure 73. The First-order Plot of Formulation XV and XVI Matrices

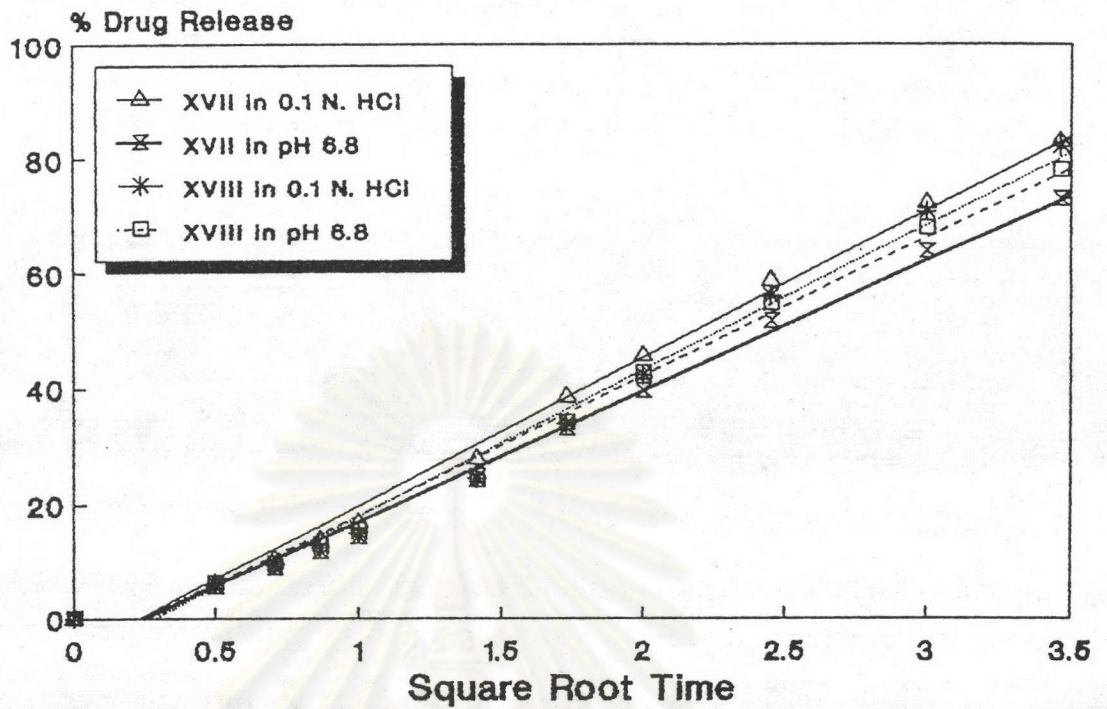


Figure 74. The Higuchi Plot of Formulation XVII and XVIII Matrices

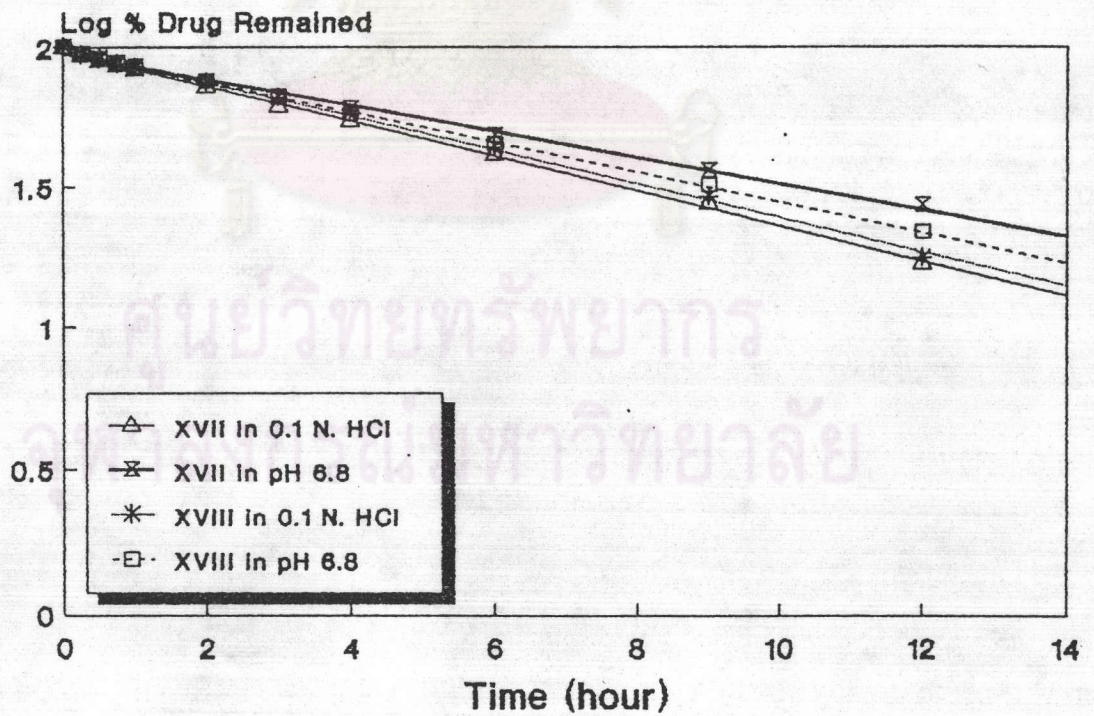


Figure 75. The First-order Plot of Formulation XVII and XVIII Matrices

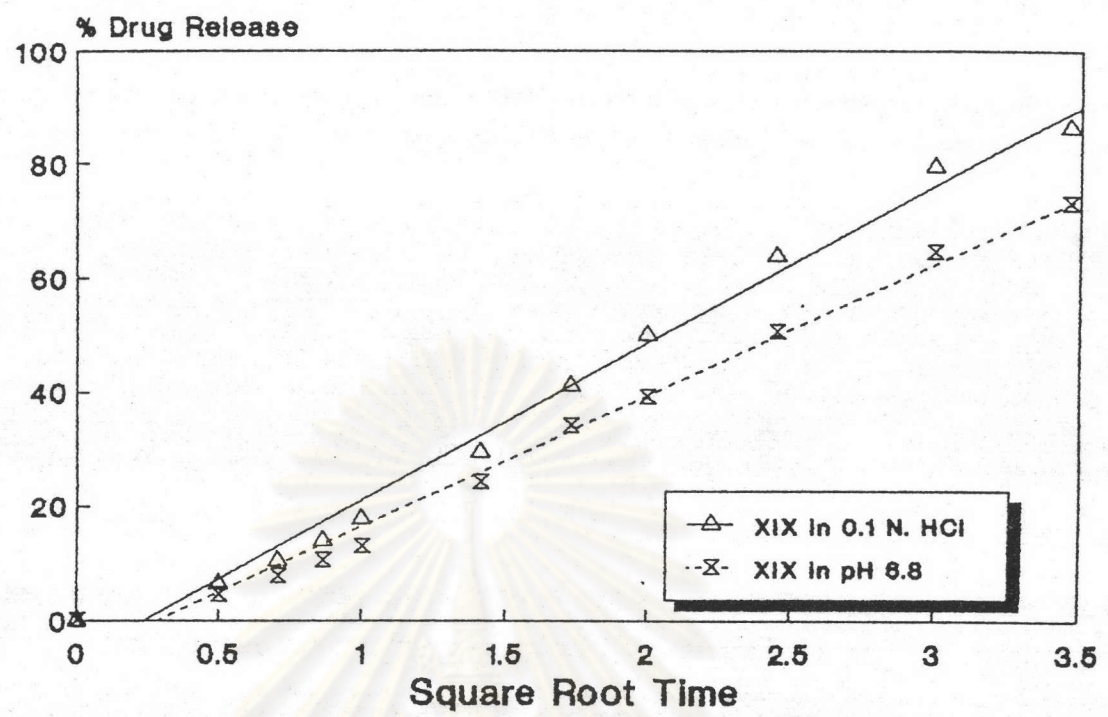


Figure 76. The Higuchi Plot of Formulation XIX Matrices

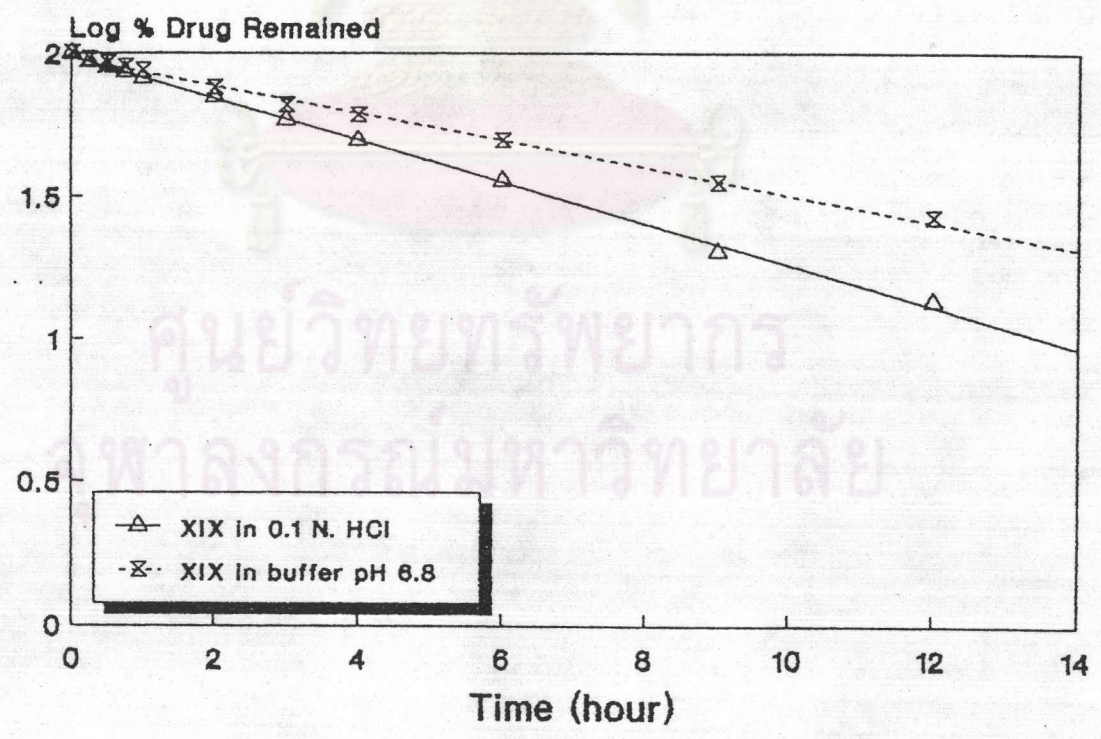


Figure 77. The First-order Plot of Formulation XIX Matrices

4.2.7 Quibron^(R)

The Higuchi plot and first-order plot for Quibron^(R) were shown in Figure 78 and 79, respectively. The highest correlation coefficient as presented in Table 19 obtained from the Higuchi plot, however, both the first-order model and Higuchi model were interested. In further treatment, the correlation coefficient of rate of release versus Q was higher than that of rate versus $1/Q$ as shown in Table 22-23 and the statistical significance difference of Quibron^(R) in buffer pH 6.8 was found as presented in Table 66 (Appendix F), these indicated that first-order model would possibly be followed.

4.2.8 Theodur^(R)

The Higuchi plot and first-order plot were shown in Figure 80 and 81, respectively. In 0.1 N.HCl, the highest correlation coefficient was 0.9977 that obtained from first-order plot (Table 19). In buffer pH 6.8, the highest correlation coefficient was 0.9871 that obtained from zero-order plot (Table 19). In further treatment, the release profile of Theodur^(R) in 0.1 N.HCl would probably follow Higuchi model with the correlation coefficient of rate of release against $1/Q$ was higher than that of rate against Q as tabulated in Table 22.

4.2.9 Nuelin^(R)

From the Figure 82-83 and the values of correlation coefficient of relationship tabulated in Table 19 pointed out that the highest correlation coefficient value in 0.1 N.HCl and

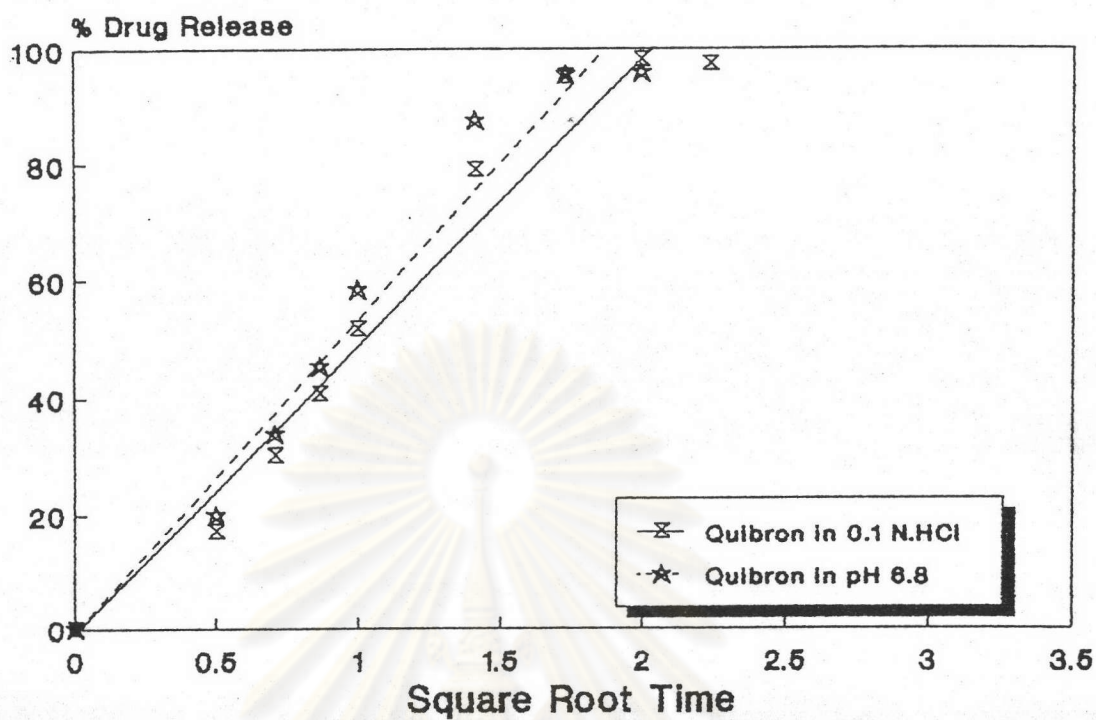


Figure 78. The Higuchi Plot of Quibron T/SR

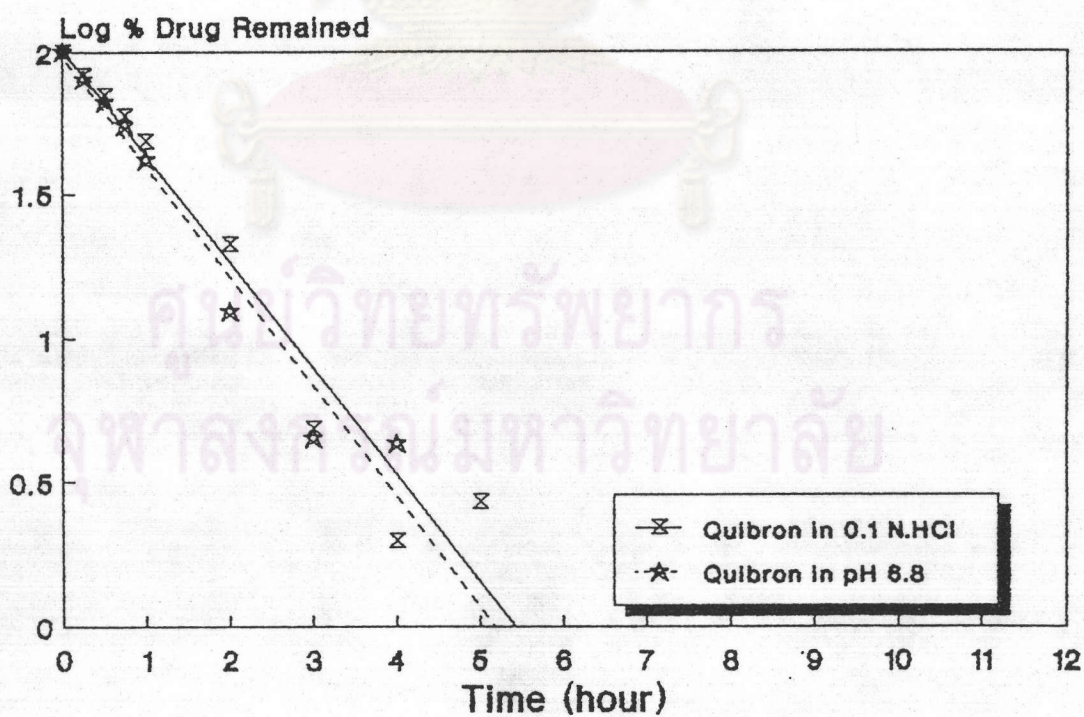


Figure 79. The First-order Plot of Quibron T/SR

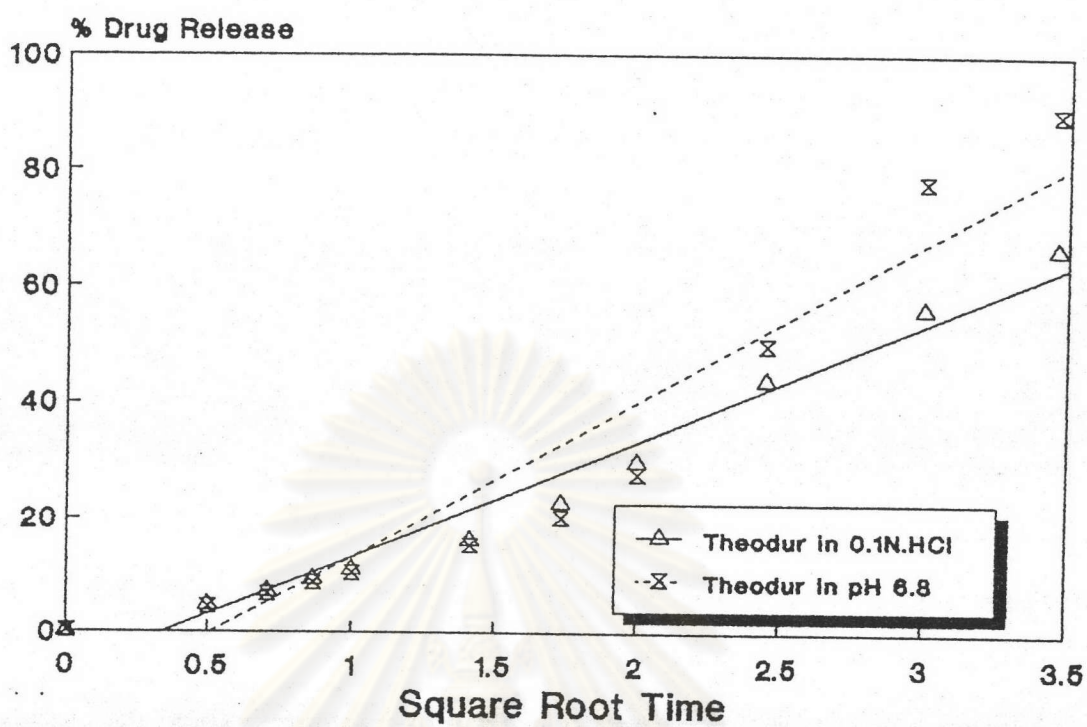


Figure 80. The Higuchi Plot of Theodur(R)

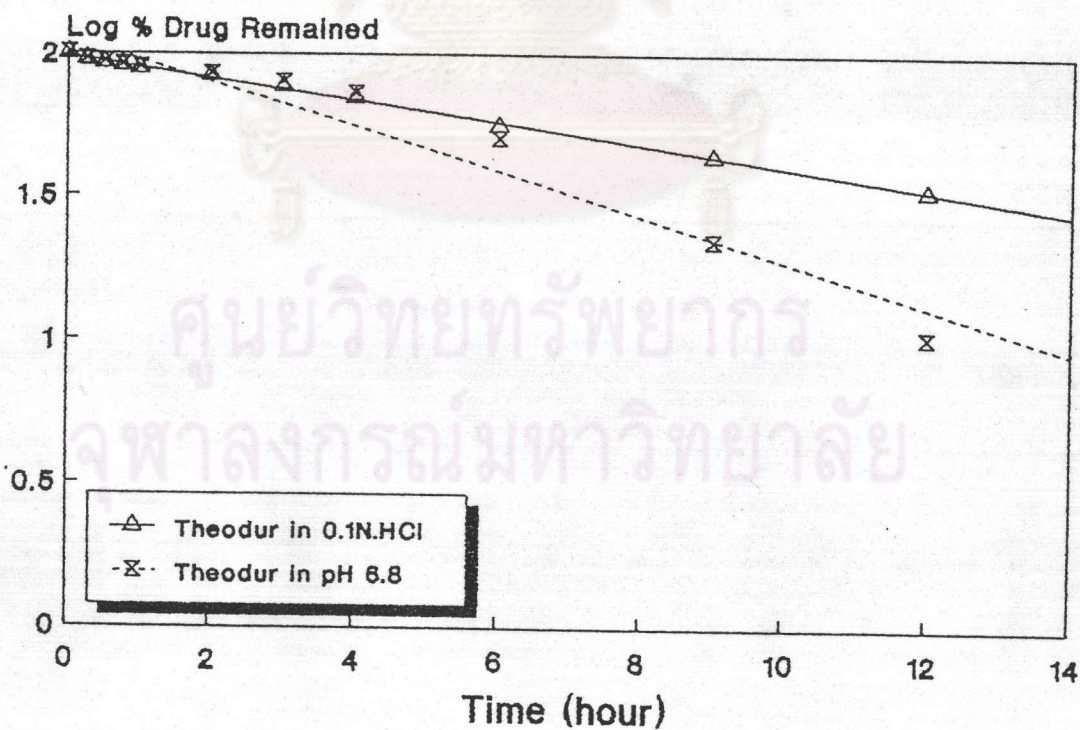


Figure 81. The First-order Plot of Theodur(R)

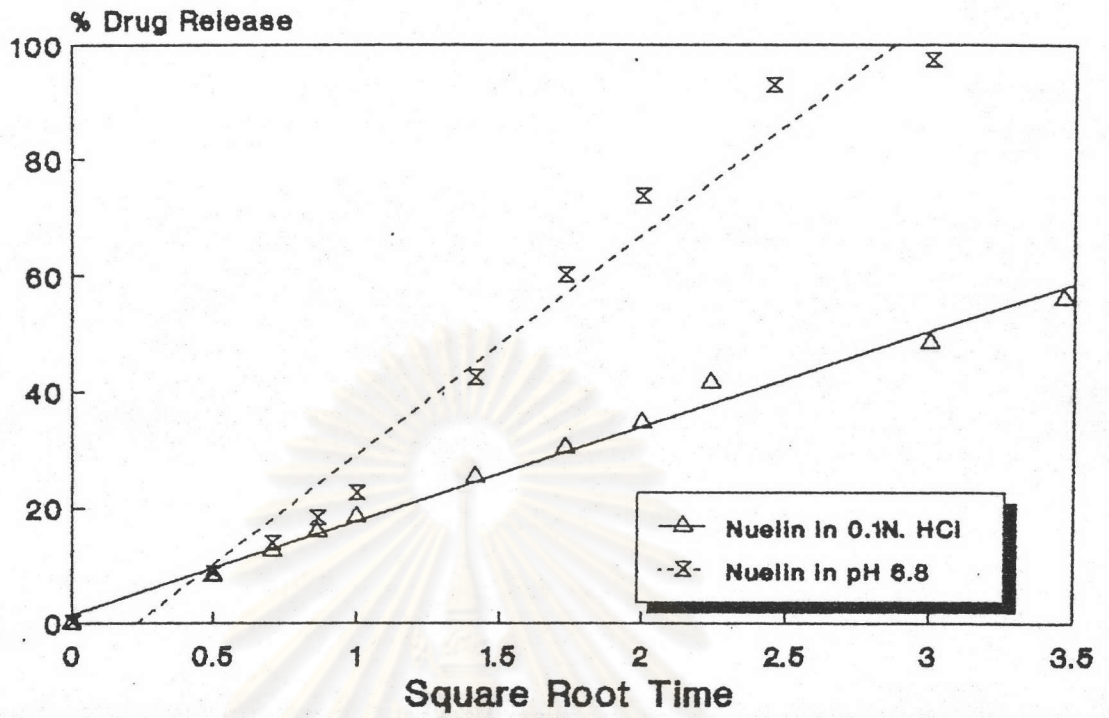


Figure 82. The Higuchi Plot of Nuelin^(R)

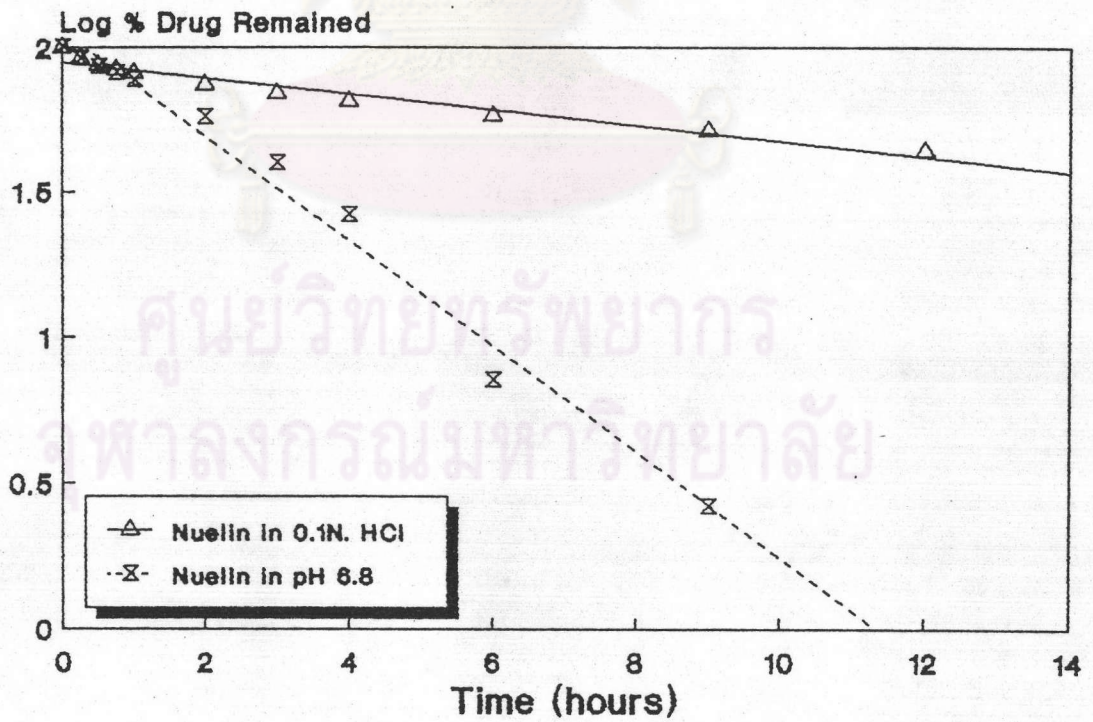


Figure 83. The First-order Plot of Nuelin^(R)

buffer pH 6.8 obtained from Higuchi plot and first-order plot, respectively. In further treatment, the linearity between plot of rate of release against $1/Q$ and Q of Nuelin^(R) in buffer pH 6.8 was rather indifferent and the t-value showed no statistical significance difference (Table 66, Appendix F), but in 0.1N.HCl the correlation coefficient value of rate of release against $1/Q$ was higher than that of rate against Q . In conclusion, the Higuchi model would possibly be operative in 0.1N.HCl.

4.2.10 The Products Tested in pH Change Method

4.2.10.1 Theodur^(R)

From Figure 60, 84, and 85 and the highest value of correlation coefficient in Table 24 that obtained from zero-order plot indicated that the release of this product would possibly follow zero-order model.

4.2.10.2 Nuelin^(R)

The Figure 84-85 and the values of correlation coefficient in Table 24 showed that the first-order model and Higuchi model were interested. In further evaluation, the correlation coefficient value of rate versus $1/Q$ was higher than that of rate versus Q as shown in Table 25 and indicated that Higuchi model would probably be operative.

4.2.10.3 Formulation XIX

The Figures 84-85 and the correlation coefficient values in Table 24 indicated that first-order

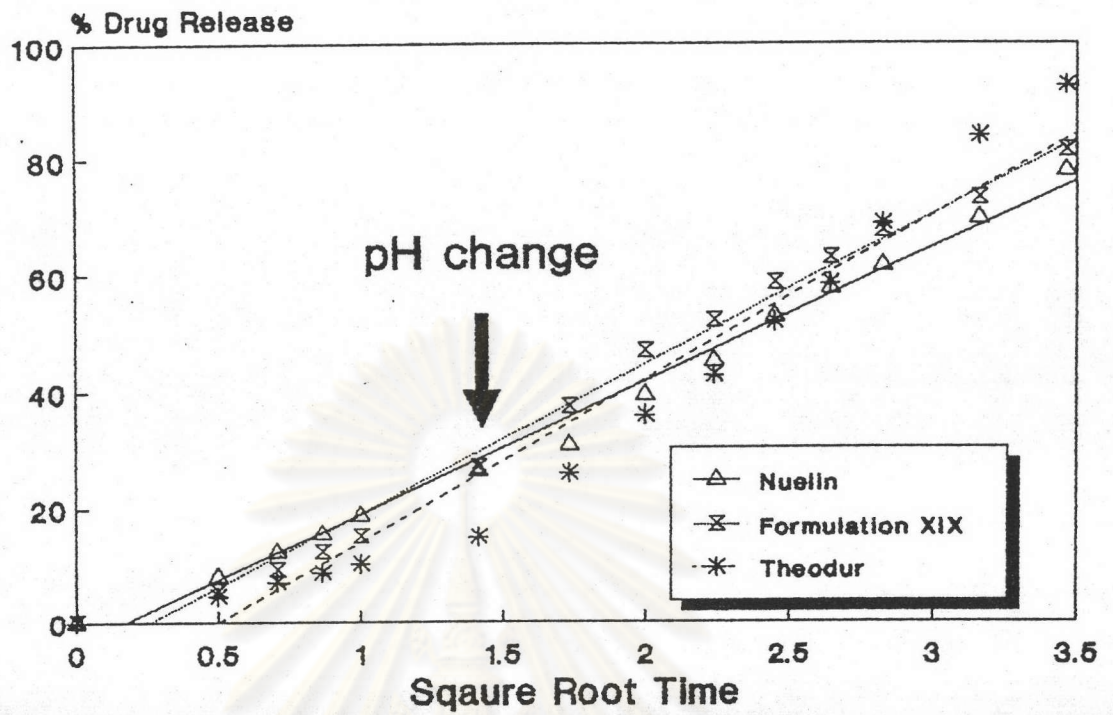


Figure 84. The Higuchi Plot of Formulation XIX Matrices, Nuellin^(R) and Theodur^(R) in pH Change Method

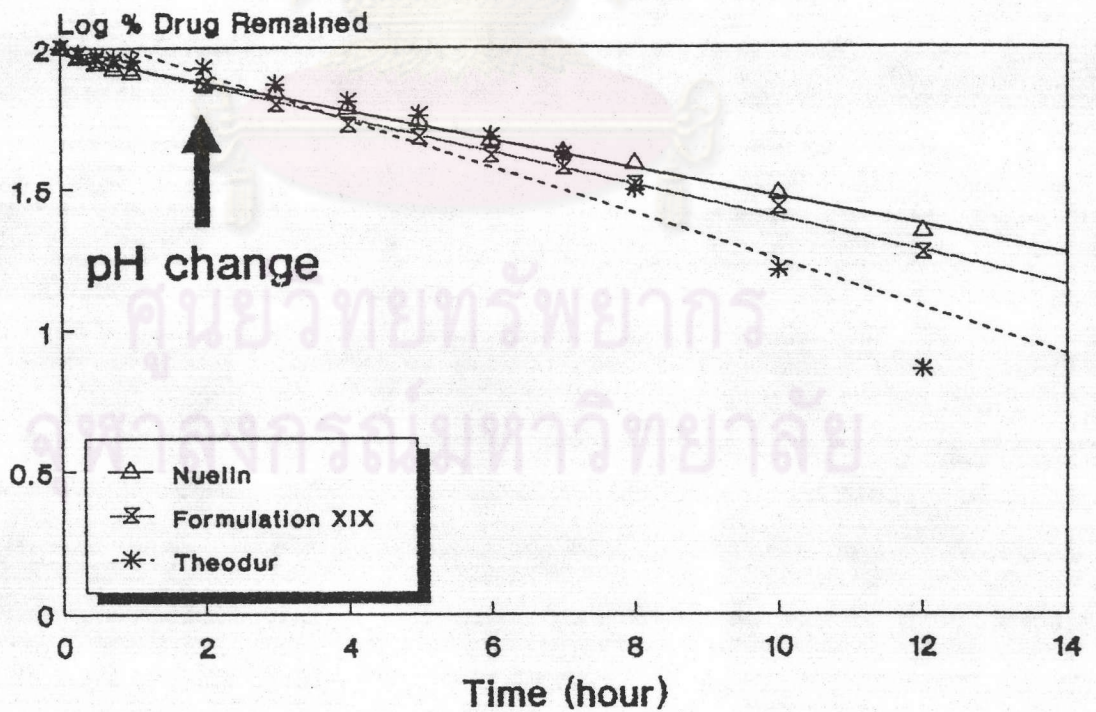


Figure 85. The First-order Plot of Formulation XIX Matrices, Nuellin^(R) and Theodur^(R) in pH Change Method

model and Higuchi model were interested. In further evaluation, the correlation coefficient value of rate against $1/Q$ was higher than that of rate against Q and the statistical significance difference was observed as presented in Table 66(Appendix F), these pointed out that Higuchi model would possibly be operative.

Table 24. Correlation coefficient of the relationships between percent drug released versus time (A), percent drug released versus square root time (B), and log percent drug remained versus time (C) in pH change method.

Product	A	B	C
XIX	0.9392	0.9897	0.9964
Nuelin ^(R)	0.9650	0.9918	0.9948
Theodur ^(R)	0.9952	0.9437	0.9177

Table 25. Comparison of linearity between plots of rate of release against reciprocal amount ($1/Q$) and amount (Q) of theophylline release from the Formulation XIX and commercial products from pH change method

Products	Correlation Coefficient of Rate dQ/dt	
	versus Q	versus $1/Q$
XIX	0.8252	0.8483
Nuelin ^(R)	0.5508	0.9392
Theodur ^(R)	0.1150	0.3439

4.3 The Evaluation of Drug Release Mechanism

The dissolution data was analyzed to clarify drugs release mechanism using equation $M_t/M_\infty = kt^n$ (Equation 7) as previous discussion in the section of the analysis of drug release mechanism. The Datatest computer program as presented in Appendix D was employed for this interpretation. All results were shown in Table 26-28.

Table 26. The values of kinetic constant (k), release exponent (n) and correlation coefficient (r^2) following linear regression of dissolution data for values of M_t/M_∞ in 0.1 N.HCl.

Formulation	n Release Exponent	k Kinetic Constant	r^2 Coefficient of Correlation
BLANK	0.77	0.380	0.9995
I	0.57	0.193	0.9984
II	0.52	0.164	0.9973
III	0.54	0.126	0.9993
IV	0.51	0.121	0.9990
V	0.73	0.117	0.9980
VI	0.64	0.110	0.9985
VII	0.55	0.112	0.9993
VIII	0.51	0.121	0.9990
IX	0.61	0.208	0.9921
X	0.71	0.207	0.9912
XI	0.63	0.198	0.9892
XII	0.62	0.192	0.9926
XIII	0.57	0.183	0.9906
XIV	0.55	0.187	0.9916
XV	0.70	0.222	0.9903
XVI	0.65	0.253	0.9914
XVII	0.69	0.173	0.9981
XVIII	0.73	0.152	0.9996
XIX	0.76	0.176	0.9995
Quibron ^(R)	0.79	0.516	0.9997
Nuelin ^(R)	0.45	0.183	0.9980
Theodur ^(R)	0.75	0.112	0.9744

จุฬาลงกรณ์มหาวิทยาลัย

Table 27. The values of kinetic constant (k), release exponent (n) and correlation coefficient (r^2) following linear regression of dissolution data for values of M_t/M_∞ in phosphate buffer pH 6.8

Formulation	n Release Exponent	k Kinetic Constant	r^2 Coefficient of Correlation
BLANK	0.87	0.304	0.9999
I	0.53	0.158	0.9980
II	0.56	0.129	0.9995
III	0.52	0.124	0.9992
IV	0.51	0.116	0.9990
V	0.58	0.082	0.9983
VI	0.55	0.075	0.9988
VII	0.54	0.090	0.9996
VIII	0.54	0.085	0.9996
IX	0.75	0.349	0.9982
X	0.92	0.406	0.9994
XI	0.81	0.338	0.9994
XII	0.53	0.422	0.9897
XIII	0.56	0.183	0.9949
XIV	0.55	0.187	0.9961
XV	0.85	0.222	0.9975
XVI	0.88	0.253	0.9992
XVII	0.71	0.173	0.9990
XVIII	0.70	0.152	0.9991
XIX	0.73	0.176	0.9926
Quibron ^(R)	0.78	0.578	0.9986
Nuelin ^(R)	0.84	0.237	0.9982
Theodur ^(R)	1.12	0.072	0.9113

Table 28. The values of kinetic constant (k), release exponent (n) and correlation coefficient (r^2) following linear regression of dissolution data for values of M_t/M_∞ in pH change method.

Formulation	n Release Exponent	k Kinetic Constant	r^2 Coefficient of Correlation
XIX	0.73	0.162	0.9965
Nuelin ^(R)	0.61	0.096	0.9938
Theodur ^(R)	0.93	0.072	0.9935

These exponent values were compared with the value of cylindrical sample in Table 7, except the values obtained from Formulations V-VIII were compared with the value of cylindrical sample in Table 8.

4.3.1 The Blank Theophylline Matrix

The blank matrix was dissolved both in 0.1 N. HCl and in phosphate buffer pH 6.8, the release exponent n were 0.77 and 0.87, respectively (Table 26-27). These results indicated that the mechanism of drug release was anomalous (non-Fickian) transport.

4.3.2 The Formulations I-IV Matrices

The theophylline-ethylcellulose matrices were not dissolved and not swelled. The value of n , k , r^2 were shown in Table 26-27. In 0.1 N. HCl and phosphate buffer pH 6.8, the trends of the release exponent n was decrease when the ethylcellulose was increased. These indicated that at low concentration of ethylcellulose the mechanism was not only Fickian diffusion but have other mechanism such as leaching from the water channel. In higher ethylcellulose, the release exponent n was approached to 0.45 that indicated that the main mechanism was closer to Fickian transport and the other mechanism was decreased. From this evaluation, it could be predicted that when the concentration of ethylcellulose was increased until the critical concentration was reached, the mechanism would be Fickian transport.

4.3.3 The Formulations V-VIII Matrices

The theophylline-HPMC matrices were formed a gelatinous matrix and swelled. The release exponent n , the kinetic

constant k and the correlation coefficient r^2 were shown in Table 26-27. The release exponent value would be compared with the value in Table 8. The release mechanism was anomalous (non-Fickian) transport. The release exponent value tended to be decreased when the amount of HPMC was increased.

4.3.4 The Formulations IX-XII Matrices

The theophylline-HPMCP matrices would be separated the evaluation into two parts according to the characteristic in the dissolution medium. In 0.1 N. HCl, The matrix was ruptured into special pattern. The highest release exponent value was obtained from 10% HPMCP matrix. This may be that this concentration was an optimum concentration of HPMCP for using as disintegrant. The release exponent n which compared to Table 7 was indicated that the mechanism was anomalous transport. In phosphate buffer pH 6.8, the matrix was dissolved completely in the range of the testing time. The highest release exponent n was obtained when using 10% of HPMCP. The release mechanism was seemed to be anomalous transport.

4.3.5 The Formulation XIII-XVI Matrices

To increase release of theophylline from matrix tablets containing ethylcellulose, water soluble additives such as PVP K30 and lactose were incorporated as channeling agents.

The ethylcellulose-PVP K30 matrices were not dissolved but had some erosion. The value of n , k and r^2 were shown in Table 26-27. In both medium, the release exponent n of

Formulations XIII and XIV indicated that the release mechanism was anomalous transport. When ethylcellulose was reduced to 1% w/w (in Formulations XV and XVI), it was found that the matrix was completely dispersed in phosphate buffer pH 6.8 within 9 hours. The release exponent n pointed out that the release mechanism was anomalous transport. The value of n from phosphate buffer pH 6.8 was higher than the value from 0.1 N. HCl, it was possibly according to the matrix erosion in phosphate buffer pH 6.8 was higher than in 0.1 N. HCl. This result might be due to the property of PVP K30.

4.3.6 The Formulations XVII-XIX Matrices

The theophylline-ethylcellulose-lactose matrix was slowly eroded in 0.1 N. HCl. The value n was increased when increasing the amount of lactose or decreasing the amount of ethylcellulose (Table 26). In phosphate buffer pH 6.8, the value n was rather steady when increasing the amount of lactose, but the value n was increase when decreasing the amount of ethylcellulose in the matrix. Finally the release mechanism of this matrix was anomalous transport. Lactose led to multiplicity of matrices which followed the same release mechanism.

4.3.7 The Commercial Products

The release mechanism of Theodur^(R) was not clear because the correlation coefficient value was rather low. The release mechanism of Quibron^(R) was anomalous transport. The n values from 0.1 N. HCl and phosphate buffer pH 6.8 were 0.79 and 0.78, respectively. The release mechanism of Nuelin^(R) in 0.1 N. HCl was Fickian diffusion with n value = 0.45. But Nuelin^(R) was eroded

in buffer pH 6.8 and the release mechanism was anomalous transport with n value = 0.84.

4.3.8 The Products Tested by pH Change Method

In the pH change method, the Formulation XIX, Nuelin^(R) and Theodur^(R) were studied. The release exponents n of Theodur^(R), Formulation XIX and Nuelin^(R) were 0.93, 0.73 and 0.61, respectively (Table 28). These indicated that the release mechanism of these three products were anomalous transport and the release mechanism of Theodur^(R) was the nearest to the zero-order transport. When the value of n approached 1.0, phenomenologically one might conclude that the release was approaching zero-order.

5. Projected *in vivo* Data

The results showed wide variations in the pattern of the *in vitro* release, both in absolute terms and in the influence of pH. Variation of these magnitudes would be expected to have significant influence *in vivo*.

Formulation XIX, Theodur^(R), and Nuelin^(R) were compared by using simulated pharmacokinetics model. All details and assumptions were as following:

1. Dissolution was the rate-limiting process for absorption
2. All drug release would be absorbed, whether in the stomach or intestine, i.e. no absorption window problems. The oral bioequivalent (F in Equation 1) equaled to one.
3. No biotransformation process occurred during absorption.
4. The elimination rate remained constant.

5. Pharmacokinetic parameters were obtained from the report of Malee Sae Jung(1988). The selected parameters were received from Thai male non-smoking group which had average body weight about 60 kg.

6. The release rate that calculated from the release profile should be used to calculate the individual dose every 15 minutes. Then, from these doses and selected pharmacokinetic parameters, the drug plasma concentration of individual could be calculated, using Equation 1. Finally, the drug plasma concentration of overall individual doses could be derived.

7. Assumed that after 12 hours, the matrices were passed through the GI tract and eliminated from the human body. The GI tract presents some unusual features that are not found in other routes of drug administration. The relatively brief transit time through the GI tract, approximately 12 hours, constrains the length of prolongation that can be expected. The variability in stomach emptying time and the rather severe chemical conditions of the stomach were additional limiting factors in the choice of prolonging mechanisms for this route. Regarding intestinal transit time in man the data listed in Table 29(Davis et al., 1984; Ritschel, 1989) could be used as a guideline. In conclusion, overall transit time of tablets was summed and the result was 617 minutes or about 10 hours.

From these assumptions, the drug plasma concentration of individual dose could be calculated for every 15 minutes until 24 hours. The latter dose would produce the drug plasma concentration that shifted from the former for 15 minutes as shown in Figure 86 (data from Formulation XIX in pH change method). From the

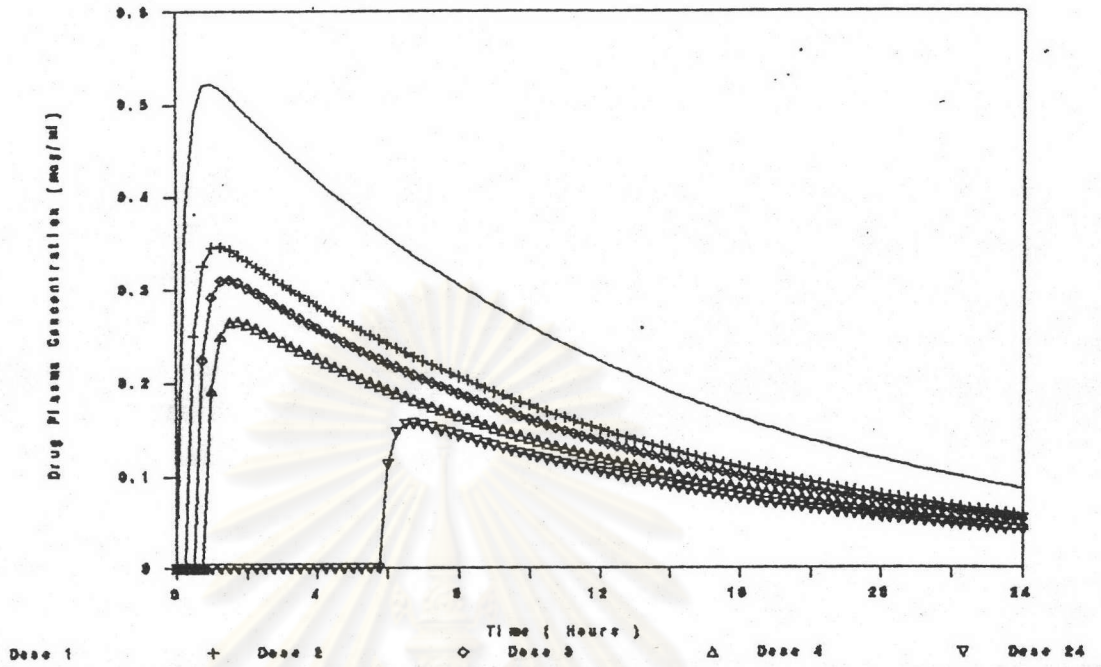


Figure 86. The Simulated Plasma Concentration of Individual Dose from Formulation XIX Matrix

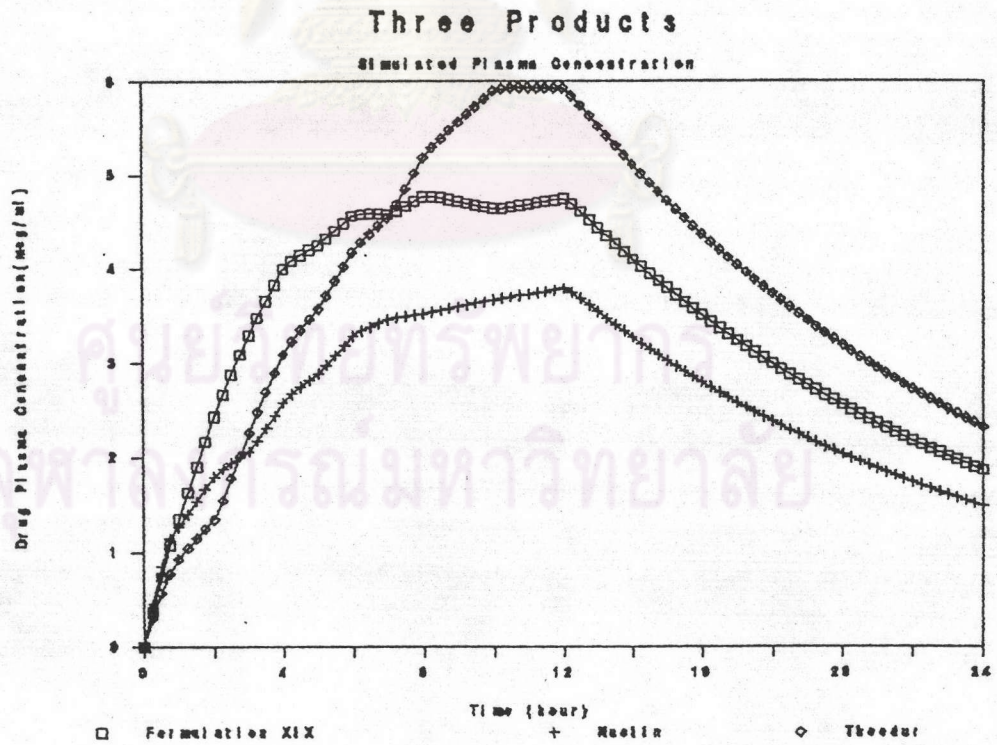


Figure 87. The Simulated Plasma Concentration Profile of Three Products Assumed that Delivered by One Dose every 15 Minutes, Amount of Dose was respected to the Release Rate

dissolution data(Formulation XIX, Nuelin^(R) and, Theodur^(R)in pH change method), each matrix could be divided to 48 individual dose, and created 48 curve of drug plasma concentration that shifted from the other for 15 minutes scale. Therefore, the cumulation curve as depicted in Figure 87 could be derived by summation the individual curve together.

Table 29. Gastrointestinal transit time in minutes \pm SD of pellets and intact tablets in humans.

Formulation	Gastric Emptying Time [min]	Small Intestine Transit Time [min]	Colonic Arrival Time [min]
Pellets (*)	79 \pm 20	277 \pm 82	305 \pm 100
Tablets	164 \pm 92	188 \pm 23	265 \pm 59

* For pellets the transit time is for 50% of the particles to leave or arrive at the particular site.

Theodur^(R) showed a highest predicted blood level than any of the other products, the peak of blood level which was reached at ten hours and maintained for two hours was about 6 μ g/ml.

Formulation XIX matrix showed a intermediate predicted blood level. The plateau of blood level was reached at time about four hours and maintained for about eight hours. The peak of plateau was about 5 μ g/ml.

Nuelin^(R) had a lowest peak of blood level which was about 3.5 μ g/ml. The nearly plateau state was reached within five hours and maintained for seven hours.